

191

$$V_0 = 2/k^2 = 1/2 \cdot 5^{-2} = 1/50$$



National Library
of Canada

Bibliothèque nationale
du Canada

Canadian Theses Division Division des theses canadiennes

Ottawa Canada
K1A 0N4

6047

PERMISSION TO MICROFILM — AUTORISATION DE MICROFILMER

- Please print or type Écrire en lettres moulées ou dactylographier

Full Name of Author Nom complet de l'auteur

• 100 •

Date of Birth Date de naissance

Quality of Birth: The Impression

Permanent Address Residence Tax

Title of thesis Title in abstract

1888-9. 1889-90.

¹See also the discussion of the relationship between the concept of "cultural capital" and the concept of "cultural value" in the introduction to this volume.

TECHNICAL SUPPORT SERVICES - A PRELIMINARY SURVEY OF THE FIELD

Nature's Way of Saving the Best

PERMISSION IS HEREBY GRANTED BY THE NAT'L LIBRARY OF CANADA TO LIBRARIES AND OTHER USERS TO MAKE ONE COPY

The author reserves the right at all times to prohibit the thesis from extensive editing, to have it printed or otherwise reproduced without his/her written permission.

THE SATELLITE AND TELEVISION SECTION OF THE CRTC. THE
FEDERATION CANADA SECTION HAS PREPARED THESE COMMENTS
FOR YOUR INFORMATION.

Date

T. J. S. STANLEY

CANADIAN THESES ON MICROFICHE

ISBN

THESES CANADIENNES SUR MICROFICHE



National Library of Canada
Collections Development Branch

Canadian Theses on
Microfiche Service

Ottawa, Canada
K1A 0N4

Bibliothèque nationale du Canada
Direction du développement des collections

Service des thèses canadiennes
sur microfiche

NOTICE

The quality of this microfiche is heavily dependent upon the quality of the original thesis submitted for microfilming. Every effort has been made to ensure the highest quality of reproduction possible.

If pages are missing, contact the university which granted the degree.

Some pages may have indistinct print, especially if the original pages were typed with a poor typewriter ribbon or if the university sent us a poor photocopy.

Previously copyrighted materials (books, articles, published tests, etc.) are not filmed.

Reproduction in full or in part of this thesis is governed by the Canadian Copyright Act (R.S.C. 1970 c. C-30). Please read the authorization forms which accompany this thesis.

THIS DISSERTATION
HAS BEEN MICROFILMED
EXACTLY AS RECEIVED

AVIS

La qualité de cette microfiche dépend essentiellement de la qualité de la thèse soumise pour microfilmage. Nous avons tout fait pour assurer une qualité supérieure de reproduction.

S'il manque des pages, veuillez communiquer avec l'université qui a conféré le grade.

La qualité d'impression de certaines pages peut大致上是欲求的, surtout si les pages originales ont été photostatées à l'aide d'un rubanuse moins bon que ce que nous avons parvenu une photocopie de mauvaise qualité.

Tous documents qui font de l'objet d'une protection copyright, articles de revue, examens, publications et autres pas à nommer.

La reproduction en totalité ou en partie de cette thèse est soumise à la Canadian Copyright Act (R.S.C. 1970 c. C-30). Veuillez prendre connaissance des formulaires d'autorisation qui accompagnent cette thèse.

LA THÈSE A ÉTÉ
MICROFILMÉE TELLE QUE
NOUS L'AVONS REÇUE

Canada

THE UNIVERSITY OF ALBERTA

Sedimentology and Clay Mineralogy of the Glauconitic Sandstone Suffield Heavy Oil
Sands, Southeastern Alberta



by

Barbara J. Tilley

A THESIS

SUBMITTED TO THE FACULTY OF GRADUATE STUDIES AND RESEARCH
IN PARTIAL FULFILMENT OF THE REQUIREMENTS FOR THE DEGREE
OF Master of Science

Department of Geology

EDMONTON, ALBERTA

Fall 1982

THE UNIVERSITY OF ALBERTA
RELEASE FORM

Permission is hereby granted to THE UNIVERSITY OF ALBERTA LIBRARY to reproduce single copies of this thesis and to lend or sell such copies for private scholarly or scientific research purposes only

The author reserves other publication rights, and neither the thesis nor extensive extracts from it may be printed or otherwise reproduced without the author's written permission

(SIGNED)

PERMANENT ADDRESS

DATED

THE UNIVERSITY OF ALBERTA
FACULTY OF GRADUATE STUDIES AND RESEARCH

The undersigned certify that they have read and recommend to the Faculty of Graduate Studies and Research, for acceptance, a thesis entitled "Sedimentology and Clay Mineralogy of the Glauconitic Sandstone, Suffield Heavy Oil Sands, Southeastern Alberta" submitted by Barbara J. Tilley in partial fulfilment of the requirements for the degree of Master of Science

Fred J. Longstaffe

Supervisor

J. J. Lubick

F. J. Scott

Date October 13, 1982

Abstract

Heavy gravity oil occurs in the Glauconitic Sandstone of the Lower Cretaceous Mannville Group in the Suffield area southeastern Alberta. The Glauconitic Sandstone ranges in thickness from zero to over 45 metres and has a pay zone averaging 20 metres thick. The thickest sandstones occur in a northwest to southeast trending broad arch which represents an ancient shoreline position with the sea to the east. Facies present in the sandstone include in ascending order coarsening-upward sandstone, medium- to coarse-grained sandstone, laminated sandstone, argillaceous sandstone, carbonaceous sandstone and shale, and very fine grained sandstone, siltstone and shale. These facies represent in order the lower, middle shoreface, middle, upper shoreface-foreshore, backshore, marsh and lagoonal or continental zones of a progradational beach system. The environment is microtidal with the sandstone belt including the reservoir dissected by few tidal inlets and channels.

The thickness of the pay zone depends upon the amount of structural movement on local basement faults during subsequent deposition as well as the facies distribution. Movement on basement faults may also have resulted in the continuous abnormally thick progradational beach sequence.

The Glauconitic Sandstone is a litharenite composed of quartz, chert, other sedimentary rock fragments and trace amounts of feldspar. Kaolinite is the dominant clay mineral present in all sandstones. Depotassified chloritized illite and interstratified illite-smectite occur in minor amounts and smectite abundance varies from a trace in the oil saturated sandstones to 10% in some sandstones below the oil-water interface. Chlorite is present in trace amounts. The paragenetic sequence is: 1) first stage calcite cementation and pyrite crystallization; 2) quartz cementation and kaolinite growth; 3) second stage calcite cementation, feldspar leaching, minor kaolinite illite crystallization and still later precipitation of calcite crystals; and 4) smectite chlorite growth and hydrocarbon emplacement.

The abundance of detrital kaolinite present in the sandstone is the main control on its reservoir quality. The laminated facies has the best reservoir qualities: high porosity, low clay content and good lateral continuity. Authigenic phases such as kaolinite, quartz and deformed rock fragments cause only minor reduction in porosity and permeability.

The argillaceous or bioturbated facies, characterized by irregular argillaceous zones, has poor reservoir qualities.

The main concern related to fluid sensitivity is the dispersion of fine kaolinite. Pyrite and Fe-chlorite are sensitive to acidization, but occur in minor amounts. An increase in temperature of the reservoir during combustion may cause a reduction in permeability as a result of formation of smectite, and the dissolution and reprecipitation of silica.

Acknowledgements

This study is based on core from the Suffield Heavy Oil Pilot project operated by Alberta Energy Company with ACOSSHA, Lime Petroleum, and Westcoast Petroleum as partners. I would like to thank each of these companies for their permission to examine and freely sample the confidential project core and for access to other confidential geological information. Without this access and permission to publish the findings, this thesis would not have been possible. Brian Wells, Allan Ohauser and Bill Male were very helpful in providing materials and information in relation to the SHOP project and their comments at various stages helped guide the direction of study. I also acknowledge the various suggestions made by members of the SHOP project technical committee during monthly meetings.

Fred Langstaffe at the University of Alberta supervised the project with particular emphasis on the mineralogy section and provided instructive criticism of various drafts of the manuscript. Fred Hein suggested improvements in an early draft of the thesis. John Kramers supervised the project at the Alberta Geological Survey. Gary Wrightman, Doug Lant, Peter Frazer, Ray Kanman, Brian Kettensasser, Karen Harris, and Grant Mississipi offered advise and criticism at various stages throughout the study.

Numerous people provided technical support both at the Research Institute and at the University of Alberta. Thin sections, SEM mounts, extra thin and grain size analyses were done by Tim Bereznik, Mark Baaske, David Edwards, and Campbell Kidston. A survey of the clay mineralogy was provided by XRD analyses run by Susan Nutz (Dane Card) at the University of Alberta Geotexture and Petrotextural Research Laboratory. Sample to detailed X-ray diffraction and powder X-ray analyses (FAB) and data was processed by Bruno Jintdassier and interpreted by Anatoly Voshch. Most diagrams were drafted by the Research Institute drafting department and photographic plates were printed by Leslie Curran, Sandra Vanasse, and Linda Hugar. I would like to thank all assistance and dear Chechenko, Linda, Linda, Ruth, Sherry, and Linda Bindra typed the tables and figure captions. I wish to express my appreciation to all of these people and to all others who helped in any way.

Table of Contents

Chapter		Page
I	INTRODUCTION	1
	A Purpose of this Study	1
	B Geological Setting	3
	C History of the Term Glauconitic Sandstone	3
	D Previous Work	5
	E Methods	6
II	FACIES ANALYSIS	8
	A Facies Descriptions	8
	Facies 6 Coarsening upward sandstone	8
	Facies 5 Medium to coarse grained sandstone	14
	Facies 4 Laminated sandstone	15
	Facies 3 Argillaceous sandstone	15
	Facies 2 Carbonaceous sandstone and shale	17
	Facies 1 Very fine grained sandstone siltstone and shale	18
	Regional Facies Descriptions	18
	B Facies Interpretation	19
	Facies 6	19
	Facies 5	22
	Facies 4	22
	Facies 3	23
	Facies 2	24
	Facies 1	24
	Summary	24
III	PALYNOLOGY	25
IV	REGIONAL DEPOSITIONAL SETTING	29
V	TECTONIC SETTING	36
	A SHOP Project Site	36
	B Regional Sulfide Area	39

C	Petroleum Trapping Mechanism	41
D	Tectonic Control on the Glauconitic Sandstone Thickness	43
VI	MINERALOGY	45
A	Bulk Mineralogy	45
B	Clay Mineralogy	47
	Descriptive Clay Mineralogy	47
	Assemblages of Clay Minerals	55
	Distribution of Clay Mineral Assemblages	56
C	Diagenetic Sequence	79
	First Stage Diagenesis	79
	Second Stage Diagenesis	80
	Third Stage Diagenesis	81
	Fourth Stage Diagenesis	81
VII	RESERVOIR QUALITY	82
A	Facies 4	82
B	Permeability and Continuity	83
C	Detrital clay	83
D	Irreducible Water Saturation	83
E	Fluid Sensitivity	84
	Effect of the Application of Wet Forward Combustion on the Reservoir	84
VIII	CONCLUSIONS	86
A	Sedimentological Controls	86
B	Structural Controls	86
C	Mineralogical and Diagenetic Controls	87
D	Recommendations for Future Work	87
X	REFERENCES	111
X	APPENDICES	112
	Appendix A Core Logs for Wells from the SHOP Project see attached pocket	113
	Appendix B Analytical Methods for Detailed XRD Analyses	114

Tables

Table 1 Grain percentages based on thin section point counts for well O1	9
Table 2 Summary of grain size analyses	12
Table 3 Average porosities	13
Table 4 Summary of facies descriptions	21
Table 5 Relative percentages of clay minerals in SHOP project samples <2 micrometre size fractions	48
Table 6 Relative percentages of clay minerals in the <2 micrometre size fraction from detailed XRD analyses	49
Table 7 X-ray powder camera results for sample 6-18	50

Figures

Figure 1 Location of the Suffield heavy oil project

Figure 2 Map of the SHOF project site showing the location of the production (P), injection (I) and observation (O) wells

Figure 3 Stratigraphic correlation chart

Figure 4 Northwest-southeast structural cross section through the SHOF project area showing the distribution of facies and samples in each well relative to the geophysical logs

Figure 5 Southwest-northeast structural cross section through the SHOF project area showing the distribution of facies and samples in each well relative to the geophysical logs

Figure 6a Generalized profile of a barrier-beach environment showing the spatial relationships of the sedimentary facies and their positions on the shore

Figure 6b Generalized litholog from SHOF project core showing the vertical sequence of facies, grain size, percent clay, geophysical log shapes and the facies interpretations

Figure 7 Gamma-ray log cross sections showing the distribution of samples analyzed for polymorphs and dinoflagellates

Figure 8 Map showing the 15 metre sandstone thickness contour for the Glauconitic Sandstone

Figure 9 Sequence of sedimentary facies within regionally spaced wells from a the western side of the Western and to the eastern side of the thick sandstone belt

Figure 10 Gamma-ray log stratigraphic cross section illustrating the relative vertical position of sandstone bodies when the datum coal bed was deposited

Figure 11 Geophysical-log stratigraphic cross section showing an interruption in the continuity of the sandstone reservoir by a facies change

Figure 12 Litholog of a channel deposit within the Glauconitic Sandstone interval

Figure 13 Location of the study area relative to various components of the North Battleford Arch, a northern extension of the Sweetgrass Arch

Figure 14 Correlation of gamma-ray logs for two wells IP2 and O2 75 metres apart hung on a series of datum lines

Figure 15 Gamma ray log structural cross section with a correlation line joining approximate correlative horizons	40
Figure 16 Two cross sections demonstrating the effect of structural movements on the relative positions of the oil/water interface	42
Figure 17 Schematic cross-section showing the thickening of sediment over a zone of relatively rapid subsidence	44
Figure 18 A and B Typical X-ray diffractograms of the <2 micrometre fraction for type I samples	58
Figure 19 A and B Typical X-ray diffractograms of the <2 micrometre fraction for type II samples	61
Figure 20 A and B X-ray diffractograms representative of shale samples from immediately above and below the Glauconitic Sandstone type III clay assemblage	64
Figure 21 A and B X-ray diffractograms representative of a very fine grained sandstone in facies 6 and a bioturbated sandstone of facies 3 type III clay assemblage	67
Figure 22 A and B X-ray diffractograms representing a shale interbed in the carbonate cemented sandstone of facies 6 type III clay assemblage	70
Figure 23 A and B X-ray diffractograms representing the <2 micrometre fraction of an oil-saturated sandstone of facies 4 type IV clay assemblage	73
Figure 24 A and B X-ray diffractograms representing the <2 micrometre fraction of an oil-saturated sandstone of facies 4 type IV clay assemblage	76

Plates

Plate 1 Core photographs for facies 6 to facies 3d	89
Plate 2 Core photographs for facies 3c to facies 1	91
Plate 3 Thin section textures for facies 5 and facies 3bi	93
Plate 4 Bulk mineralogy	95
Plate 5 Bulk mineralogy and texture of argillaceous sandstones	97
Plate 6 Pore space reduction by kaolinite and quartz	99
Plate 7 Morphologies of illite and smectite	101
Plate 8 Paragenetic sequence	103
Plate 9 Pore morphology	105

I. INTRODUCTION

Heavy gravity oil (33 API) occurs in the Glauconitic sandstone of the Lower Miette or Mannville Group in southeastern Alberta. This study is based largely on cores from the Suttfield Heavy Oil Pilot SHOP project. The pilot, which taps the Glauconitic Sandstone, is located north of Medicine Hat on the northwestern corner of a Special Oil Production Area within the Suttfield Military Range Field. The experimental aspect of the SHOP project is the application of in-situ wet combustion to a reservoir where the zone is underlain by water. The project consists of an inverted five-spot pattern (Fig. 2) with the production well in a singular area of the target zones. The project is operated by Alberta Energy Company with Alberta Energy Research Institute, Alberta, Imperial Oil, Canadian West Coast Petroleum and Petro-Canada as partners.

A. Purpose of this Study

The main goal of the core programme was to take advantage of the unique nature of the cores to determine the entire basin-wide distribution of intercalated shales and dolomites within the oil-bearing zone. The purpose of this study was to extend the knowledge obtained from these cores to a wider field and to develop a comprehensive understanding of the sedimentary environment, the lithofacies, principles of deposition and the characteristics of the rock properties of the area covered by the study area.

Determining the depositional environment and facies distribution is important in order to predict the types of reservoirs developed and related to the range of the environmental conditions at the time of deposition. This information is also important in order to predict the types of reservoirs developed and related to the range of the environmental conditions at the time of deposition.

From the rock material available, it is hoped to deduce the characteristics of the oil-bearing hydrocarbon reservoirs, determine the reservoir facies and to relate these to the original environment and the range of deposition. This will lead to the prediction of the future oil and gas potential of the area.

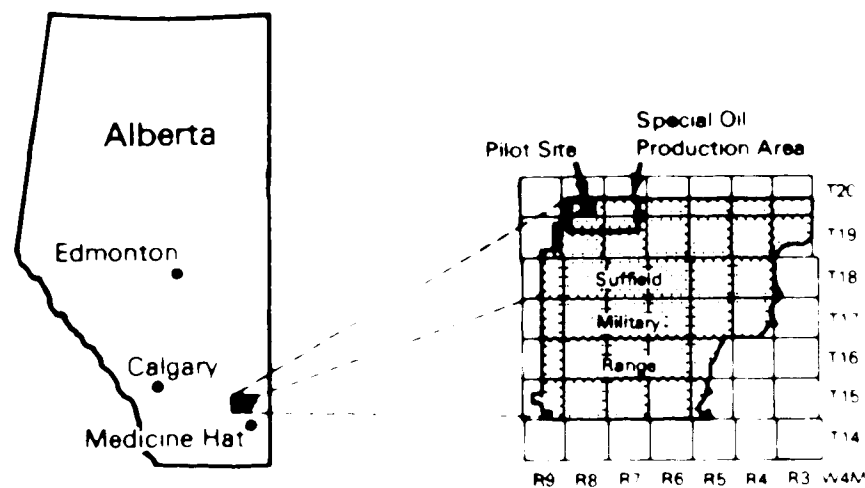


FIGURE 1 Location of the Sulfur & Heavy Oil Project

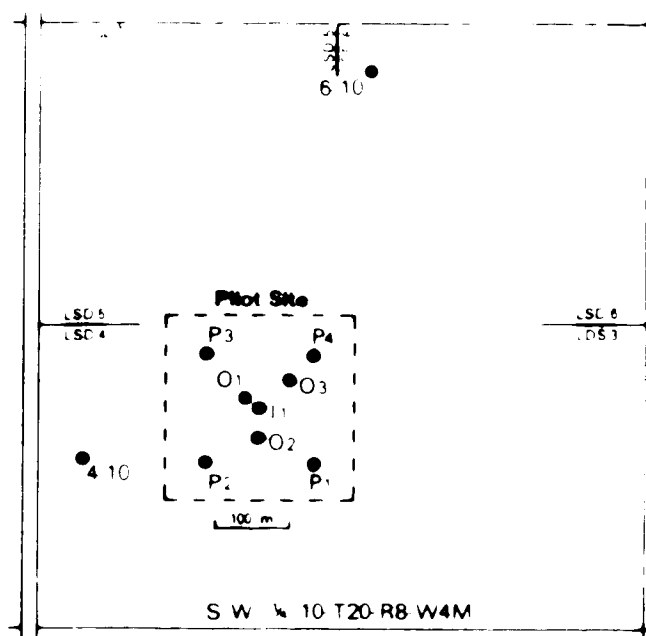


FIGURE 2 Map of the SHOF project site showing the locations of the Production Wells and observation wells.

reservoir is essential, especially where large volumes of fluids are pumped through a formation at high temperatures, as in the wet combustion recovery process.

B Geological Setting

The Glauconitic Sandstone occurs at the base of the Lower Cretaceous Upper Mannville Formation. It is underlain by calcareous sediments of the ostracode zone and overlain by a continental sequence of sand, silt, shale and coal in south and central Alberta (Fig. 3). In the SHOF project area, the Glauconitic Sandstone is 45 metres thick with an average pay thickness of 20 metres. Thick sandstone (>15m) occurs in a broad arch extending to the northwest and southeast of the pilot site, Map 1, in pocket. This belt of sandstone, which is 5 to 10 kilometres wide and a minimum of 35 kilometres long, is the focus of this study. A less extensive belt of thinned sandstone occurs four miles to the east of the major sandstone belt but was not studied in detail. The stratigraphic equivalent to the Glauconitic Sandstone to the west of the thick sandstone belt is an indistinct sequence of thin sandstone, siltstone, shale and coal and to the east the sandstone has a different character.

C History of the Term "Glauconitic Sandstone"

The Glauconitic Sand Series was first described in the Edmonton area (Tett et al. 1949), who divided the Mannville Group sediments into the Clayey Series, Glauconitic Sand Series and the Quartz Sand Series. Corringer (1951) began the division of the Glauconitic Sand Series into the Glauconitic Sandstone and the Ostracode Zone (Alberta Society of Petroleum Geologists 1961). Other workers studying the Mannville Group correlated the glauconitic sandstone over a large part of Alberta. This was correlated with the Bluesky Formation in northwest Alberta, the Wabiskaw Member of the Clearwater Formation in northeast Alberta and the upper part of the Lummeluk Member in east-central Alberta (Fig. 3; Rudkin 1964). In other areas throughout Alberta, the glauconitic Sandstone has been called the Bluesky, Wabiskaw, or dolomitic.

The ostracode zone was originally described by Corringer (1951) as a lithostratigraphic zone. Years of incorrect usage of the term "ostracode zone" has resulted in its common recognition as a lithostratigraphic unit correlative to the Calcareous Member of the southern Foothills (Rudkin 1964).

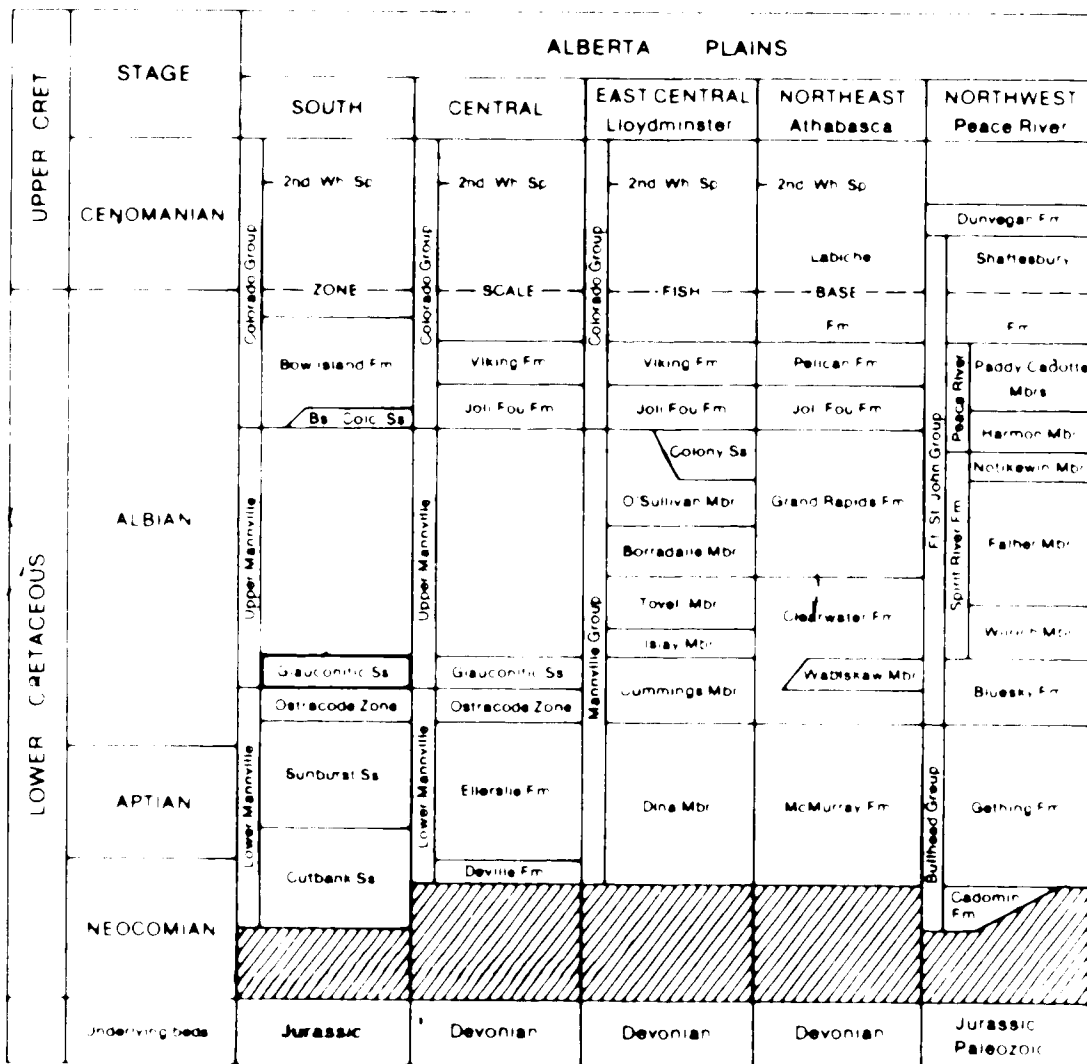


Fig. 4. Regional stratigraphic chart for the Alberta Plains showing the correlation of the various groups and formations. Modified after R. J. Campbell, 1964.

Islay and Kerkhoff

Glauconitic Sandstone is not an approved geological name for a formation. In 1959 Workman proposed the term Bluesky Formation be re-defined and extended from the Peace River region to designate the sandstone previously called the Glauconite Sandstone. He advocated an approved geological name for the Glauconitic Sandstone for the following reasons: (1) the unique stratigraphic position of the Glauconitic Sand; (2) its widespread occurrence; (3) its importance to the oil and gas industry; (4) because glauconite can not always be detected in it; and (5) there are other glauconite sands in the Blairmore. (Workman 1959). His proposal was largely ignored by later workers who perpetuated the terms Glauconitic Sandstone (Rudkin 1964; Herbaly 1974); Glauconite Sandstone (Conybeare 1976); and Glauconite Sand (Holmes and Rivard 1976). As can be seen there is no consistent title used for this sandstone.

Since the Glauconitic Sandstone in the study area contains only trace amounts of glauconite the term glauconitic is a misnomer. However the name Glauconitic Sandstone is recognized by the operators in the area and various other workers in southern Alberta. In order to avoid confusion the term Glauconitic Sandstone will be continued in this thesis.

D Previous Work

The Glauconitic Sandstone in the Suffield area of southeastern Alberta was examined briefly by Herbaly 1974 and Holmes and Rivard 1977. Herbaly 1974 described the sandstone (>100 ft thick) as an almost dune-like development cut by silt-filled channels. Holmes and Rivard 1977 studied cores from two pools in the Jennerfield Twp 20 & 21 Rge 8 W4 and interpreted the sandstone as a barrier-island deposit representing the last marine deposition of the Upper Mannville section. They also described the petrology of the sandstone.

Regional studies indicate that the percentage of glauconite in the Glauconitic Sandstone decreases east of the 5th meridian and south of Edmonton (Gairster 1959 and Conybeare 1976). The sandstone is predominantly marine in the Edmonton area and

¹Blairmore is the Mannville equivalent in the southern Foothills.

becomes more nonmarine towards the south. The thickness of the sandstone ranges from an average of 6 to 9 metres to greater than 30 metres and changes markedly over a distance of a few kilometres (Conybeare 1976 Workman 1958).

Individual field studies provide some understanding of the regional variation in depositional environment. The Glauconitic Sandstone in southernmost Alberta (Twp 1-15 Rges 16-20 W4) has been interpreted as representing floodplain and channel deposits (Herbaly 1974 and Brown 1976). Herbaly (1974) also postulated channel deposition in the Countess field area (Twp 18-20 Rges 15-17 W4). In the Little Bow area (Twp 14 & 15 Rge 20 W4) Hermanson et al. (1982) described subtidal marine bars locally cut by channels. In the Carbon field (Twp 29 Rge 22) the Glauconitic Sandstone has been interpreted as a tidal channel (Conybeare 1976).

E Methods

The eight cores from the SHOP project which form the basis of this study were examined in detail and sedimentary facies were defined. Core logs for each well are included in Appendix A. A total of 42 samples representing units of varying lithology, grain size, sedimentary structures or oil saturation within each well were analyzed for grain size properties and examined in thin section and by scanning electron microscopy (SEM) for mineralogy, texture, pore morphology and diagenesis. A survey of the clay minerals present in the < 2 micrometre size fraction of the SHOP project sandstones was obtained from X-ray diffraction analyses performed by Alberta Research Council.

In order to obtain a regional perspective on the sedimentary environment represented by the Glauconitic Sandstone and to observe any regional mineralogical variations, cores from a total of 71 wells surrounding the pilot site were also examined. Unfortunately many of these cores are only 10 to 20 metres long and include only the mid portion of the Glauconitic Sandstone. Therefore the sequence of facies could only be defined from the SHOP project cores and correlated to regional wells wherever there was sufficient core. Thirty-five samples representing 15 regional wells were examined in thin section and by SEM. A detailed clay mineralogical study involved XRD of these

samples as well as re-examination of sandstone samples from well O2 XRD procedures for these analyses are described in Appendix B

A sandstone thickness map for the Glauconitic Sandstone (Map 1) was computer-generated from a data base of 758 wells. The sand thickness for each well was determined based on the 70 per cent sand/shale line on the gamma-ray logs.

Twelve shale or silty-shale samples from below within and above the Glauconitic Sandstone were selected for palynological analysis. The samples were examined for palynomorphs and dinoflagellates by C Singh.



II FACIES ANALYSIS

A Facies Descriptions

The Glauconitic Sandstone consists of six lithological facies in ascending order; these include coarsening-upward sandstone, medium- to coarse-grained sandstone, laminated sandstone, argillaceous sandstone, carbonaceous sandstone and shale, and fine-grained sandstone, siltstone and shale. Although these facies have been defined entirely on the basis of the eight cores from the SHOF project, they are generally applicable within the regional framework. Three cores, wells 1, 2, and 3 from the SHOF project include almost the entire Glauconitic Sandstone interval, whereas cores from wells in the regional setting generally include only small portions of the interval. The most important variations within facies are described as subfacies. These subfacies apply to a phenomenon which is of limited lateral extent.

The grain mineralogy of the Glauconitic Sandstone is summarized in Table 1, showing that quartz appears approximately equal proportions to feldspar and other sedimentary rock fragments, and trace amounts of feldspar. Only minerals of clastic origin are discussed in the facies descriptions. The distribution of facies within the lithological intervals relative to geophysical logs is shown in figures 4 and 5. A summary of grain size analyses for samples representing each facies is given in Table 1. Table 2 is a summary of properties for each facies.

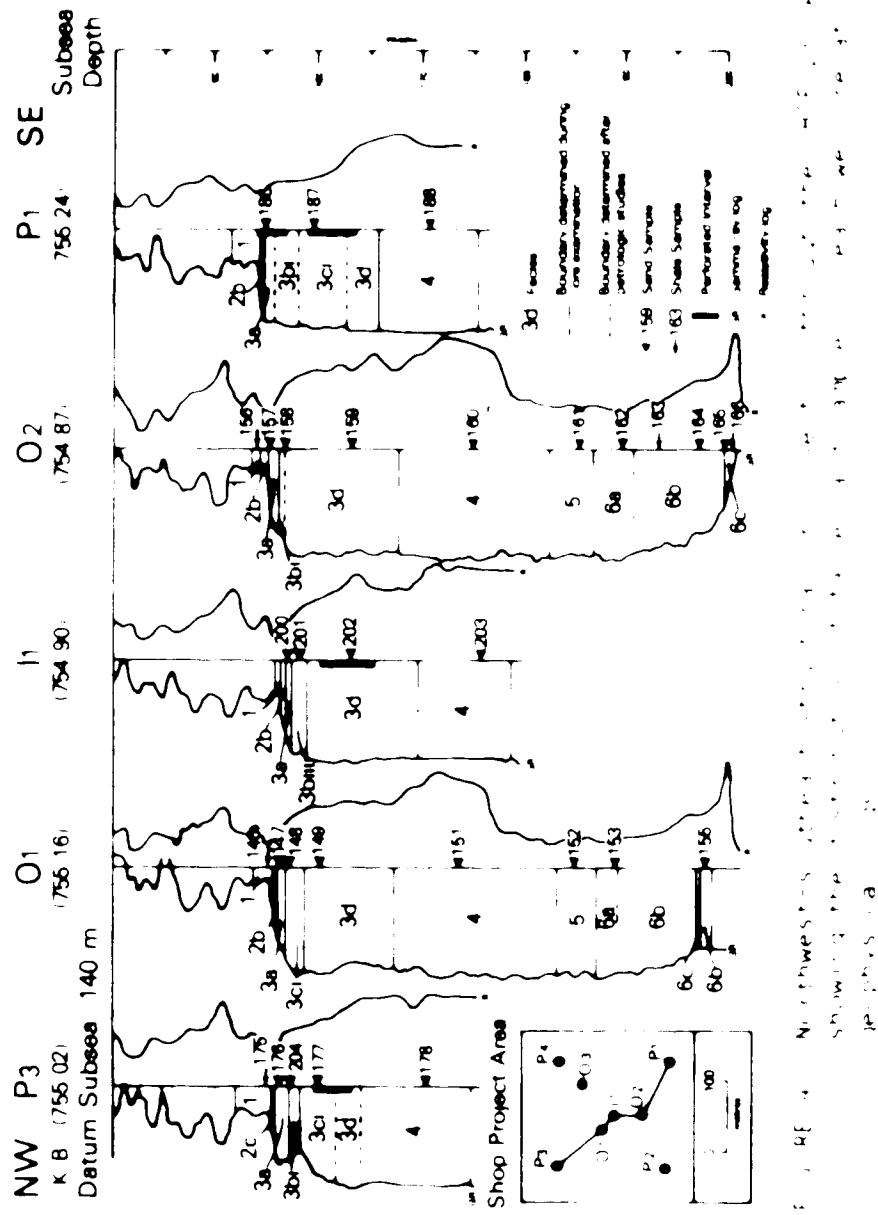
Facies 6 Coarsening-upward sandstone

Facies 6 is the lowermost unit of the Glauconitic Sandstone and is gradational above the laminated zone. It consists of a thin bed of well-laminated sandstone which gradually coarsens upward to a fine-grained sandstone. The sandstone is medium-well sorted and contains up to 15 percent clay. Subangular to subrounded grains of the total thickness for facies 6 is characterized by a light grey to light brown color. The fine-grained sandstone which has well-defined laminations (Plate 1) is carbonaceous debris commonly outlines laminations, especially in the lower portion of facies 6. Sedimentary structures include horizontal planar laminations, cross laminations, wave

^aFacies are defined on the basis of observed lithologic variations within the Glauconitic Sandstone and the descriptions include all the characteristics that make an environmental interpretation possible. See Krumbiegel and Siess, 1963, for a detailed discussion of the definition of facies.

Sample	Date	Initial Percentages Based on Number of Responses		Final Percentages Based on Number of Responses	
		Male	Female	Male	Female
3a	147	31.1	3	51.	4
3c	48	31.2	3	61.	4
3d	49	91.5	2	61.	4
4	51	92.9	2	91.	2
5	54	94.0	5	91.	2
6a	53	34.4	2	51.	2
6c	55	95.3	4	91.8	2
6e	54	45.2	4	47.	2

300.000 were included in each sample.



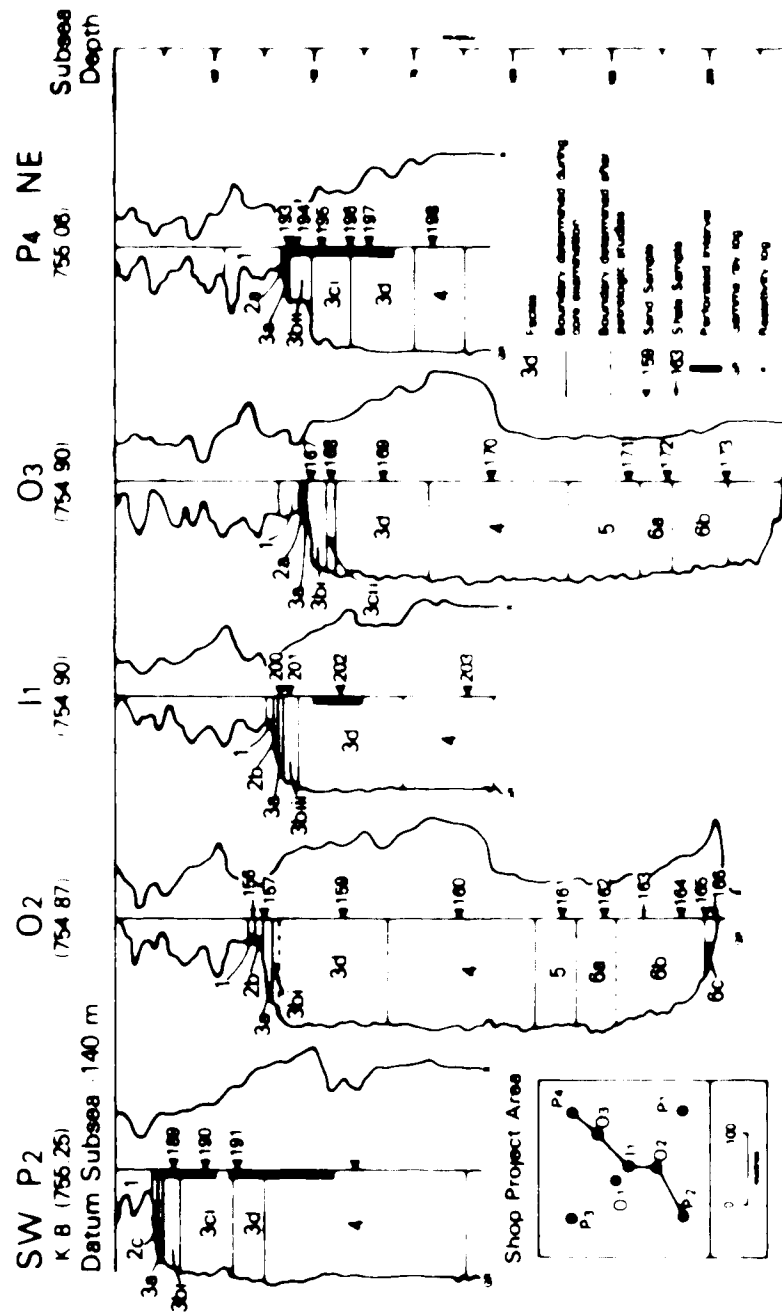


Fig. 1: Southwest - northeast seismic reflection profiles.
 Shows the locations of some of the main project areas.
 The profiles are stacked.

Table 2. Summary of Data - Stage Area 1983

Sample No.	Depth (m) ²	Composition (%)			Depth (m)	Age (yr)	Depth (m)	Depth (m)
		SiO ₂	Al ₂ O ₃	TiO ₂				
<u>ve - 0</u>								
87	30	91.1	9.18	0.70	73.00	14.70	9.74	146
88	30	91.2	9.12	0.71	81.80	6.56	9.6	146
89	30	91.5	9.15	0.72	81.28	6.79	9.94	147
90	30	92.9	9.29	0.74	86.88	5.74	2.7	147
91	30	94.0	9.40	0.78	92.00	4.28	3.83	148
92	60	94.2	9.42	0.76	94.40	4.74	9.31	148
93	60	95.1	9.51	0.77	95.20	4.08	2.6	149
<u>ve - 1</u>								
94	30	91.0	9.10	0.71	69.10	6.1	14.64	149
95	30	91.6	9.16	0.70	82.20	6.07	0.04	150
96	30	91.8	9.18	0.70	89	6.0	2.1	150
97	30	92.9	9.29	0.74	86.80	5.74	14.79	152
98	30	94.0	9.40	0.78	90.40	4.28	14.79	152
99	60	94.4	9.44	0.76	94.40	4.28	14.79	152
100	60	95.2	9.52	0.77	96.70	4.08	14.79	152
<u>ve - 12</u>								
101	30	91.4	9.14	0.70	56.50	11.9	9.55	153
102	30	91.6	9.16	0.70	56.50	9.67	9.55	153
103	30	92.1	9.21	0.72	81.20	8.88	5.62	153
104	30	91.4	9.14	0.70	87.80	9.39	3.07	154
105	30	91.6	9.16	0.70	91.80	9.39	3.07	154
106	60	95.0	9.5	0.85	95.80	8.88	6.0	154
107	60	95.6	9.56	0.81	95.80	8.88	5.50	154
<u>ve - P</u>								
86	30	91.4	9.14	0.70	58.79	12.1	9.51	155
87	30	91.5	9.15	0.70	81.50	6.8	14.81	155
88	60	92.6	9.26	0.77	86.10	5.38	14.04	156
<u>ve - P'</u>								
89	30	90.8	9.08	0.72	67.42	16.70	5.84	159
90	30	90.8	9.08	0.72	71.42	8.44	14.2	159
91	30	90.7	9.07	0.71	84.91	7.8	14.26	159
92	60	91.9	9.19	0.73	92.01	9.8	14.26	159
<u>ve - P1</u>								
76	30	91.5	9.15	0.71	62.01	16.7	21.80	168
204	30	91.2	9.12	0.70	76.26	14.5	9.59	169
205	30	91.5	9.15	0.71	75.80	16.75	7.94	169
19	60	92.6	9.26	0.77	90.27	7.58	2.15	169
<u>ve - Pn</u>								
93	30	91.3	9.13	0.71	36.51	15.36	28.1	170
94	30	91.3	9.13	0.71	66.6	17.79	15.60	170
95	30	91.6	9.16	0.71	67.64	15.38	16.79	170
96	30	91.5	9.15	0.71	77.07	13.02	9.92	170
97	30	92	9.23	0.76	84.26	7.03	6.7	170
98	60	92.7	9.27	0.76	90.16	6.99	2.84	170
<u>ve -</u>								
200	30	91.7	9.17	0.70	75.22	14.78	0.00	176
20	30	91.2	9.12	0.70	82.5	7.69	10.36	177
202	30	91.7	9.17	0.71	91.31	7.65	1.04	178
203	60	93.0	9.3	0.77	92.27	7.18	1.37	179

² Sample numbers not listed are either shale samples, carbonate cemented, or repetitions of samples already listed.

³ Depth = Log depth corresponds to depths on geophysical well logs.

Table 3 - Average Resistivities¹

<u>Facies</u>	<u>Resistivity</u>								<u>Average</u>
	<u>P1</u>	<u>P2</u>	<u>P3</u>	<u>P4</u>	<u>P5</u>	<u>P6</u>	<u>P7</u>	<u>P8</u>	
3a	10	-	-	14	18	10	-	-	11
3b	-	22	-	14	13	-	-	-	14
3c	-	-	-	-	-	-	-	-	-
3d	-	-	-	-	-	-	-	22	22
3e	22	-	-	2	20	2	21	21	21
3f	-	-	21	-	-	-	-	-	21
3g	25	25	26	2	25	27	25	26	26
4	26	27	29	28	27	27	29	27	27
5	25	25	29	-	-	-	-	-	26
6a	26	28	29	-	-	-	-	-	28
6b	23	22	27	-	-	-	-	-	24
6c	15	10	-	-	-	-	-	-	12

¹ Values from core analyses by Core Laboratory test Canada Ltd.

ripples (Plate 1), and small scour and fill structures c. 3 cm diameter. Burrows and bioturbated zones are rare in subfacies 6c, and thin shale beds occur mainly in the lower portion. Bedding thickness is commonly greater than 20 centimetres. The SHOF project cores do not penetrate the base of the facies, with Sandstone subfacies 6b c. at least 1–2 metres thick.

Subfacies b1, the sandstone cemented siltstone or very fine grained sandstone, is commonly laminated to slightly burrowed with some partially bioturbated carbonaceous shale interbeds with synheretic cracks (Plate 1). The sandstone cemented zone may represent the lowermost strata of the Sandstone subfacies 6b, which may be underlain by at least a metre of the more carbonate cemented subfacies 6b1.

Buttress facies occurs in the upper part of the facies and where a 2–3 m transition from talus to bedrock is 10–15 centimetres thick. It contains no burrowed structures, and the thin laminated facies is replaced by the massive, fine-grained subfacies b1, but finer than talus.

Facies 5. Medium-to-coarse grained sandstone

Facies 5 is found in the deltaic environment of coarse material and has the same lithology and sedimentary structures as the deltaic facies described above, except that the facies is thicker and the grain size is larger. It is also laminated to laterally discontinuous laminae, and may contain interbedded siltstone, shale and/or mudstone. The facies is characterized by the presence of large, irregular, angular blocks of talus material, up to 10 cm in diameter, scattered throughout the facies. Relative abundance of talus blocks increases downwards through the facies, and they are absent from the uppermost part of the facies.

The talus blocks are angular to subangular, and are derived from the bedrock surface. They are well sorted, angular to subangular, and are derived from the bedrock surface. They are well sorted, angular to subangular, and are derived from the bedrock surface. They are well sorted, angular to subangular, and are derived from the bedrock surface. They are well sorted, angular to subangular, and are derived from the bedrock surface. They are well sorted, angular to subangular, and are derived from the bedrock surface. They are well sorted, angular to subangular, and are derived from the bedrock surface. They are well sorted, angular to subangular, and are derived from the bedrock surface.

The talus blocks are derived from the bedrock surface, the talus blocks are derived from the bedrock surface. The talus blocks are derived from the bedrock surface, the talus blocks are derived from the bedrock surface. The talus blocks are derived from the bedrock surface, the talus blocks are derived from the bedrock surface. The talus blocks are derived from the bedrock surface, the talus blocks are derived from the bedrock surface.

Angular blocks of talus material are derived from the bedrock surface, and are derived from the bedrock surface. They are well sorted, angular to subangular, and are derived from the bedrock surface.

gradational contact. Coarser interbeds gradually becoming less abundant upwards.

Facies 4. Laminated sandstone

Facies 4 occurs structurally relatively clear ($>4\%$ fine clay content). The grained sandstone which is characteristically massive has horizontal planar laminations and low-angle cross-lamination. Facies 4 is benthic. The sandstone is well sorted with an enrichment of dark-coloured siltstones defining the laminations rather than significant grain-size variation. No shale laminations in bed are present. Higher angled laminations in disturbed beds and disturbed laminations are mainly due to current structures in beds and bedding planes. Disturbed laminations in facies 4 are mostly due to penetration by burrows and burrow casts. Horizontal planar laminations are mainly due to the presence of a tidal meter or at least a meter of thickness.

The laminated facies is the most common facies in the study area and is found in the following environments: back-barrier, embayment, coastal plain, deltaic, coastal, and coastal.

Facies 3. Argillaceous sandstone

Facies 3 is represented by a dark greyish-green sandstone. It is well sorted and contains abundant tabular interbeds of the facies 3. The sandstone has an enrichment of fine-grained material. The facies 3 is often found in tidal flats, back-barrier areas, and the top of the coastal plain. The facies 3 is also found in the deltaic environment. The facies 3 is represented by a dark greyish-green sandstone.

The facies 3 is represented by a dark greyish-green sandstone. It is well sorted and contains abundant tabular interbeds of the facies 3. The sandstone has an enrichment of fine-grained material. The facies 3 is often found in tidal flats, back-barrier areas, and the top of the coastal plain. The facies 3 is also found in the deltaic environment. The facies 3 is represented by a dark greyish-green sandstone. It is well sorted and contains abundant tabular interbeds of the facies 3. The sandstone has an enrichment of fine-grained material. The facies 3 is often found in tidal flats, back-barrier areas, and the top of the coastal plain. The facies 3 is also found in the deltaic environment. The facies 3 is represented by a dark greyish-green sandstone. It is well sorted and contains abundant tabular interbeds of the facies 3. The sandstone has an enrichment of fine-grained material. The facies 3 is often found in tidal flats, back-barrier areas, and the top of the coastal plain. The facies 3 is also found in the deltaic environment.

The facies 3 is represented by a dark greyish-green sandstone. It is well sorted and contains abundant tabular interbeds of the facies 3. The sandstone has an enrichment of fine-grained material. The facies 3 is often found in tidal flats, back-barrier areas, and the top of the coastal plain. The facies 3 is also found in the deltaic environment.

subfacies 3d and limits reservoir potential. Clay content varies from 1 to 6 percent in the samples analyzed from this subfacies. Angular, randomly oriented breccia blocks (Plate 1) found in a 1.6-metre thick interval in well C2 are laminated. The matrix of the breccia is a slightly coarser clay-rich sandstone.

Subfacies 3e gradationally overlies subfacies 3d and represents the uppermost mollusc-rich bedding or laminations within the Glauconitic Sandstone, excluding facies 3f. It differs from subfacies 3d in being more angular clasts of clay and in lacking any regular bedding. The units vary from 1.8 metres thick to less than 1.5 metres thick. The clasts are quite variable within a particular wavelength. In the sandstone may be the turbated structures of heterotypically bedded Plate 2. Magnetite grains are concentrated along sigmoidal laminae in the sandstone (Fig. 1). The greenish grey fine sandstone in these areas has been distinguished as facies 3f.

The sandstone at Plate 2 is equivalent to subfacies 3e, but it is more massive and contains no distinct mollusc-bearing laminae. The magnetite-rich laminae are thin and dark brown and in this area have been distinguished as facies 3g.

THE sandstone at Plate 3 is equivalent to subfacies 3d, but it is more massive and contains no distinct mollusc-bearing laminae. The magnetite-rich laminae are thin and dark brown and in this area have been distinguished as facies 3h.

At Plate 4 the sandstone is equivalent to subfacies 3e, but it is more massive and lacks any distinct mollusc-bearing laminae. The magnetite-rich laminae are thin and dark brown and in this area have been distinguished as facies 3i. The differences between the sandstones at Plate 2 and Plate 4 are that the sandstone at Plate 2 contains more magnetite-rich laminae and that the sandstone at Plate 4 contains more dolomite-rich laminae. The dolomite-rich laminae are thin and light grey, and the magnetite-rich laminae are thin and dark brown. The magnetite-rich laminae are thin and dark brown and in this area have been distinguished as facies 3j.

At Plate 5 the sandstone is equivalent to subfacies 3e, but it is more massive and lacks any distinct mollusc-bearing laminae. The magnetite-rich laminae are thin and dark brown and in this area have been distinguished as facies 3k. The dolomite-rich laminae are thin and light grey, and the magnetite-rich laminae are thin and dark brown. The magnetite-rich laminae are thin and dark brown and in this area have been distinguished as facies 3l.

Petrologically and texturally subfacies 3bi is distinctive from the other facies. The thin section photograph on Plate 3-2 demonstrates the preferential horizontal fabric resulting from compaction flattening of soft rock fragments and the orientation of elongate chert grains. Feldspars (K-feldspar and plagioclase) are more abundant than in other facies. Also illite content is 5 percent, an abnormally high percentage for a zone with such low porosity. Average porosity from core analyses is 11 percent, an average lower than other facies.

Facies 3bi also occurs in the same stratigraphic position as subfacies 3b, but is distinguished from both 3b and 3bi by its w-w angle planar laminations defined by coarse sand-sized magnetite grains (Plate 2-4). It is present only in well 1 and is 1.5 metres thick. The sandstone is light grey, fine grained and clay-rich, with clay-out, but mostly relatively light (2.2). The lower boundary of the unit is gradational and poorly defined. The uppermost few centimetres of the unit are bioturbated and reworked and therefore lack a sharp contact with the overlying angularous sandstone. Facies 3b and 3bi are most clearly seen in sandstone facies 3c, which occurs at the top of the 3b facies. Sandstone in the 3b facies is well sorted, typically a medium grey, and thin, very angular, lens-like graded sandstone with scattered, larger, chert grains and carbonaceous laminae (Plate 2-5). The sandstone is structureless, or bioturbated. The high standard deviation of grain size (cf. 3.8% Table 2) indicates the very poor sorting. The contrast in the median grain size of the graded sandstone and the mean diameter of sized particles vary considerably between 1 and 83 cm, reflecting the fact that the latter decreases with increasing thickness (metre scale) to 10 cm (metre scale).

Facies 2 Carbonaceous sandstone and shale

The facies is subdivided into two distinct facies, the carbonaceous sandstone and the dark grey shale. The sandstone facies is characterized by a high content of bentonite and illite, and contains scattered, angular, dark grey, angular, carbonaceous laminae. In these, the angular dolomitic and doleritic, and about 10 mm, angular dolomitic lenses are common, indicating the sandstone unit has been subjected to some degree of weathering.

bioturbated. The transition from facies 3 to 2 is generally quite abrupt with an irregular boundary marked by a colour change from medium or light grey facies 3 to dark grey facies 2. Plate 2-6. Carbonaceous material in the underlying facies 3a is commonly most abundant near this boundary.

Facies-1. Very fine grained sandstone, siltstone, and shale

A maximum of 6 metres of rock above facies 2 is represented in the SHOF project cores and is described here as 'lowermost facies'. Overlies facies 2 gradually and consists of structureless or laminated medium grey shale with light grey silt interlaminations. Plate 2-7. Very small burrows and ripples < 1 mm. are present locally in the shale and carbonaceous chips are common. Silt interbeds and lenses gradually become more abundant upwards such that interbeds of shale and interlaminated silt and shale alternate on a one or two metre scale. Sedimentary structures (Plate 2-8) include ripples, planar laminations, burrows, matting, truncated burrows, contorted laminations, structureless beds, and rare rootlets. Fyrite is common, it has nodules averaging 1 centimetre in diameter and may contain thin laminations. The uppermost metre or so is composed of fine-grained carbonate cemented very fine grained sandstone. Lenticular ripples are defined by light-coloured debris. Microfauna and carbonaceous bioturbated shale interbeds are also present. This sandstone lies with a sharp flat contact on the underlying thick (> 1.5 m) shale bed.

Regional Facies Descriptions

Although the facies descriptions in the preceding section are based entirely on cores from the SHOF project cores, they can be adapted slightly to apply to a more regional scale. The characteristics of facies 1 in a regional scale are consistent with those described in the SHOF project, though never taken together. Considerably thicker, generally fine-grained sandstone interbedded with the coarser sandstone described in the SHOF project may consist of pebbles (e.g. Fig. 2-11A). Thick, graded sandstone, i.e. medium grained sandstone with tabular, or sigmoidal, cross-bedding (Fig. 2-11B) may consist of medium to coarse grained sandstone. In fact, rather than the graded sandstone being away from single planar laminated fine sandstone, tabular may be angular as both are generally tabular. The grain size of the sedimentary structures in the coarsest interbedded

structureless with only isolated laminated zones. A carbonaceous equivalent of facies 2 and a shale-siltstone sequence of facies 1 are represented in most wells.

B Facies Interpretation

The criteria suggesting the deposition of the Glauconitic Sandstone in the SHOP project area in a prograding shoreline and nearshore environment are abundant. Palynological analysis of shales from immediately below the Glauconitic Sandstone indicate restricted marine depositional conditions (See section on Palynological Results). 2. The contact of the Glauconitic Sandstone with the ostracode zone is gradational with the lower portion of the Glauconitic Sandstone coarsening upwards from silt or very fine grained sandstone. 3. The zones present on a modern day beach (shoreface, foreshore, backshore) are all represented in the Glauconitic Sandstone (Fig. 6) and 4. The uppermost part of the sandstone contains carbonaceous root markings and coal and is overlain by a energy shales and siltstones of probable back-barrier origin.

Well-documented studies of modern barrier-island systems have resulted in a relatively good understanding of sedimentary structures and other features of sediments in beach environments. Several review papers (e.g. Flint 1978; Reinson 1981; and McCubbin 1982) have both summarized the characteristics of barrier and strandplain sandstone facies which have been recognized in modern environments and described several ancient analogues. The most intensively studied modern barrier-island environments are the East Coast and Gulf Coast examples in the United States described by LeBlanc and Madsen 1959; Shepard 1961; Bernard, LeBlanc and Madsen 1962; 1964; and Weimer 1963; and Kraft 1977. Other well-known studies of modern shorelines include those by Hayes and Kara 1976 and Curran and Moore 1964. The latter work interpretation of beach facies represented in the Glauconitic Sandstone is based on a comparison with facies from various barrier-island settings as described mainly in the review papers. A summary of the characteristics of each facies of the beach and strandplain facies described in the previous section is given in Table 4 and Figure 6.

Facies 6

Facies 6 represents the lower-middle shoreface zone. The very fine grained sandstone and thin shale interbeds of the strandplain were deposited in the lower

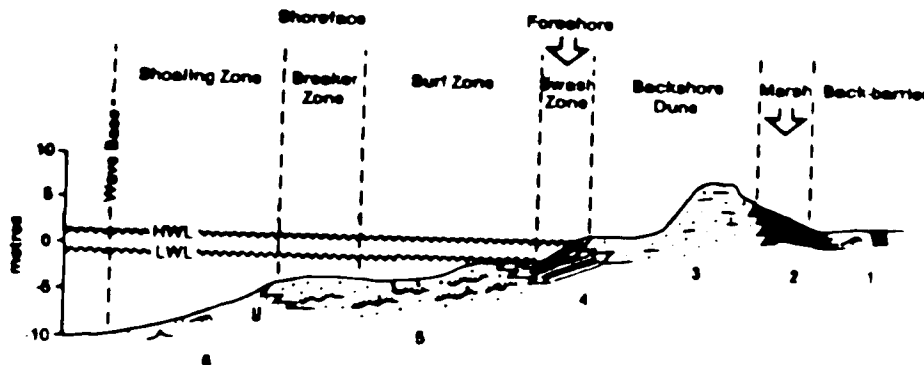


Fig. RE-6a. Generalized profile of a barrier-beach environment showing the spatial relationships of the sedimentary facies and their positions on the shore. (Shore profile modified from Reinson, 1980).

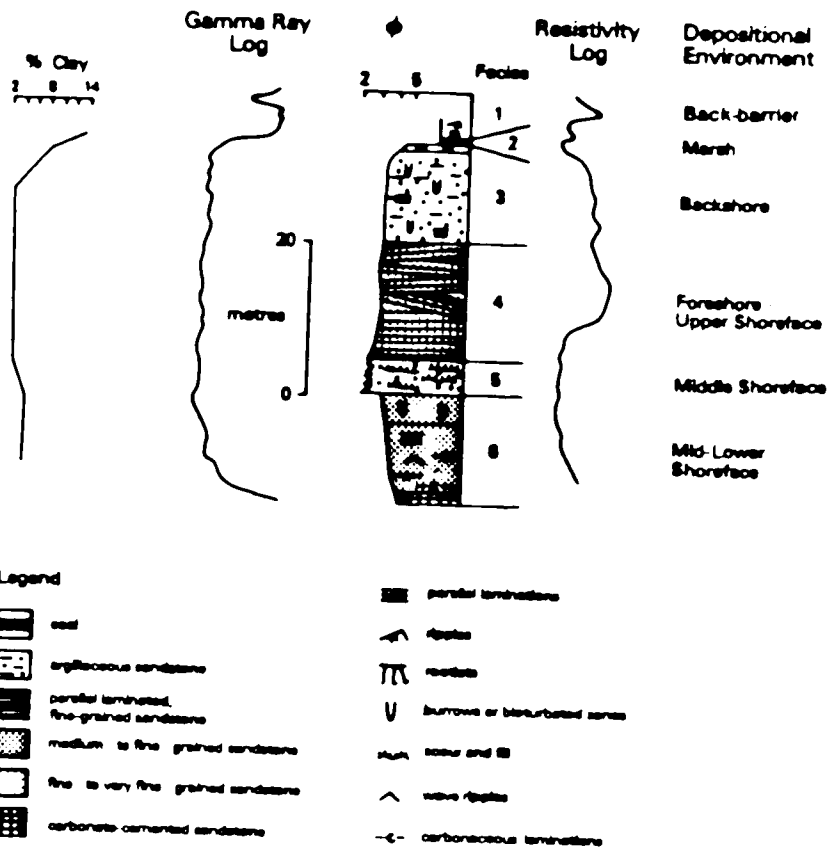


Fig. RE-6b. Generalized litholog from SHOP project core showing the vertical sequence of facies, grain size, per cent clay, geophysical log shapes and the facies interpretations.

POOR COPY
COPIE DE QUALITEE INFERIEURE

Table 4. Summary of Factors Describing Tasks

FINE PRINT

shoreface. In his review paper, Reinson (1980) described the lower shoreface as a relatively low energy transitional zone, where waves begin to affect the bottom, but where offshore shelf or basinal depositional processes also occur. The coarsening upwards to fine-grained sandstone represents the transition into the middle shoreface. The low-angle cross-laminations, horizontal planar laminations, wave ripples (Plate 1) and scour and fill structures were produced by shoaling and breaking waves in this zone. The predominance of primary sedimentary structures in the shoreface zone of the sandstone bands is in contrast with the bi-turbated shoreface zones described by Bernard et al. (1962). In contrast to sandstone preservation of primary structure indicates a high wave energy setting where biogenic structures are not developed (wave action preserving potential; Botha 1990).

The last element of subfacies 5 probably came at the end of the wave-dominated phase, the end of the band of after-breaker sandstone, at the start of the breaker zone. The right-hand side generally structures reflect a turbulent zone (Plate 1), representing a part of the middle shoreface with high energy, and little time for maturing and sorting of sand.

Facies 5

The last element of subfacies 5 probably came at the end of the wave-dominated phase, the breaker zone of the middle shoreface (Hammer et al. 1971; Galloway 1976). The absence of sandstone in the lower shoreface (Fig. 1) and sandstone in the upper shoreface (Fig. 2) suggests that the lower shoreface was dominated by rippled, upward-sandstone bands, the upper shoreface by tabular, laminated sandstone. In the freshwater zone there is the same variation in facies, but that facies was deposited in the breaker zone.

Flebble beds (Fig. 1) are the products of the wave-dominated phase, indicating a shallow, wave-based, and tidal system. These features suggest the presence of a coastal marshland deposit, probably close to a wave-related embayment.

Facies 4

The first three subfacies (subfacies 1, 2 and 3) are all derived from the same facies, which is the lower shoreface of the wave-dominated phase (Fig. 1). Hammer (1962), Botha (1974) and Moll (1976) described the lower shoreface as the wave-breaking and the general lack of sedimentation in the area, implying

conditions of deposition such as occur in the wave zone. The ~~swash~~ backwash mechanism is mainly responsible for the subhorizontal to ~~cw angle~~ planar laminations.

Facies 3

The depositional setting of facies 3 is the backshore zone of a beach. Subfacies 3C represents the transition from the foreshore to backshore zone. Backshore energy conditions in coastal areas have allowed significant bioturbation. The laminated fine-grained clavate (Plate 1) are probably capsize products of the banks of a small tidal creek. Downstream decrease in wave energy will take effect as current velocity decreases, resulting in a decrease in bioturbation.

After 1978, described below, a backwash-laminated sand facies (backwash-laminated facies) was deposited in a beach area. This facies is characterized by a tendency to contain angular and abundant heavy minerals, probably very similar to facies 3C. The backwash-laminated facies. The backwash-laminated facies is the coarsest sand facies, containing gradational contacts with the laminated sand facies, and it is characterized by angular grains, sand-size and an upward decrease in heavy mineral content. This facies is commonly in the backwash bar at the seaward margin of the beach. It is also found in the intertidal area and in areas where backwash is dominant, and it is absent in the beach face margin. The angular heavy mineral represented in facies 3C may be a different share than that of the facies after interpretation of a wave-tale, and therefore, were unable to deposit. The laminated sand facies is the most common facies in the beach margin, and it is heavily represented in the backwash-laminated facies. The difference between the end of the facies after interpretation of a wave-tale and facies 3C is the absence of angular heavy minerals in the backwash-laminated facies. The angular heavy mineral is slightly different in that it is very heavy, probably composed of magnetite.

Table 10 illustrates the presence of angular heavy mineral in the backwash-laminated facies. The remaining data differ in suggesting that angular heavy mineral is present in the facies after interpretation of a wave-tale, and it is absent in the facies.

The angular heavy mineral data of facies 3C suggest that the angular heavy mineral is highly dispersed, and the data of facies 3C suggest a low concentration of angular heavy mineral. The result after wave-tale generation of angular heavy mineral in the backwash-laminated facies is unclear, because it is absent in the facies after interpretation of a wave-tale.

The deposits are generally thin, ranging from a few centimeters to two metres for each washover event facies. Some 1.5 metres thick, perhaps representing one washover event. The perturbation and ripples at the top suggest the development of vegetation on a sand flat.

Energy of the backshore environment fluctuates between calm during calm periods and high during storm. Vegetated zones - up to one metre in the area where the area does not contain water - are the variable primary productivity areas. High energy areas, turbulent, sandy, rippled, are variable productivity areas due to the variability of vegetation and methods of the backshore environment.

Facies 2

The antidiagonal materials of facies 2 represent a marine environment. The antidiagonal materials are materials that the land has been washed off by the tide. Individually different, but similar in that they contain sand, silt, and organic material. The sediments are fine textured and are derived from the land. (See Fig. 10)

Facies 3

Facies 3 is the backshore. Backshore environments are characterized by low energy and low sedimentation rates. At certain times, the backshore is dominated by sand, at other times it is dominated by silt. Depositional environments are dependent on the time of the year. The seasonal differences in the backshore facies are due to the amount of wind and wave energy. Odd that the antidiagonal elements are the dominant sand facies, but have been washed away. Perhaps this is formed a sand flat before the change. The antidiagonal elements are also associated with some marine influence.

Summary

The data of the washover deposit in the study area indicate that there is a gradual transition from land to sea environments. The backshore facies is characterized by a low energy environment. The main difference between the land and the backshore is the amount of energy and the amount of the material. The materials in the backshore are mainly sand, silt, and organic material. The backshore materials are derived from the land. Most of the materials are derived from the land. A possible explanation is that the land and the sea are interconnected.

III. PALYNOLGY

Palynological results provide additional support for an environmental interpretation based on sedimentary structures and lithology. Shale and silty shale samples from below, above and within the mudstone bandstone are regionally spaced wells were examined for polymorphs and dinoflagellates. The distribution of samples within each well indicated two distinct environments (dotted and the geographic position of wells is shown in Figure 1).

Samples containing dinoflagellates represent deposition in a marine environment at the base of the overlying sandstone facies. The dinoflagellate assemblage (Table 4) includes *G. hirsutus*, *H. gracilis* and *P. sinense*. In these samples, species diversity is extremely low, consistent with higher Marine Index values at the base of the mudstone bandstone. Marine Index values are consistently higher in the overlying sandstone, indicating higher diversity. It is likely that the environment at the base of the mudstone bandstone was deposited in a very restricted marine environment, possibly a lagoon or a small embayment.

All other samples examined contain dinoflagellates in the mudstone facies, although some samples contain dinoflagellates in the sandstone facies. These include *G. hirsutus* and medospores. Whereas there are incomplete dinoflagellate samples at the bottom of the upper part of the mudstone bandstone, complete samples are found in the sandstone facies. In addition, dinoflagellates are present in all samples. The presence of dinoflagellates suggests they are distributed throughout the sample. At the top of the mudstone bandstone, evidence of a marine environment is indicated by the presence of dinoflagellates in the sandstone facies. A dinoflagellate assemblage similar to that found in the mudstone bandstone is present in the sandstone facies. This indicates that dinoflagellates are present in the marine environment throughout the mudstone bandstone.

The dinoflagellate data indicate that the mudstone bandstone is deposited in a relatively dry environment. An indication of the dry environment is the absence of dinoflagellates in the sandstone facies. In other words, if

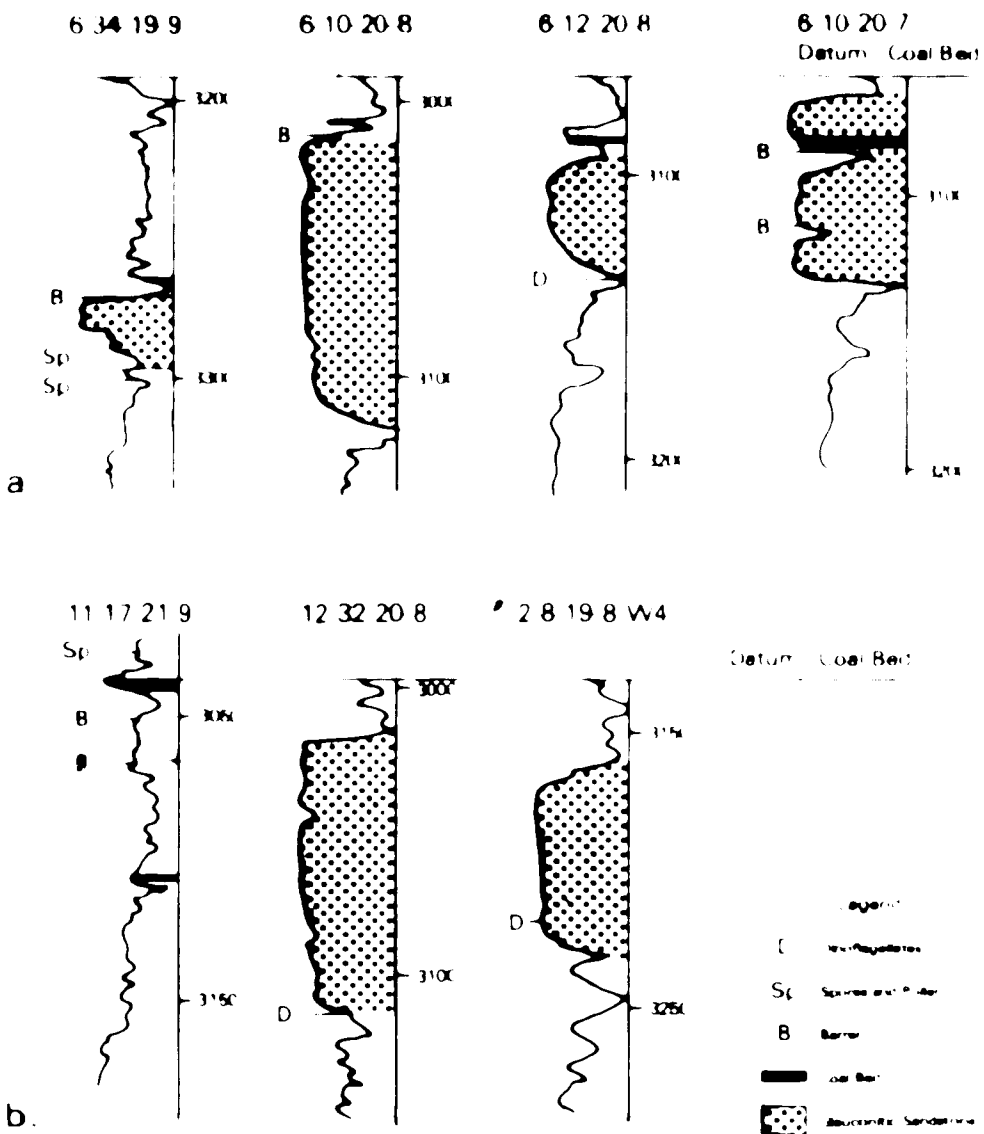
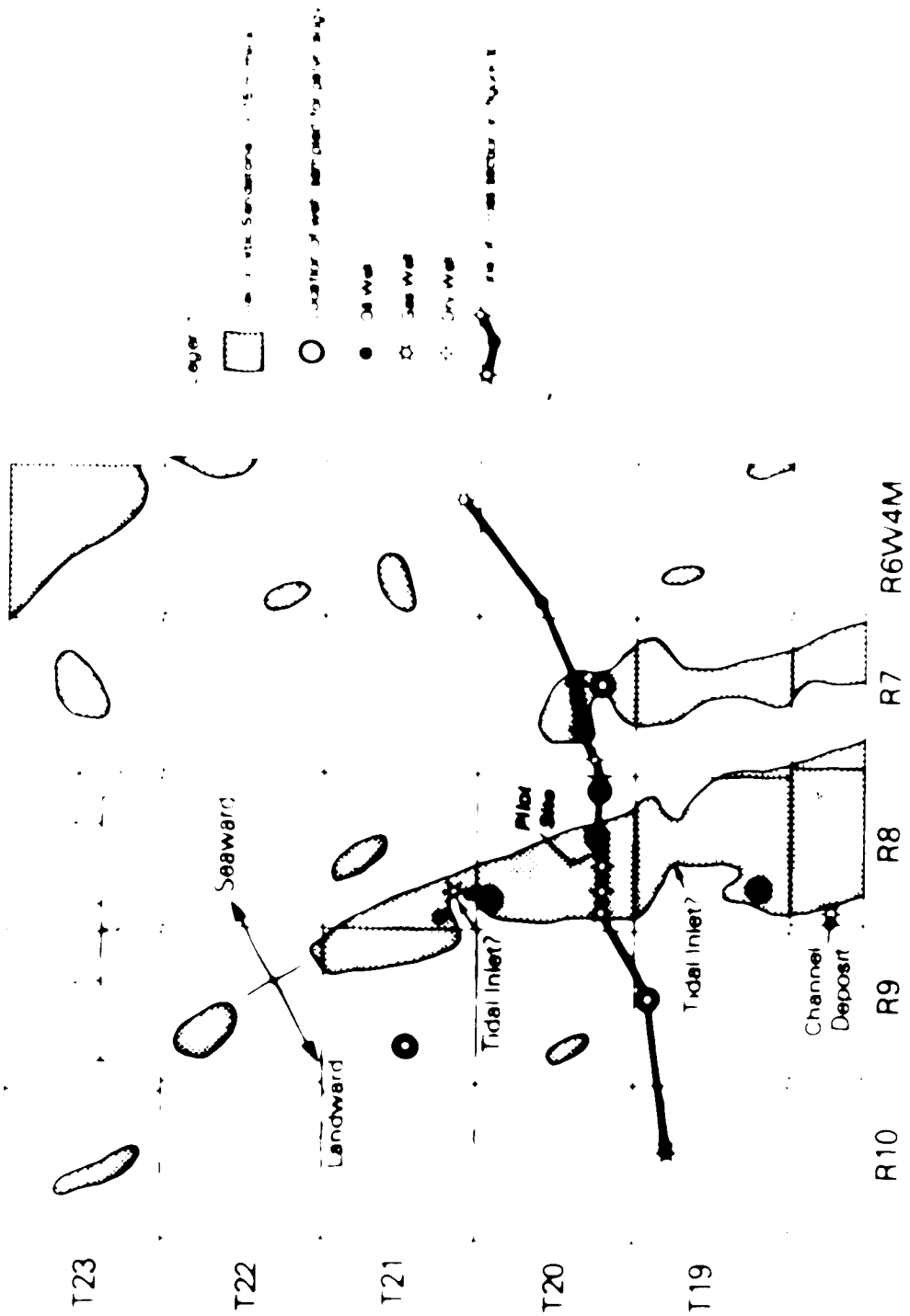


FIG. 6. - Stratigraphic columns showing thicknesses of the various facies. The thicknesses are based on the seismic sections shown in Figures 4 and 5. The thicknesses are approximate and were determined by extrapolating the thicknesses measured at the datum coal bed to the top of the section. The thicknesses were taken from the seismic sections shown in Figures 4 and 5.



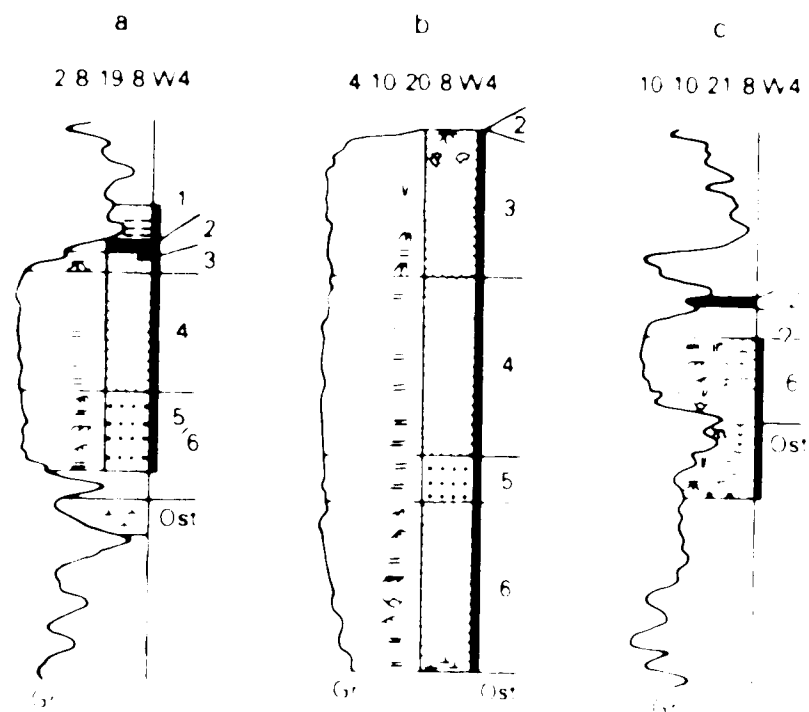
e - a prograding beach complex with restricted marine sediments at the base of the Glauconitic Sandstone to continental sediments at the top.

IV REGIONAL DEPOSITIONAL SETTING

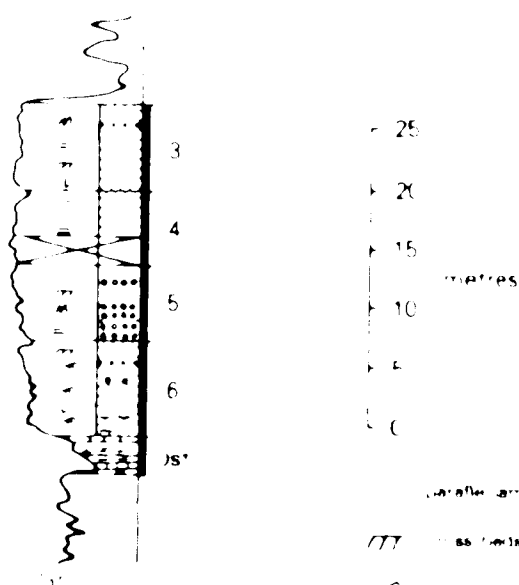
Major lithologies are mostly determined based on the lithology map of the area and the following table summarizes the major lithology and their distribution in the area. In general, the lithology is determined based on the major material found in the sample, although the minor material may also be present in the sample. For example, the shale matrix may contain some sandstone or siltstone. The evidence of the presence of the latter is represented by the sandstone/siltstone in the shale matrix. It can be suggested that the major lithology is determined by the major material and the minor material is not important in determining the major lithology.

The major lithology is divided into four categories: clastic, carbonaceous, organic-rich, and the others. The first three categories are determined based on the major material found in the sample. The last category is determined based on the minor material found in the sample. For example, the shale matrix may contain some sandstone or siltstone. The evidence of the presence of the latter is represented by the sandstone/siltstone in the shale matrix. It can be suggested that the major lithology is determined by the major material and the minor material is not important in determining the major lithology.

The major lithology is divided into four categories: clastic, carbonaceous, organic-rich, and the others. The first three categories are determined based on the major material found in the sample. The last category is determined based on the minor material found in the sample. For example, the shale matrix may contain some sandstone or siltstone. The evidence of the presence of the latter is represented by the sandstone/siltstone in the shale matrix. It can be suggested that the major lithology is determined by the major material and the minor material is not important in determining the major lithology.



1 32 29 8 W4



LEGEND

[diagonal lines]	Highly laminated
[diagonal lines with dots]	Dense, fine-grained grained sandstone
[horizontal lines]	Fine-grained sandstone
[diagonal lines with dots]	Medium-grained sandstone
[triangles]	Angular arenous shale
[triangles with dots]	Angular arenous dolomite
[solid black]	Shale
[solid black]	0.0
Lithological abbreviations	
[diagonal lines]	Lam.
[diagonal lines with dots]	Sand.
[triangles]	Aren.
[triangles with dots]	Aren. dol.
[solid black]	Sh.
[solid black]	0.0

Fig. 10. Stratigraphic columns for wells 2 8 19 8 W4, 4 10 20 8 W4, 10 10 21 8 W4, and 1 32 29 8 W4. The numbers 1, 2, 3, 4, 5, 6 refer to the numbered horizons shown in Fig. 9.

the base of the dolomitic limestone, which is overlain by a thin dolomitic shale.

The dolomitic limestone is overlain by a thin dolomitic shale, which is overlain by a thin dolomitic limestone.

The dolomitic limestone is overlain by a thin dolomitic shale, which is overlain by a thin dolomitic limestone.

Figure 1. The eastern section of the Glauconitic Sandstone extending perpendicular to the sandstone belt (Fig. 8). To the west of the sandstone belt, the Glauconitic Sandstone is replaced by an interbedded sequence of thin sandstone interbeds, shales and sandstones. In the far east the Glauconitic Sandstone has its distinctive character.

Opposite to talus in the three sandstones in the western side of the sandstone belt, talus in the thick sandstone between the shale, which is talus, has been preferentially thickened at the expense of the thin thick sandstone, representing areas where the surface was stable with abundant talus sedimentation and talus denudation. This vertical variation of talus is more intense than the lateral variation of talus thickness and is seen in the eastern talus setting. The talus thickness decreases from the thick sandstone and thick talus to the thin sandstone and thin talus. In the western talus setting, the talus thickness is constant at about 10 cm, but in the eastern talus setting the talus thickness is variable, ranging from 10 to 50 cm. The talus thickness is correlated with the thickness of the sandstone, and the greater the sandstone thickness the greater the talus thickness. The talus thickness is also correlated with the degree of weathering, and the greater the degree of weathering the greater the talus thickness. The talus thickness is also correlated with the degree of glaciogenesis, and the greater the degree of glaciogenesis the greater the talus thickness. The talus thickness is also correlated with the degree of permafrost, and the greater the degree of permafrost the greater the talus thickness. The talus thickness is also correlated with the degree of desertification, and the greater the degree of desertification the greater the talus thickness. The talus thickness is also correlated with the degree of aridification, and the greater the degree of aridification the greater the talus thickness. The talus thickness is also correlated with the degree of desertification, and the greater the degree of desertification the greater the talus thickness.

The talus thickness is also correlated with the degree of desertification, and the greater the degree of desertification the greater the talus thickness. The talus thickness is also correlated with the degree of desertification, and the greater the degree of desertification the greater the talus thickness. The talus thickness is also correlated with the degree of desertification, and the greater the degree of desertification the greater the talus thickness.

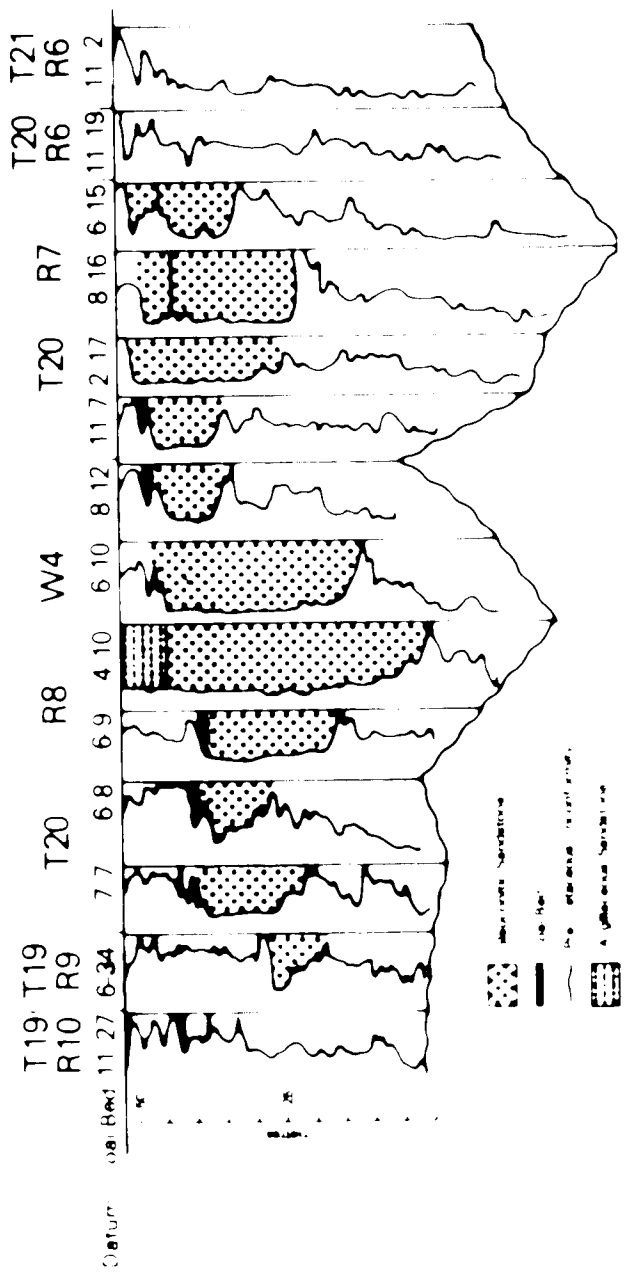
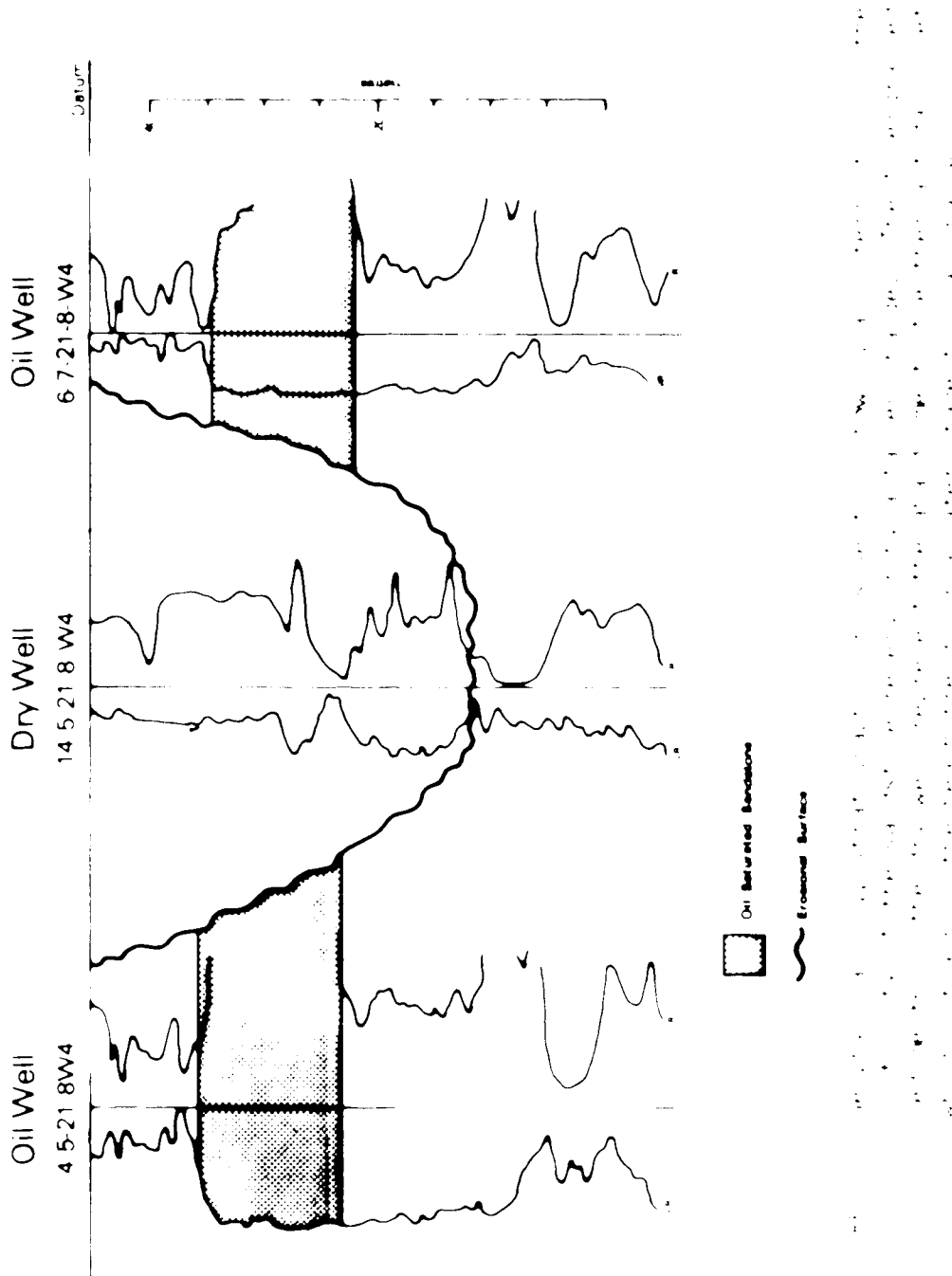


Fig. 1. Geologic cross-section showing locations where the detector was tested. The cross-section shows the detector was not detectable in the 11-27-6-34, 10-W4 and 11-20-21-22, due to adjacent weathered zones. In the 11-20-21-22, we can see the detector was detectable across the entire section. However, in the 11-27-6-34, the detector was not detectable in the upper portion of the section.

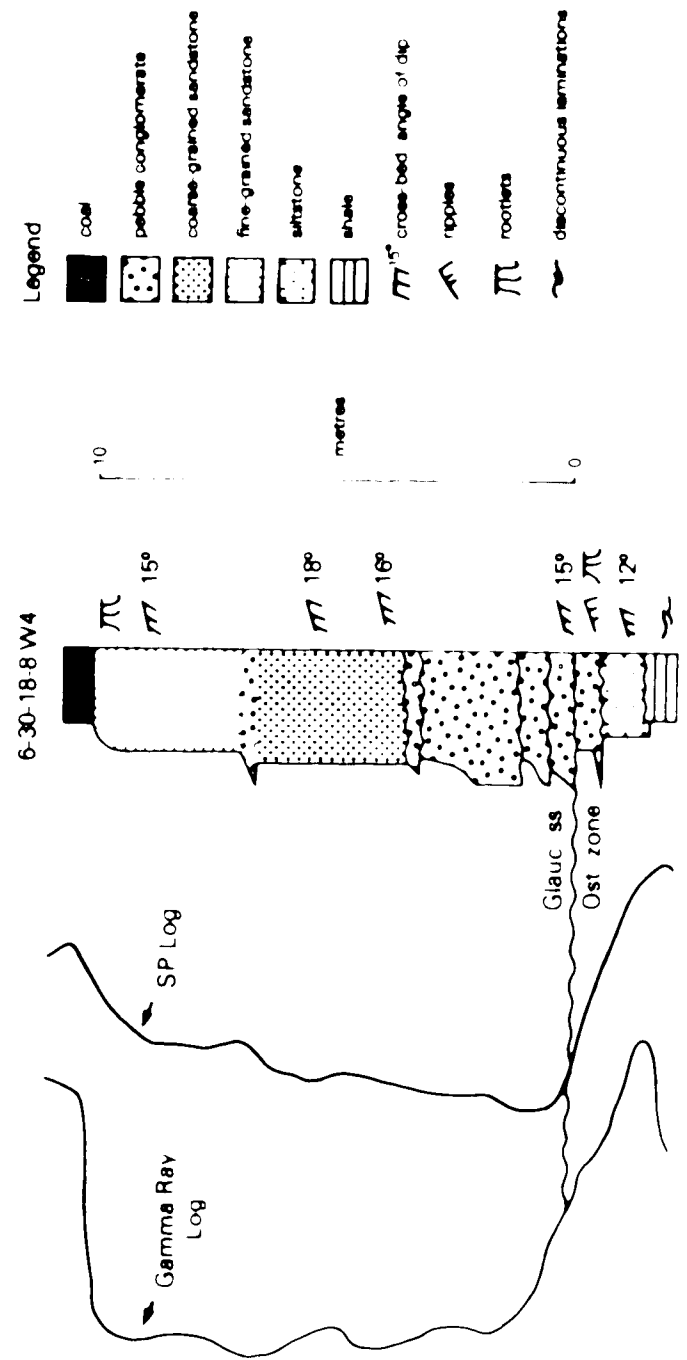


dry whereas wells immediately to the north and south (4, 5, 21, 8 W4 and 6, 7, 21, 8 W4; Fig. 11) have the typical Glauconitic Sandstone beach facies and are oil producers. The silty sandstone of the dry well represents a facies change from the beach facies in the surrounding wells and probably is the fill of an abandoned portion of a tidal inlet or the abandonment of a later stage fluvial channel. Similar abandoned portions of tidal inlets are described by Tye (1978) in South Carolina.

A 10-metre-thick channel sandstone occurs at the 30-18-8 W4 (Fig. 12). The base of the sandstone is erosional into the underlying calcareous silt shale and sand of the stratocade zone. The lower portion of the sandstone unit consists of a series of thinning upward cycles with erosional bases, from cobbles and pebbles through intercalates to coarse grained sandstone. In the upper portion of the unit, the sandstone has fined upwards to fine grained sandstone and is topped by a horstled surface of thin laminae. Tipping at about 15 degrees are the dominant sedimentary structures.

Other wells probably penetrate tidal inlet or channel deposits, but unfortunately they rarely include the base of the Glauconitic Sandstone. The difficulty in identifying channel versus beach deposits is based in geophysical and character differences indicated by the tools. The gamma ray log indicates a high gamma ray reading associated with anerobic bacterial activity suggesting a beach deposit, whereas the resistivity log indicates a low reading between two wells suggesting a channel deposit in the same depth interval.

In summary, the depositional setting can be inferred from the tidal channel sandstone marker and the seaward direction of the east. The thick sandstone marker is not expected to extend to the south of the 21-18-8 W4, although it may be the result of the presence of a buried tidal inlet or the absence of a channel to the west of the marker sandstone.



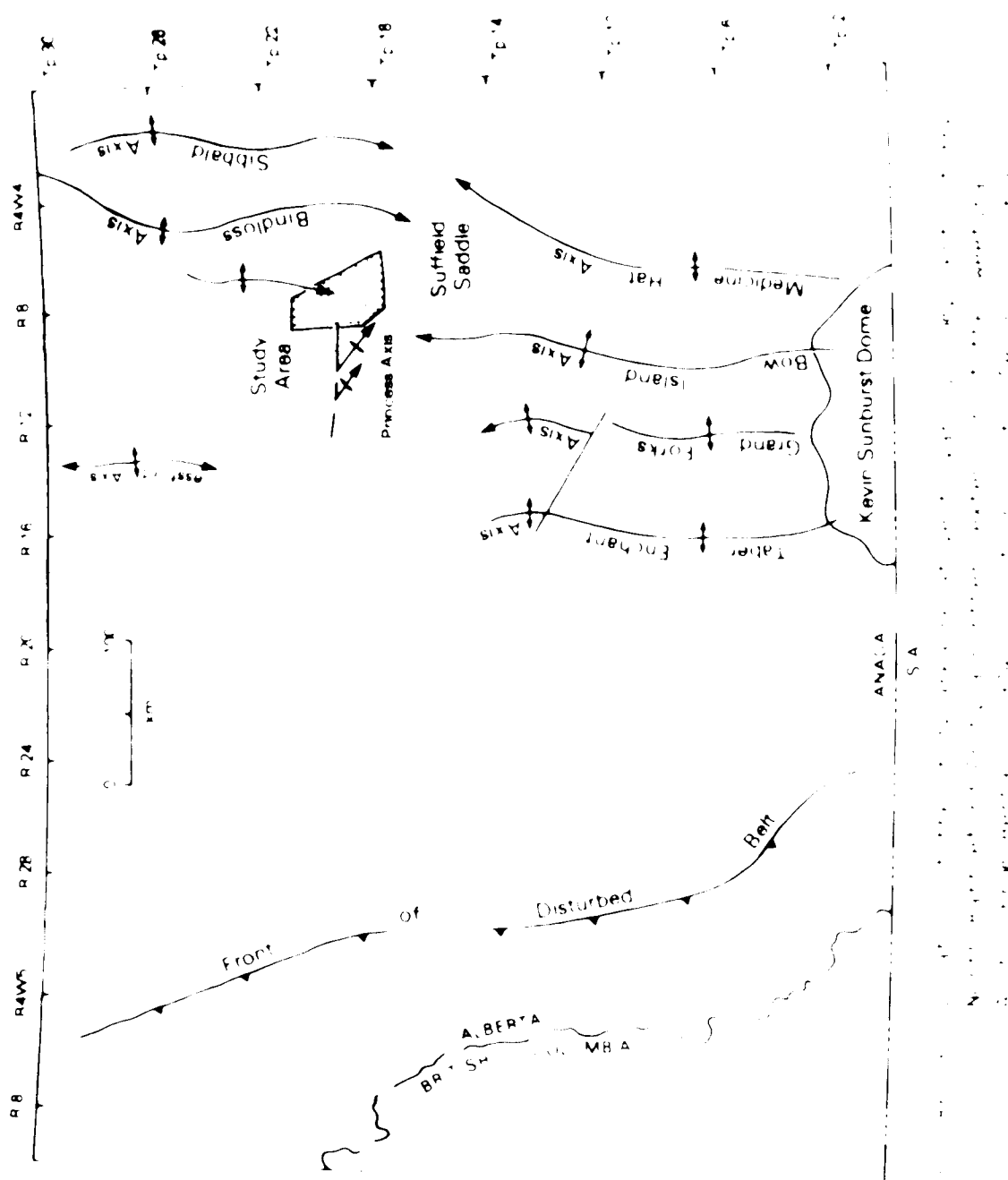
V TECTONIC SETTING

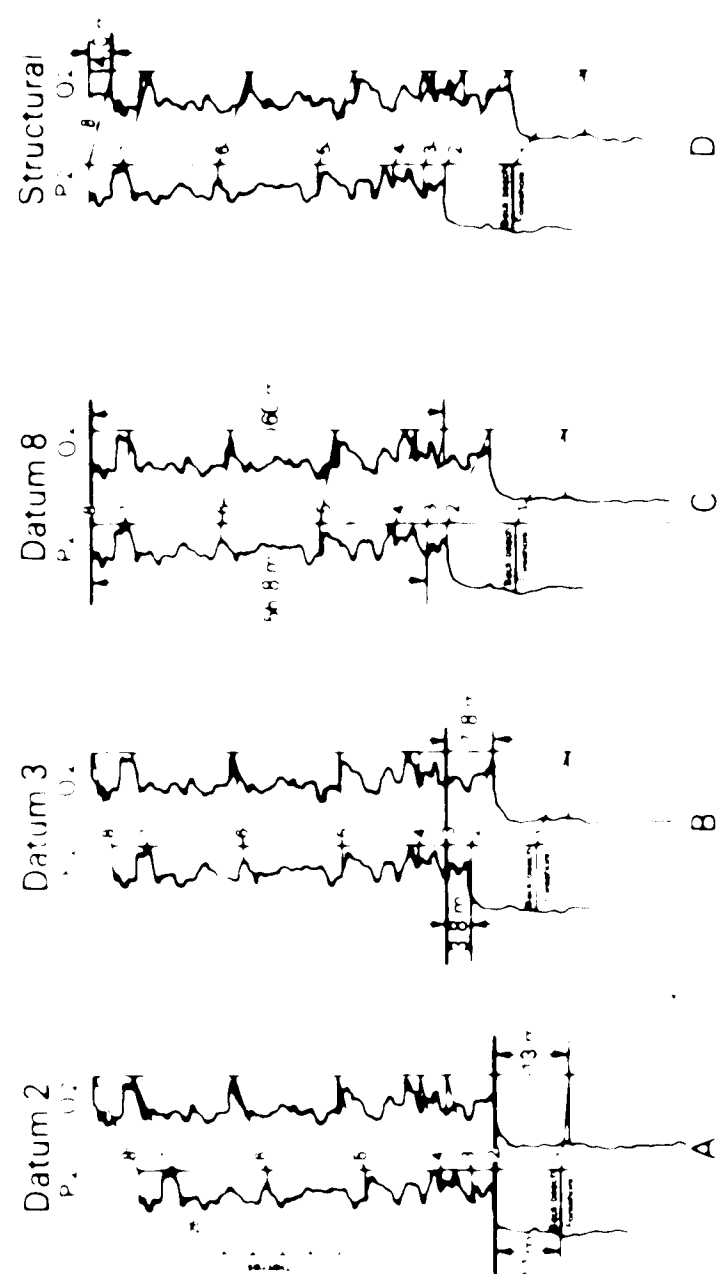
The study area is located immediately west of the Ninth Battleford Arch and northward extension of the Sweetgrass Arch. The westernmost ridge line from the arch extends into the northern portion of the study area (Fig. 13). Evidence of periods of uplift along the Sweetgrass Arch indicate Precambrian movement, the Tertiary (e.g., the Miocene), and Early Tertiary. By close examination of the rock units it is noted that there were several episodes of uplift and erosion and young periods of nondeposition in the Sweetgrass Arch. Dipping southward from the Ninth Battleford Arch during the Tertiary caused the arch to translate as evidenced by subcrop patterns and thinning of clastic facies in the axial zone of the positive trend. Major reactivation of the arch occurred during the late Tertiary and Early Tertiary (aramatic) (Rogers, Grove, 1985) and eastward slippage of the arch resulted in the north of the saddle (Baddie, Fig. 13) dipping toward the west. The Ninth Battleford Arch retained its original southward dip during the Miocene, as indicated by evidence of lateral faulting to the west of the Sweetgrass Arch (Fig. 13) and by the Miocene reactivation. The present evidence shows that extensive faulting and various types of displacement (Ridge, Saddle, and Mountain) have taken place in the area of the Sweetgrass Arch in Miocene times.

A SHOP Project Site

The dense limestone within the Ninth Battleford Arch is the primary source of limestone in the small-scale sandstone beds which are distributed throughout the area. Late Tertiary movement associated with the Ninth Battleford Arch caused the limestone to move. Many veins of

thin, very closely spaced, well-sorted, fine-grained sandstone lenses are found in the limestone bed. The lenses are at the top of the limestone zone (layer 4) and in the base of the sandstone bed (Fig. 14). Figure 14 shows these two lenses, F and G, in their approximate vertical positions. The horizontal to subhorizontal lines between the two lenses are massive beds and represent surfaces which were near horizontal during deposition.

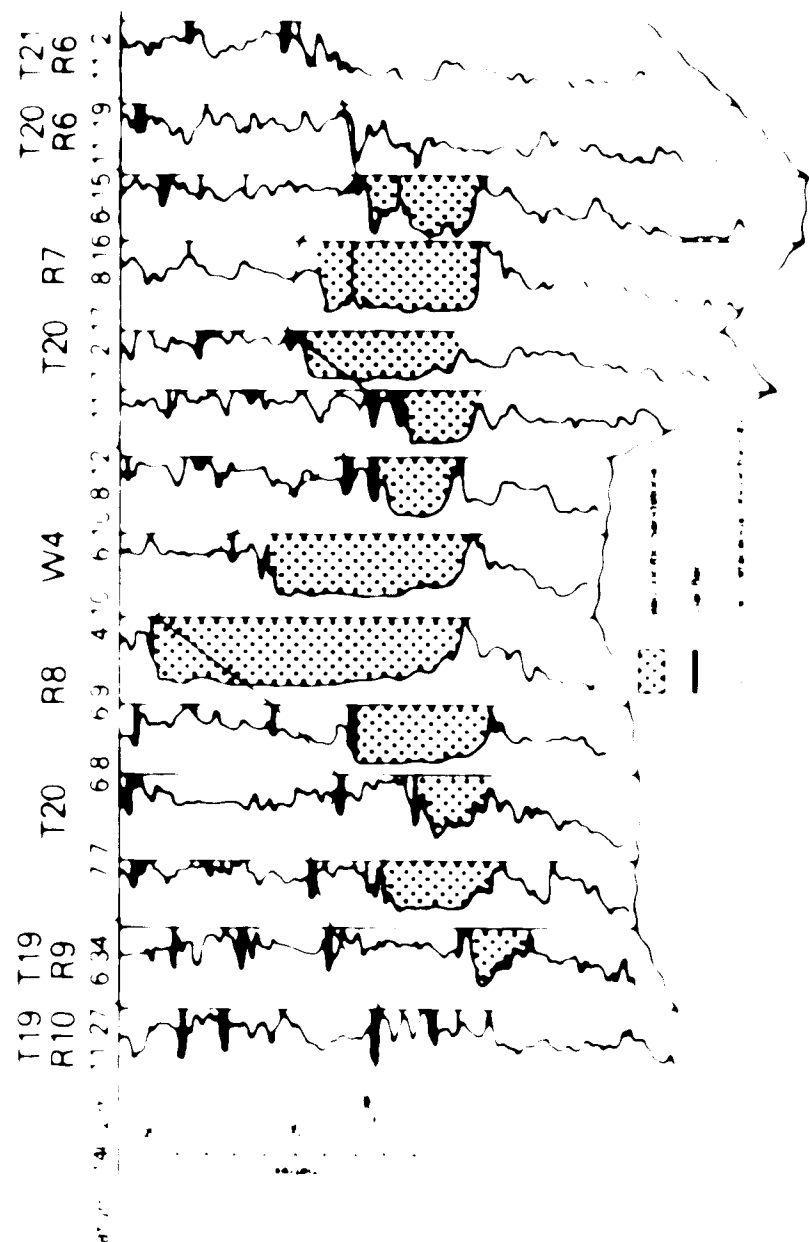




that particular datum. Figure 14A shows the position of the two wells with the carbonaceous bed on the top of the sandstone as the datum #2. Note that the interval from the top of the foreshore zone facies A to the carbonaceous bed at the top of the sandstone is thicker in well 14A by 1.4 metres. Figure 14B shows the datum #3 which is a thickening of 4 metres added to the datum #2 to #3. This is the interval of most significant thickening in the upper Mannville sequence. Figure 14C shows the top of the Mannville as the datum #3 and the lower datum #2 is at 185.5 and adds 1.4 metres to the Kananaskis sandstone. The top separation of the Mannville is the top of the Kananaskis sandstone at 187.5 metres. At the present time, the top of the Mannville is at 189.5 metres. The Mannville sequence has a total thickness of 1.4 metres and a 1.4-metre vertical adjustment to the present datum #3. It is noted that the Kananaskis sandstone is about 1.4 metres higher than the original base of the Mannville sequence. The Mannville sequence has a total thickness of 1.4 metres and a 1.4-metre vertical adjustment to the present datum #3. It is noted that the Kananaskis sandstone is about 1.4 metres higher than the original base of the Mannville sequence.

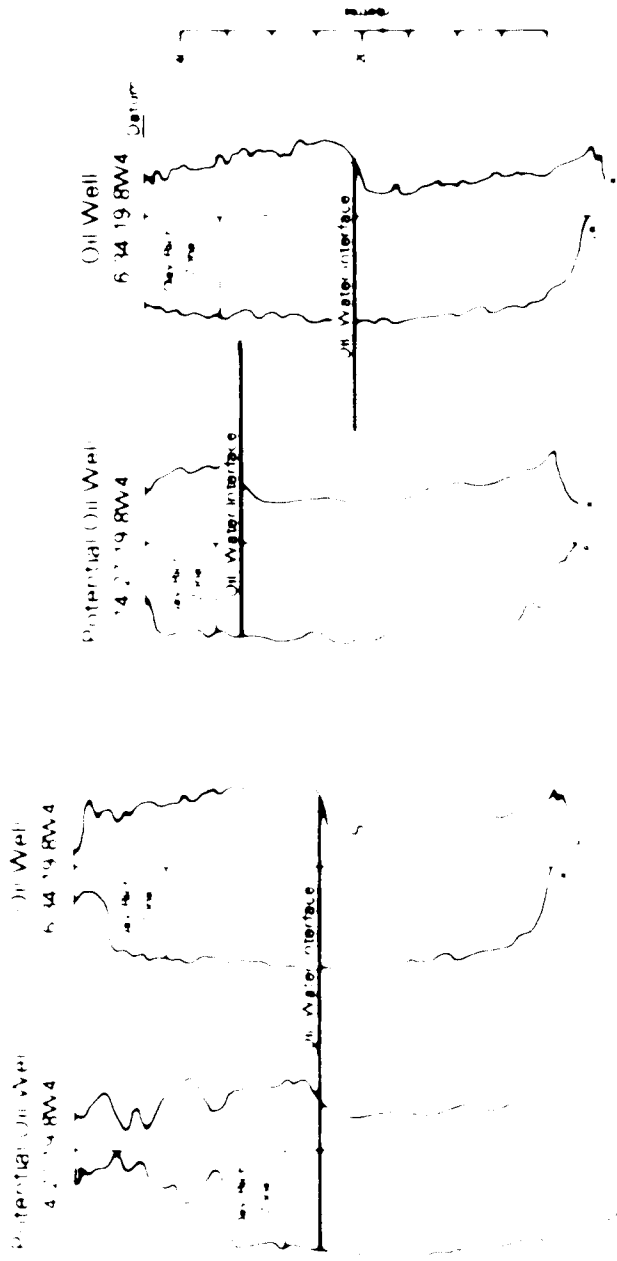
E. Regional Suffield Area

Information on the Mannville sequence is limited to the Suffield area. In the Suffield area, it is necessary to estimate the vertical thickness of the Mannville sequence to determine the vertical thickness of the regional Mannville sequence. The Mannville sequence is divided into three major facies zones. The upper facies zone is characterized by thick, coarse-grained sandstones. The middle facies zone is characterized by thin, fine-grained sandstones. The lower facies zone is characterized by thin, fine-grained sandstones. The upper facies zone is characterized by thick, coarse-grained sandstones. The middle facies zone is characterized by thin, fine-grained sandstones. The lower facies zone is characterized by thin, fine-grained sandstones.



the following example. A component \mathcal{C} has a frame \mathcal{F} that is well-known (achieved so that the component can be easily integrated) and the component depends on another component \mathcal{D} which is not yet known. The dependency of \mathcal{C} on \mathcal{D} is denoted by $\mathcal{C} \rightarrow \mathcal{D}$.

Perrin sum trapping mechanism



A Structural Cross Section

B Stratigraphic Cross Section

D Tectonic Control on the Glauconitic Sandstone Thickness

As mentioned previously parts of the Glauconitic Sandstone are unusually thick (in a beach sequence) in light of the evidence for tectonic activity immediately after deposition of the sandstone. It seems reasonable that movement by basement faults was responsible for controlling the rate of subsidence during deposition of the glauconitic sandstone (figure 11). A schematic cross section showing the thickening of sediment facies in a relative rapid subsidence area. A fault is present west of the crest of a ridge and to the east of the ridge sandstone becomes thicker. The thicknesses of the facies representing the shallowest, intermediate and deepest zones are shown as thick, medium and thin respectively. The greater sediment accumulation to the south of the ridge indicates relatively rapid subsidence caused by the faulting.

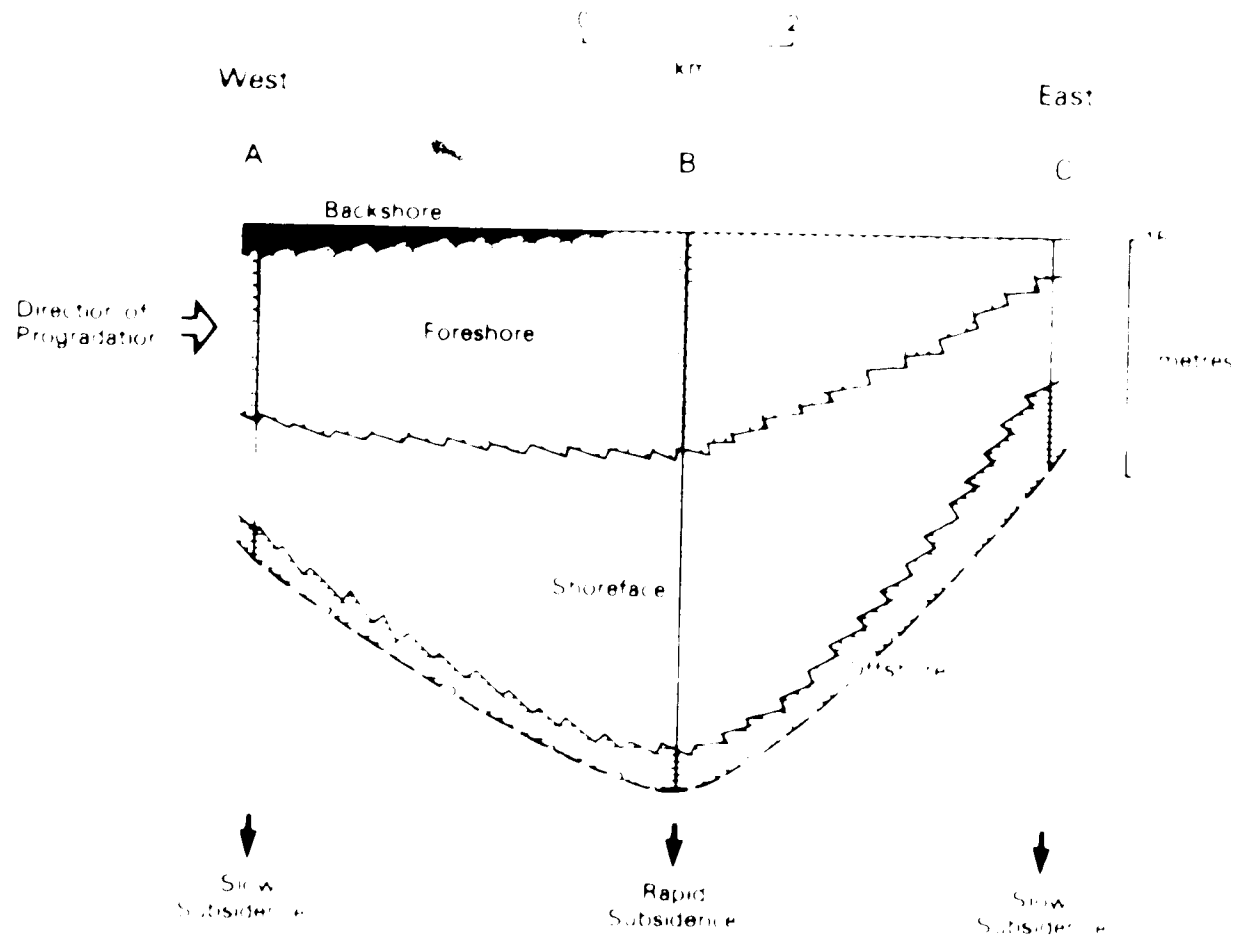


Fig. 1. Schematic cross-section of a coastal profile showing the effect of subsidence on the development of a shoreface. The profile is oriented with West at the top left and East at the top right. The horizontal scale bar indicates 2 km. The vertical axis on the right is labeled 'metres' with a scale from -10 to +10. The profile shows three main zones: 'Backshore' (top), 'Foreshore' (middle), and 'Shoreface' (bottom). The 'Backshore' and 'Foreshore' areas are relatively flat, while the 'Shoreface' area shows a steep gradient. Three arrows point downwards from the 'Shoreface' area towards the bottom of the diagram, labeled 'Slow Subsidence' (left), 'Rapid Subsidence' (center), and 'Slow Subsidence' (right). A curved arrow on the left side of the diagram indicates the 'Direction of Progradation' moving from West to East.

VI MINERALOGY

A Bulk Mineralogy.

The grain mineralogy of the dolomitic sandstone is not included here in the sedimentary rock fragment and mineral analysis because it is not yet determined. The distribution of the various minerals and mineraloids is discussed below. The following section is concerned with the sedimentary rock fragments and the associated minerals.

Analyses of the dolomitic sandstone indicate the presence of dolomite, calcite, and dolomite-calcite intergrowths. Calcite is present in the dolomitic sandstone in the form of dolomite-calcite intergrowths, dolomite, and dolomite-calcite intergrowths. Calcite is also present in the dolomitic sandstone in the form of dolomite-calcite intergrowths, dolomite, and dolomite-calcite intergrowths.

The dolomitic sandstone contains dolomite, calcite, and dolomite-calcite intergrowths. The dolomitic sandstone contains dolomite, calcite, and dolomite-calcite intergrowths. The dolomitic sandstone contains dolomite, calcite, and dolomite-calcite intergrowths.

The dolomitic sandstone contains dolomite, calcite, and dolomite-calcite intergrowths. The dolomitic sandstone contains dolomite, calcite, and dolomite-calcite intergrowths. The dolomitic sandstone contains dolomite, calcite, and dolomite-calcite intergrowths. The dolomitic sandstone contains dolomite, calcite, and dolomite-calcite intergrowths.

Other sedimentary rock fragments consist of siltstone, shale and silty shale. Fragments in the siltstone fragments are dominantly quartz with some feldspar. Some siltstone fragments have been so deformed that they are almost indistinguishable from the matrix. Fragments of rock fragments with a significant clay content tend to be deformed and rounded. Impact of shale & silt rock fragments are most abundant in samples A, C, D, E, G and H. In sample H, impact of shale fragments is significantly reduced.

Metamorphic minerals are present in the metamorphic fragments. The most common are the mica-schistose minerals that will typically leave irregular, folded and broken mineral fragments. Commonly, garnet, omphacite, and/or kyanite are found within the fragment. In sample H, the mica-schistose fragments are relatively small and rounded. In sample G, the mica-schistose fragments are larger and more angular than in sample H. Metamorphic minerals are also found in the pelitic material, which are mainly composed of the mica-schistose minerals.

Quartzite fragments are the most abundant and the most common fragment in the sand and gravel. The size of the quartzite fragments varies from small to large. Quartzite fragments are often angular and irregular. They are usually light grey in colour and may contain small amounts of feldspar and/or mica. The angular shape of the quartzite fragments suggests that they were derived from a weathered source. The angular shape of the quartzite fragments suggests that they were derived from a weathered source. The angular shape of the quartzite fragments suggests that they were derived from a weathered source. The angular shape of the quartzite fragments suggests that they were derived from a weathered source.

Chert fragments are also common in the sand and gravel. They are usually angular and irregular. They are often light grey in colour and may contain small amounts of feldspar and/or mica. The angular shape of the chert fragments suggests that they were derived from a weathered source. The angular shape of the chert fragments suggests that they were derived from a weathered source. The angular shape of the chert fragments suggests that they were derived from a weathered source.

B Clay Mineralogy

Descriptive Clay Mineralogy

• 11 •

FINE PRINT

48

Table 2. Relative Percentage of the Number of Species in Some of the 3000 Samples

Relative
Percentage

#	Species	Log Dose	No. of sp.	%	No. of sp.	%	No. of sp.	%	No. of sp.	%
1	9.1	10	01	1	1	01	1	01	1	01
2	9.1	11	01	1	1	01	1	01	1	01
3	9.1	12	01	1	1	01	1	01	1	01
4	9.1	13	01	1	1	01	1	01	1	01
5	9.1	14	01	1	1	01	1	01	1	01
6	9.1	15	01	1	1	01	1	01	1	01
7	9.1	16	01	1	1	01	1	01	1	01
8	9.1	17	01	1	1	01	1	01	1	01
9	9.1	18	01	1	1	01	1	01	1	01
10	9.1	19	01	1	1	01	1	01	1	01
11	9.1	20	01	1	1	01	1	01	1	01
12	9.1	21	01	1	1	01	1	01	1	01
13	9.1	22	01	1	1	01	1	01	1	01
14	9.1	23	01	1	1	01	1	01	1	01
15	9.1	24	01	1	1	01	1	01	1	01
16	9.1	25	01	1	1	01	1	01	1	01
17	9.1	26	01	1	1	01	1	01	1	01
18	9.1	27	01	1	1	01	1	01	1	01
19	9.1	28	01	1	1	01	1	01	1	01
20	9.1	29	01	1	1	01	1	01	1	01
21	9.1	30	01	1	1	01	1	01	1	01
22	9.1	31	01	1	1	01	1	01	1	01
23	9.1	32	01	1	1	01	1	01	1	01
24	9.1	33	01	1	1	01	1	01	1	01
25	9.1	34	01	1	1	01	1	01	1	01
26	9.1	35	01	1	1	01	1	01	1	01
27	9.1	36	01	1	1	01	1	01	1	01
28	9.1	37	01	1	1	01	1	01	1	01
29	9.1	38	01	1	1	01	1	01	1	01
30	9.1	39	01	1	1	01	1	01	1	01
31	9.1	40	01	1	1	01	1	01	1	01
32	9.1	41	01	1	1	01	1	01	1	01
33	9.1	42	01	1	1	01	1	01	1	01
34	9.1	43	01	1	1	01	1	01	1	01
35	9.1	44	01	1	1	01	1	01	1	01
36	9.1	45	01	1	1	01	1	01	1	01
37	9.1	46	01	1	1	01	1	01	1	01
38	9.1	47	01	1	1	01	1	01	1	01
39	9.1	48	01	1	1	01	1	01	1	01
40	9.1	49	01	1	1	01	1	01	1	01
41	9.1	50	01	1	1	01	1	01	1	01
42	9.1	51	01	1	1	01	1	01	1	01
43	9.1	52	01	1	1	01	1	01	1	01
44	9.1	53	01	1	1	01	1	01	1	01
45	9.1	54	01	1	1	01	1	01	1	01
46	9.1	55	01	1	1	01	1	01	1	01
47	9.1	56	01	1	1	01	1	01	1	01
48	9.1	57	01	1	1	01	1	01	1	01
49	9.1	58	01	1	1	01	1	01	1	01
50	9.1	59	01	1	1	01	1	01	1	01
51	9.1	60	01	1	1	01	1	01	1	01
52	9.1	61	01	1	1	01	1	01	1	01
53	9.1	62	01	1	1	01	1	01	1	01
54	9.1	63	01	1	1	01	1	01	1	01
55	9.1	64	01	1	1	01	1	01	1	01
56	9.1	65	01	1	1	01	1	01	1	01
57	9.1	66	01	1	1	01	1	01	1	01
58	9.1	67	01	1	1	01	1	01	1	01
59	9.1	68	01	1	1	01	1	01	1	01
60	9.1	69	01	1	1	01	1	01	1	01
61	9.1	70	01	1	1	01	1	01	1	01
62	9.1	71	01	1	1	01	1	01	1	01
63	9.1	72	01	1	1	01	1	01	1	01
64	9.1	73	01	1	1	01	1	01	1	01
65	9.1	74	01	1	1	01	1	01	1	01
66	9.1	75	01	1	1	01	1	01	1	01
67	9.1	76	01	1	1	01	1	01	1	01
68	9.1	77	01	1	1	01	1	01	1	01
69	9.1	78	01	1	1	01	1	01	1	01
70	9.1	79	01	1	1	01	1	01	1	01
71	9.1	80	01	1	1	01	1	01	1	01
72	9.1	81	01	1	1	01	1	01	1	01
73	9.1	82	01	1	1	01	1	01	1	01
74	9.1	83	01	1	1	01	1	01	1	01
75	9.1	84	01	1	1	01	1	01	1	01
76	9.1	85	01	1	1	01	1	01	1	01
77	9.1	86	01	1	1	01	1	01	1	01
78	9.1	87	01	1	1	01	1	01	1	01
79	9.1	88	01	1	1	01	1	01	1	01
80	9.1	89	01	1	1	01	1	01	1	01
81	9.1	90	01	1	1	01	1	01	1	01
82	9.1	91	01	1	1	01	1	01	1	01
83	9.1	92	01	1	1	01	1	01	1	01
84	9.1	93	01	1	1	01	1	01	1	01
85	9.1	94	01	1	1	01	1	01	1	01
86	9.1	95	01	1	1	01	1	01	1	01
87	9.1	96	01	1	1	01	1	01	1	01
88	9.1	97	01	1	1	01	1	01	1	01
89	9.1	98	01	1	1	01	1	01	1	01
90	9.1	99	01	1	1	01	1	01	1	01
91	9.1	100	01	1	1	01	1	01	1	01
92	9.1	101	01	1	1	01	1	01	1	01
93	9.1	102	01	1	1	01	1	01	1	01
94	9.1	103	01	1	1	01	1	01	1	01
95	9.1	104	01	1	1	01	1	01	1	01
96	9.1	105	01	1	1	01	1	01	1	01
97	9.1	106	01	1	1	01	1	01	1	01
98	9.1	107	01	1	1	01	1	01	1	01
99	9.1	108	01	1	1	01	1	01	1	01
100	9.1	109	01	1	1	01	1	01	1	01
101	9.1	110	01	1	1	01	1	01	1	01
102	9.1	111	01	1	1	01	1	01	1	01
103	9.1	112	01	1	1	01	1	01	1	01
104	9.1	113	01	1	1	01	1	01	1	01
105	9.1	114	01	1	1	01	1	01	1	01
106	9.1	115	01	1	1	01	1	01	1	01
107	9.1	116	01	1	1	01	1	01	1	01
108	9.1	117	01	1	1	01	1	01	1	01
109	9.1	118	01	1	1	01	1	01	1	01
110	9.1	119	01	1	1	01	1	01	1	01
111	9.1	120	01	1	1	01	1	01	1	01
112	9.1	121	01	1	1	01	1	01	1	01
113	9.1	122	01	1	1	01	1	01	1	01
114	9.1	123	01	1	1	01	1	01	1	01
115	9.1	124	01	1	1	01	1	01	1	01
116	9.1	125	01	1	1	01	1	01	1	01
117	9.1	126	01	1	1	01	1	01	1	01
118	9.1	127	01	1	1	01	1	01	1	01
119	9.1	128	01	1	1	01	1	01	1	01
120	9.1	129	01	1	1	01	1	01	1	01
121	9.1	130	01	1	1	01	1	01	1	01
122	9.1	131	01	1	1	01	1	01	1	01
123	9.1	132	01	1	1	01	1	01	1	01
124	9.1	133	01	1	1	01	1	01	1	01
125	9.1	134	01	1	1	01	1	01	1	01
126	9.1	135	01	1	1	01	1	01	1	01
127	9.1	136	01	1	1	01	1	01	1	01
128	9.1	137	01	1	1	01	1	01	1	01
129	9.1	138	01	1	1	01	1	01	1	01
130	9.1	139	01	1	1	01	1	01	1	01
131	9.1	140	01	1	1	01	1	01	1	01
132	9.1	141	01	1	1	01	1	01	1	01
133	9.1	142	01	1	1	01	1	01	1	01
134	9.1	143	01	1	1	01	1	01	1	01
135	9.1	144	01	1	1	01	1	01	1	01
136	9.1	145	01	1	1	01	1	01	1	01
137	9.1	146	01	1	1	01	1	01	1	01
138	9.1	147	01	1	1	01	1	01	1	01
139</td										

FINE PRINT

4

FINE PRINT

1
2
3
4
5
6
7
8
9
10
11
12
13
14
15
16
17
18
19
20
21
22
23
24
25
26
27
28
29
30
31
32
33
34
35
36
37
38
39
40
41
42
43
44
45
46
47
48
49
50
51
52
53
54
55
56
57
58
59
60
61
62
63
64
65
66
67
68
69
70
71
72
73
74
75
76
77
78
79
80
81
82
83
84
85
86
87
88
89
90
91
92
93
94
95
96
97
98
99
100
101
102
103
104
105
106
107
108
109
110
111
112
113
114
115
116
117
118
119
120
121
122
123
124
125
126
127
128
129
130
131
132
133
134
135
136
137
138
139
140
141
142
143
144
145
146
147
148
149
150
151
152
153
154
155
156
157
158
159
160
161
162
163
164
165
166
167
168
169
170
171
172
173
174
175
176
177
178
179
180
181
182
183
184
185
186
187
188
189
190
191
192
193
194
195
196
197
198
199
200
201
202
203
204
205
206
207
208
209
210
211
212
213
214
215
216
217
218
219
220
221
222
223
224
225
226
227
228
229
230
231
232
233
234
235
236
237
238
239
240
241
242
243
244
245
246
247
248
249
250
251
252
253
254
255
256
257
258
259
259
260
261
262
263
264
265
266
267
268
269
270
271
272
273
274
275
276
277
278
279
280
281
282
283
284
285
286
287
288
289
289
290
291
292
293
294
295
296
297
298
299
299
300
301
302
303
304
305
306
307
308
309
309
310
311
312
313
314
315
316
317
318
319
319
320
321
322
323
324
325
326
327
328
329
329
330
331
332
333
334
335
336
337
338
339
339
340
341
342
343
344
345
346
347
348
349
349
350
351
352
353
354
355
356
357
358
359
359
360
361
362
363
364
365
366
367
368
369
369
370
371
372
373
374
375
376
377
378
379
379
380
381
382
383
384
385
386
387
388
389
389
390
391
392
393
394
395
396
397
398
399
399
400
401
402
403
404
405
406
407
408
409
409
410
411
412
413
414
415
416
417
418
419
419
420
421
422
423
424
425
426
427
428
429
429
430
431
432
433
434
435
436
437
438
439
439
440
441
442
443
444
445
446
447
448
449
449
450
451
452
453
454
455
456
457
458
459
459
460
461
462
463
464
465
466
467
468
469
469
470
471
472
473
474
475
476
477
478
479
479
480
481
482
483
484
485
486
487
488
489
489
490
491
492
493
494
495
496
497
498
499
499
500
501
502
503
504
505
506
507
508
509
509
510
511
512
513
514
515
516
517
518
519
519
520
521
522
523
524
525
526
527
528
529
529
530
531
532
533
534
535
536
537
538
539
539
540
541
542
543
544
545
546
547
548
549
549
550
551
552
553
554
555
556
557
558
559
559
560
561
562
563
564
565
566
567
568
569
569
570
571
572
573
574
575
576
577
578
579
579
580
581
582
583
584
585
586
587
588
589
589
590
591
592
593
594
595
596
597
598
599
599
600
601
602
603
604
605
606
607
608
609
609
610
611
612
613
614
615
616
617
618
619
619
620
621
622
623
624
625
626
627
628
629
629
630
631
632
633
634
635
636
637
638
639
639
640
641
642
643
644
645
646
647
648
649
649
650
651
652
653
654
655
656
657
658
659
659
660
661
662
663
664
665
666
667
668
669
669
670
671
672
673
674
675
676
677
678
679
679
680
681
682
683
684
685
686
687
688
689
689
690
691
692
693
694
695
696
697
698
699
699
700
701
702
703
704
705
706
707
708
709
709
710
711
712
713
714
715
716
717
718
719
719
720
721
722
723
724
725
726
727
728
729
729
730
731
732
733
734
735
736
737
738
739
739
740
741
742
743
744
745
746
747
748
749
749
750
751
752
753
754
755
756
757
758
759
759
760
761
762
763
764
765
766
767
768
769
769
770
771
772
773
774
775
776
777
778
779
779
780
781
782
783
784
785
786
787
788
789
789
790
791
792
793
794
795
796
797
798
799
799
800
801
802
803
804
805
806
807
808
809
809
810
811
812
813
814
815
816
817
818
819
819
820
821
822
823
824
825
826
827
828
829
829
830
831
832
833
834
835
836
837
838
839
839
840
841
842
843
844
845
846
847
848
849
849
850
851
852
853
854
855
856
857
858
859
859
860
861
862
863
864
865
866
867
868
869
869
870
871
872
873
874
875
876
877
878
879
879
880
881
882
883
884
885
886
887
888
889
889
890
891
892
893
894
895
896
897
898
899
899
900
901
902
903
904
905
906
907
908
909
909
910
911
912
913
914
915
916
917
918
919
919
920
921
922
923
924
925
926
927
928
929
929
930
931
932
933
934
935
936
937
938
939
939
940
941
942
943
944
945
946
947
948
949
949
950
951
952
953
954
955
956
957
958
959
959
960
961
962
963
964
965
966
967
968
969
969
970
971
972
973
974
975
976
977
978
979
979
980
981
982
983
984
985
986
987
988
989
989
990
991
992
993
994
995
996
997
998
999
999
1000

the field, by presenting a different kind of information to the student than that presented in the text. The student may be asked to predict what will happen if certain variables are changed, or to compare two different situations. The student may also be asked to draw conclusions from a set of data, or to determine the best way to solve a problem. These types of questions encourage the student to think more deeply about the material and to apply it to real-world situations.

Another benefit of using a computer-based learning system is that it can provide immediate feedback to the student. If the student answers a question correctly, they receive positive reinforcement, which can help to motivate them to continue learning. If the student answers a question incorrectly, they receive feedback that helps them to understand where they went wrong and how to correct their mistake. This type of feedback is much more effective than traditional methods of teaching, such as lectures or readings, because it allows the student to immediately see the results of their actions and learn from them. Additionally, computer-based learning systems can track the student's progress over time, allowing the teacher to identify areas where the student may be struggling and provide additional support as needed. This can help to ensure that all students are able to succeed in the course.

Overall, computer-based learning systems offer many benefits for both teachers and students. They can help to make learning more interactive and engaging, while also providing valuable feedback and tracking tools. By incorporating these systems into their teaching, teachers can help to ensure that all students have the opportunity to succeed in the classroom.

had to be used. The reference material was prepared from material obtained by dry distillation of natural gas at 300°C. under a water vapor atmosphere and at a rate of 10 kg./hr. The water vapor was used to keep the oven dry and to reduce the chance of spontaneous ignition.

The following procedure was adopted to obtain the desired results. A sample of the reference material was weighed into a small crucible and placed in a muffle furnace. The temperature was raised to 300°C. and held constant for 10 minutes. The sample was then removed from the furnace and cooled in a desiccator. The sample was weighed again and the difference between the two weights was noted. This difference was taken as the weight of water lost during the heating process. The sample was then heated again at 300°C. for 10 minutes and cooled again. The sample was weighed again and the difference between the two weights was noted. This difference was taken as the weight of water lost during the second heating process. The sample was then heated again at 300°C. for 10 minutes and cooled again. The sample was weighed again and the difference between the two weights was noted. This difference was taken as the weight of water lost during the third heating process. The sample was then heated again at 300°C. for 10 minutes and cooled again. The sample was weighed again and the difference between the two weights was noted. This difference was taken as the weight of water lost during the fourth heating process. The sample was then heated again at 300°C. for 10 minutes and cooled again. The sample was weighed again and the difference between the two weights was noted. This difference was taken as the weight of water lost during the fifth heating process. The sample was then heated again at 300°C. for 10 minutes and cooled again. The sample was weighed again and the difference between the two weights was noted. This difference was taken as the weight of water lost during the sixth heating process. The sample was then heated again at 300°C. for 10 minutes and cooled again. The sample was weighed again and the difference between the two weights was noted. This difference was taken as the weight of water lost during the seventh heating process. The sample was then heated again at 300°C. for 10 minutes and cooled again. The sample was weighed again and the difference between the two weights was noted. This difference was taken as the weight of water lost during the eighth heating process. The sample was then heated again at 300°C. for 10 minutes and cooled again. The sample was weighed again and the difference between the two weights was noted. This difference was taken as the weight of water lost during the ninth heating process. The sample was then heated again at 300°C. for 10 minutes and cooled again. The sample was weighed again and the difference between the two weights was noted. This difference was taken as the weight of water lost during the tenth heating process.

The following table gives the results obtained from the above procedure. The first column gives the number of the heating process. The second column gives the weight of water lost during each heating process. The third column gives the percentage of water lost during each heating process. The fourth column gives the total weight of water lost during all heating processes. The fifth column gives the percentage of water lost during all heating processes. The sixth column gives the percentage of water lost during the last heating process. The seventh column gives the percentage of water lost during the first heating process. The eighth column gives the percentage of water lost during the second heating process. The ninth column gives the percentage of water lost during the third heating process. The tenth column gives the percentage of water lost during the fourth heating process. The eleventh column gives the percentage of water lost during the fifth heating process. The twelfth column gives the percentage of water lost during the sixth heating process. The thirteenth column gives the percentage of water lost during the seventh heating process. The fourteenth column gives the percentage of water lost during the eighth heating process. The fifteenth column gives the percentage of water lost during the ninth heating process. The sixteenth column gives the percentage of water lost during the tenth heating process. The seventeenth column gives the percentage of water lost during the eleventh heating process. The eighteenth column gives the percentage of water lost during the twelfth heating process. The nineteenth column gives the percentage of water lost during the thirteenth heating process. The twentieth column gives the percentage of water lost during the fourteenth heating process. The twenty-first column gives the percentage of water lost during the fifteen-

3.2. Periodicity in the Atmosphere

The periodicity of the atmosphere is a well-known phenomenon and has been studied by many authors. Several different methods have been used to study the periodicities in the atmosphere. One method is to calculate the autocorrelation function of the atmospheric variables. Another method is to calculate the power spectrum of the atmospheric variables. A third method is to calculate the periodogram of the atmospheric variables. The fourth method is to calculate the spectral density of the atmospheric variables. The fifth method is to calculate the spectral density of the atmospheric variables after the time constant has been taken into account. The sixth method is to calculate the spectral density of the atmospheric variables after the time constant has been taken into account and the time constant has been taken into account.

The first method is to calculate the autocorrelation function of the atmospheric variables. This method is based on the assumption that the atmospheric variables are stationary. The second method is to calculate the power spectrum of the atmospheric variables. This method is based on the assumption that the atmospheric variables are stationary. The third method is to calculate the periodogram of the atmospheric variables. This method is based on the assumption that the atmospheric variables are stationary. The fourth method is to calculate the spectral density of the atmospheric variables. This method is based on the assumption that the atmospheric variables are stationary. The fifth method is to calculate the spectral density of the atmospheric variables after the time constant has been taken into account. This method is based on the assumption that the atmospheric variables are stationary. The sixth method is to calculate the spectral density of the atmospheric variables after the time constant has been taken into account and the time constant has been taken into account.

The first method is to calculate the autocorrelation function of the atmospheric variables. This method is based on the assumption that the atmospheric variables are stationary. The second method is to calculate the power spectrum of the atmospheric variables. This method is based on the assumption that the atmospheric variables are stationary. The third method is to calculate the periodogram of the atmospheric variables. This method is based on the assumption that the atmospheric variables are stationary. The fourth method is to calculate the spectral density of the atmospheric variables. This method is based on the assumption that the atmospheric variables are stationary. The fifth method is to calculate the spectral density of the atmospheric variables after the time constant has been taken into account. This method is based on the assumption that the atmospheric variables are stationary. The sixth method is to calculate the spectral density of the atmospheric variables after the time constant has been taken into account and the time constant has been taken into account.

Expectations about the availability of capital. The expectations about future availability of the capital will be important and there can be no doubt. Moreover, the knowledge of the term qualities of the capital present a great advantage in the planning of the investment.

"

The ability to plan ahead is a great advantage in the long run. It is also important to have a clear idea of the quality of the capital available. This is particularly important when the capital is used for long-term projects. In such cases, the quality of the capital is often more important than the quantity. This is because the quality of the capital determines the success or failure of the project.

It is also important to have a clear idea of the quality of the capital available. This is particularly important when the capital is used for long-term projects. In such cases, the quality of the capital determines the success or failure of the project. The quality of the capital is often more important than the quantity. This is because the quality of the capital determines the success or failure of the project.

It is also important to have a clear idea of the quality of the capital available. This is particularly important when the capital is used for long-term projects. In such cases, the quality of the capital determines the success or failure of the project. The quality of the capital is often more important than the quantity. This is because the quality of the capital determines the success or failure of the project. The quality of the capital is often more important than the quantity. This is because the quality of the capital determines the success or failure of the project.

Minerals

The mineral assemblage of the metamorphic rocks is dominated by quartz and feldspar. These minerals are the most abundant and often occur in large, well-defined, well-sorted grains. They have little or no internal porphyroblasts, indicating little recrystallization after initial formation. The feldspar is usually plagioclase, although some alkali feldspar is present.

Other minerals are present in minor amounts. These include garnet, staurolite, kyanite, and sillimanite. Sillimanite is the most common of these minerals, occurring in small, irregular, elongated grains. It is associated with staurolite and kyanite, which are also present in small amounts. Garnet is less common than the other minerals, but it is often found in association with sillimanite and staurolite.

Mineral Assemblages

There are four distinct mineral assemblages in the metamorphic rocks. These assemblages are based on the presence of different minerals and their relative abundance. The first assemblage is characterized by the presence of quartz, feldspar, and sillimanite. The second assemblage is characterized by the presence of quartz, feldspar, and staurolite. The third assemblage is characterized by the presence of quartz, feldspar, and kyanite. The fourth assemblage is characterized by the presence of quartz, feldspar, and garnet.

Assemblages of the Minerals

The mineral assemblages are based on the presence of different minerals and their relative abundance. The first assemblage is characterized by the presence of quartz, feldspar, and sillimanite. The second assemblage is characterized by the presence of quartz, feldspar, and staurolite. The third assemblage is characterized by the presence of quartz, feldspar, and kyanite. The fourth assemblage is characterized by the presence of quartz, feldspar, and garnet.

Mineralogical Features

There are several mineralogical features in the metamorphic rocks.

1. The presence of large, well-sorted grains of quartz and feldspar.

2. The presence of small, irregular, elongated grains of sillimanite and staurolite.

3. The presence of small, irregular, elongated grains of kyanite and garnet.

Distribution of Clay Mineral Assemblages

Type I samples from the area of the Andes show a marked trend toward the development of the clay mineral assemblage mentioned above (see Fig. 1) and the evolution of the detrital clay minerals (the kaolinite, illite, and chlorite) during the degradation of the bedrock. The clay mineral assemblage is readily identified by the presence of the element Mn, which is either found in the clay minerals or in the interlayer spaces of the illite and chlorite layers (see Fig. 1).

When samples from the Andes and the Urals are compared, it is found that the distribution of clay minerals in the soils of the two regions is similar. This is due to the fact that the soils of the Urals were formed under conditions of relatively low temperatures and high humidity, which are typical of the climate of the Urals. The soils of the Andes, on the other hand, were formed under conditions of high temperatures and low humidity, which are typical of the climate of the Andes. The soils of the Andes are therefore more likely to contain clay minerals than the soils of the Urals. The soils of the Andes are also more likely to contain clay minerals than the soils of the Urals because the soils of the Andes are more likely to contain clay minerals than the soils of the Urals.

The soils of the Andes are more likely to contain clay minerals than the soils of the Urals because the soils of the Andes are more likely to contain clay minerals than the soils of the Urals. The soils of the Andes are also more likely to contain clay minerals than the soils of the Urals because the soils of the Andes are more likely to contain clay minerals than the soils of the Urals.

large amounts of smectite. Therefore smectite in samples from this eastern sandstone belt is probably detrital in origin. The bentonitic shale probably represents deposition of a sandstone deposit that may have occurred sometime after that of the shales in the belt immediately above the major white sandstone of the western belt.

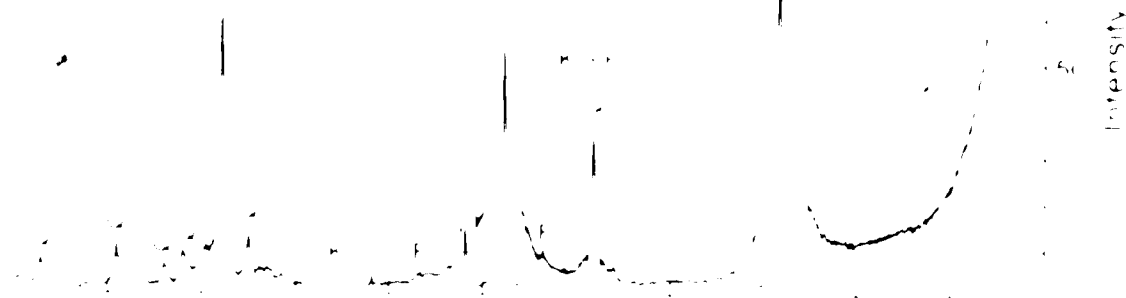
Figure 18 A and B

Typical X-ray diffractograms of the <2 micrometre fraction for type 1 samples. Type 1 samples represent the moist argillaceous sandstone at the top of the Glauconitic Sandstone (uppermost facies 3). This sample contains almost 100 per cent kaolinite (K), a minor amount of quartz (Q) and trace amounts of feldspar (F). Basal reflections for the clay minerals are indicated by brackets after the symbol for the clay. The 'A' symbol peak for kaolinite is sharp and intense. The clay symbols with no adjacent bracket indicate nonbasal reflections.

Type I

Ca-saturated
54% R.H.

K=0013



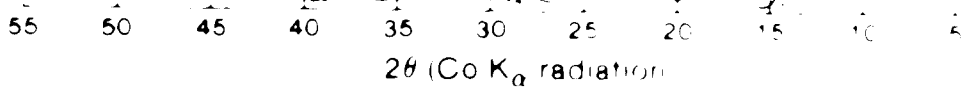
Ca-saturated
glycolated

K=0013



K-saturated
0% R.H.

K=002

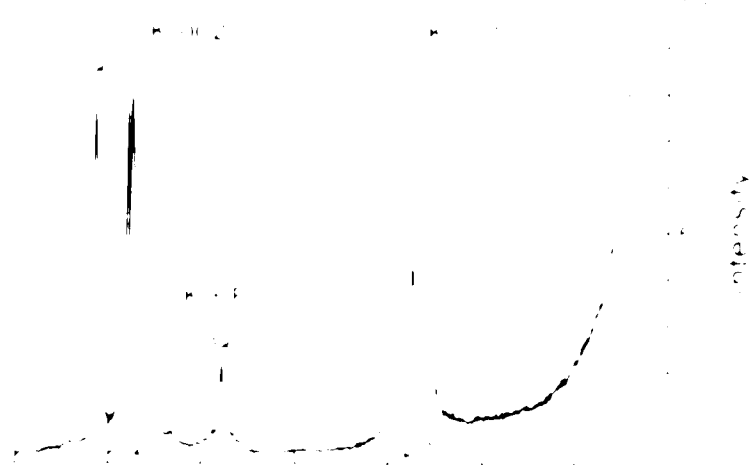


Type I cont.

K-saturated
54% R.H.



K-saturated
300 C



K-saturated
550 C

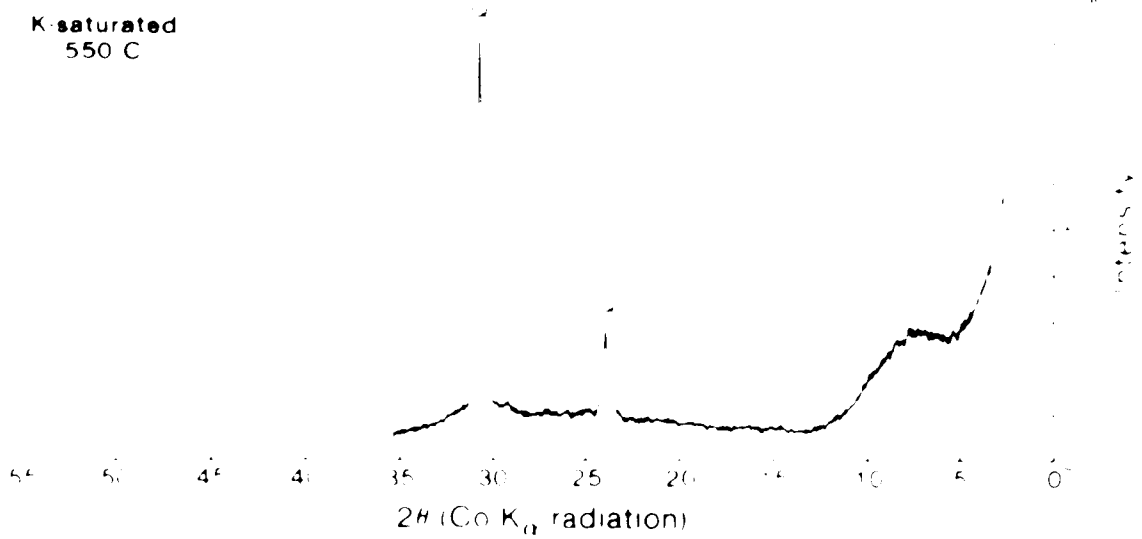


Figure 19 A and B

Typical X-ray diffractograms of the 1-2 micrometre fraction for type samples. Type I samples represent sandstones of facies 3 located stratigraphically below those of type 1. The total clay content in the sandstone is significantly lower than in type 1 samples. Illitic clay minerals are present in trace amounts. The low angle asymmetry which remains on the 10A peak (200°) after K₂ saturation (Fig. 19A) indicates the presence of chloritic material within the illitic phase.

Type II

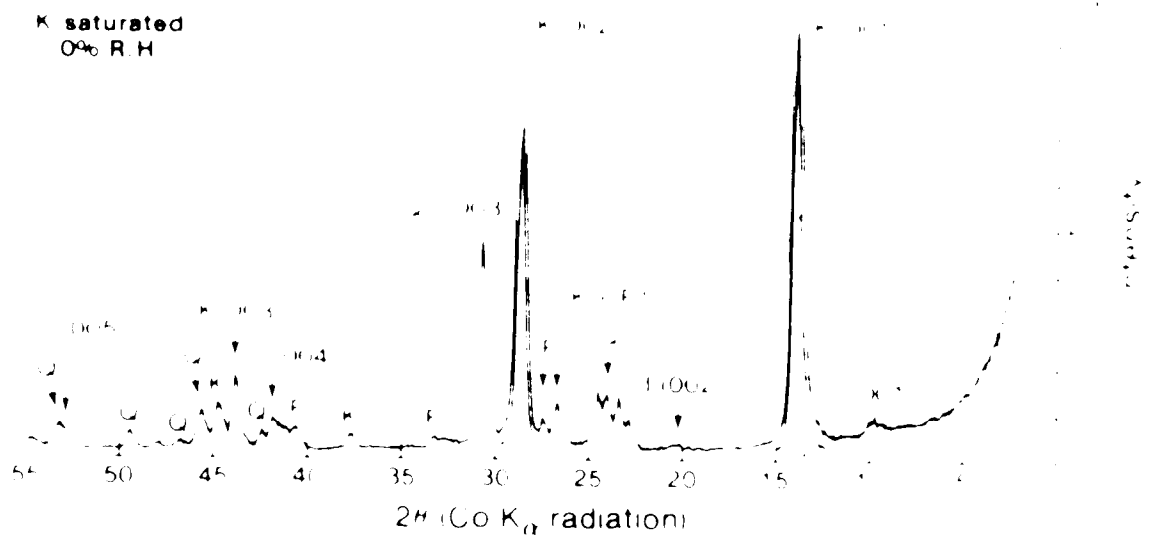
Ca-saturated
54% R.H.



Ca-saturated
glycolated

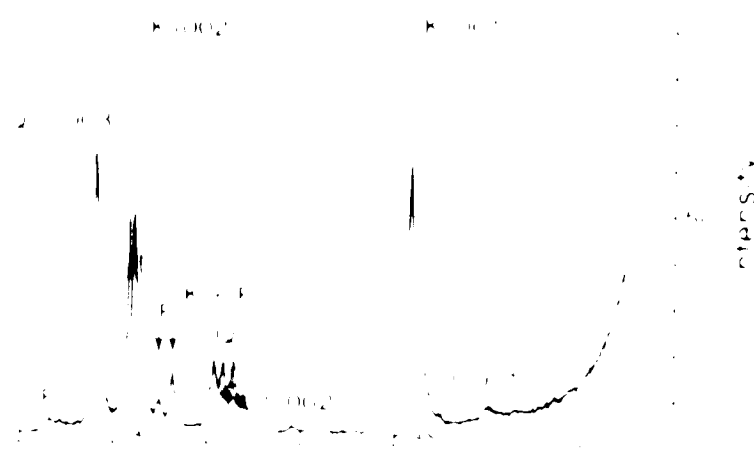


K saturated
0% R.H.

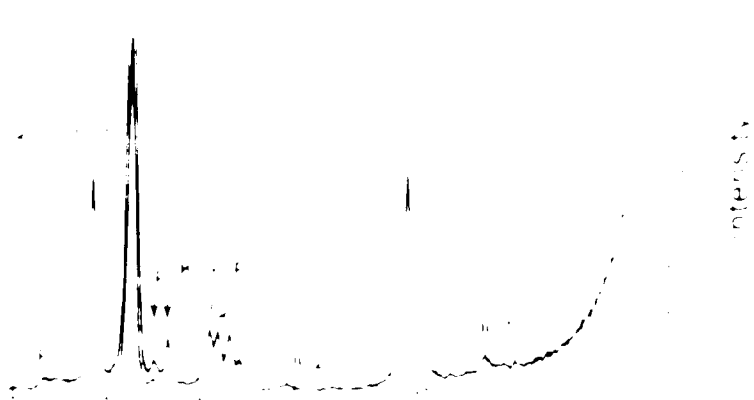


Type II cont.

K-saturated
54% R H



K-saturated
300 C



K-saturated
550 C

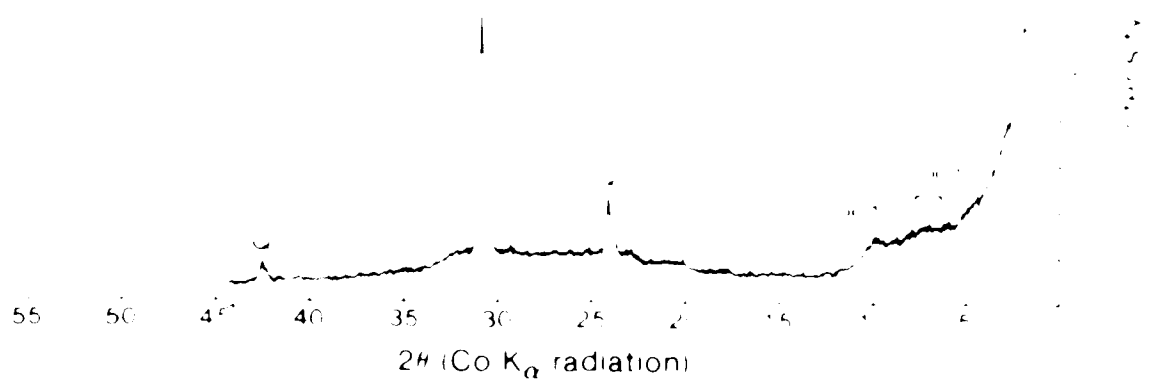
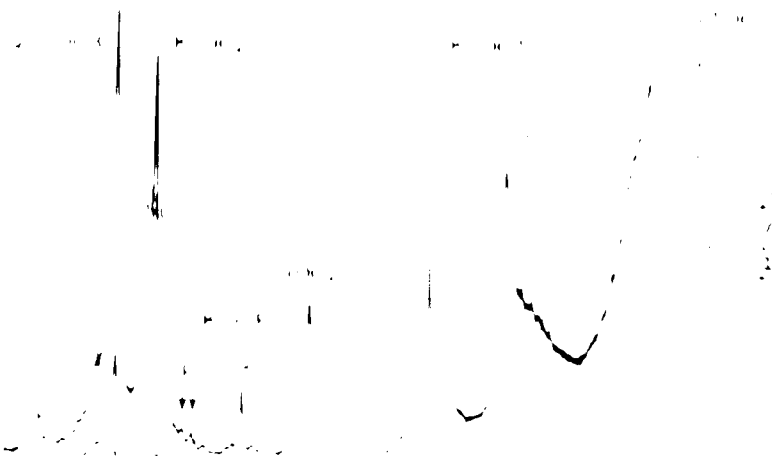
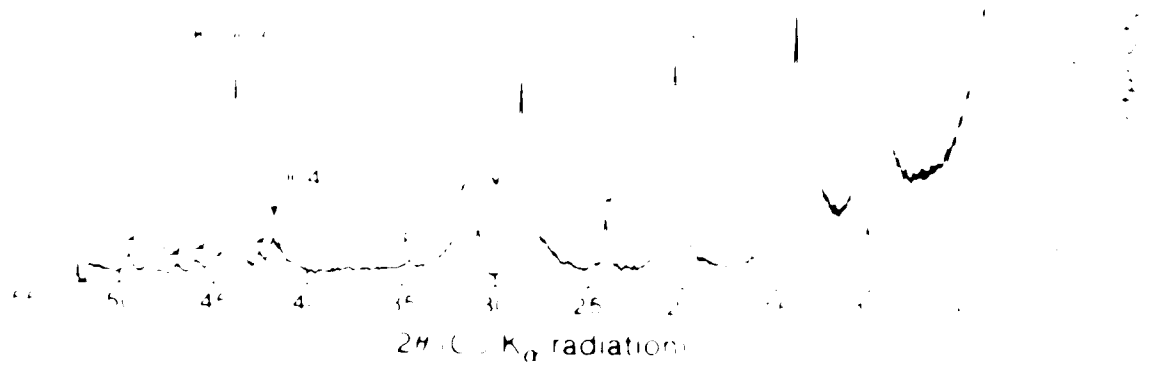


FIGURE 2. A and B.

X-ray diffractograms representative of shale samples from immediately above and below the Glauconitic Sandstone-type illite assemblage. This sample contains about 30% illite. The 10 Å (100%) reflection is sharp (at d = 5.4 Å) at 54% humidity but is asymmetric toward its low angle side. The asymmetry extends from 10 Å to 15–16 Å. Upon saturation with ethylene glycol, the 10 Å reflection remains sharp but the asymmetric tail portion expands towards higher d-spacings and a broad peak is produced at 13–14 Å. The asymmetry and swelling properties may result from edge weathering. Note the presence of chloritic material within the illite phase is indicated by the low angle asymmetry which remains in the 10 Å peak after it is saturated (Fig. 2B). At lower part of graph heating to 100°C (Fig. 2B) over pattern the illite tail is diffused indicating illite passes through an amorphous stage.

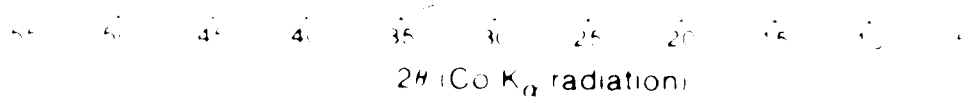
Type IIICa saturated
54% R.H.Ca saturated
glycolatedK saturated
0% R.H.

Type III cont.

K saturated
54% R.H.

K saturated
300°C

K saturated
550°C

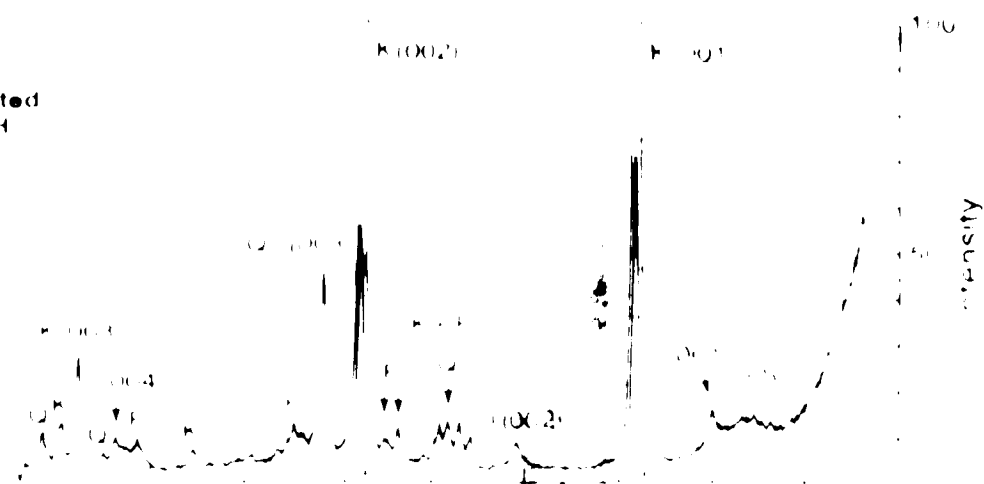


Figures A and B

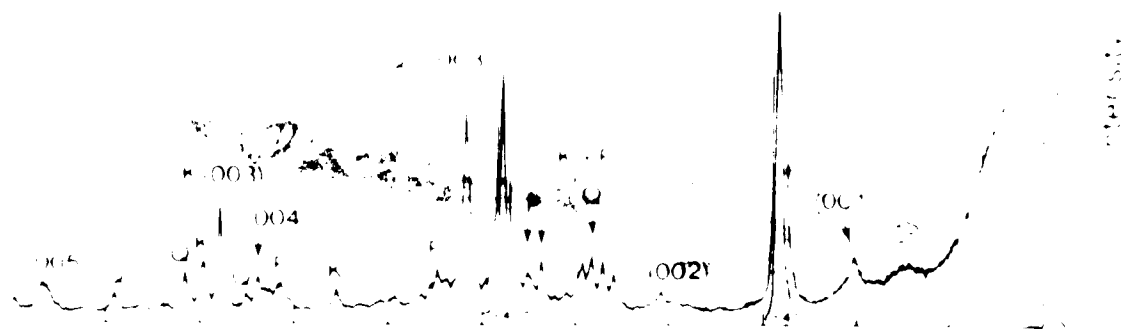
X-ray diffractograms representative of a very fine grained sandstone in facies b and a bioturbated sandstone of facies c type II clay assemblage. Both these sandstones probably have a significant detrital clay component. Note the broad peak at about 12 Å labelled 'S' on the Ca-saturated 54% RH pattern (Fig. 2, 1A). Upon glycolation, the broad 12 Å reflection loses intensity and shifts to about 14 Å. Much material does not collapse completely to 10 Å when K-saturated <1% humidity. This behaviour results in a 10 Å peak which has greater intensity but is still broadly asymmetrical on the low angle side. This clay is probably a randomly interstratified illite-smectite. The behaviour of the low angle reflections upon heating (Fig. 2, 1B) suggests that the clay is also randomly interstratified.

Type III

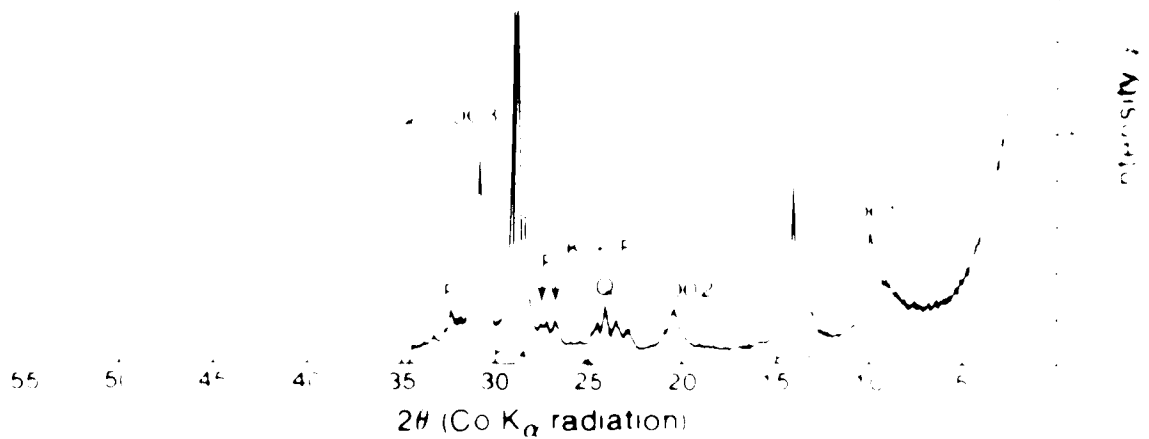
Ca-saturated
54% R H



Ca saturated
glycolated

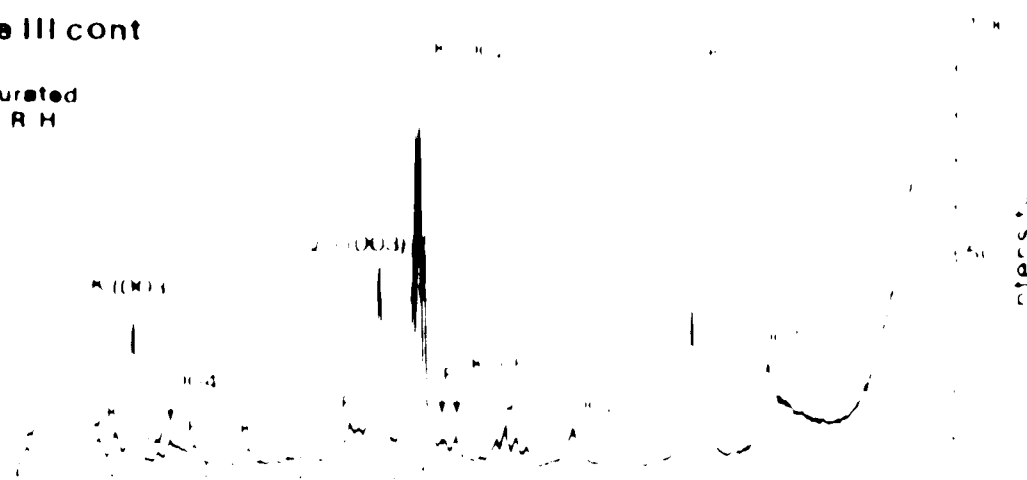


K-saturated
0% R H

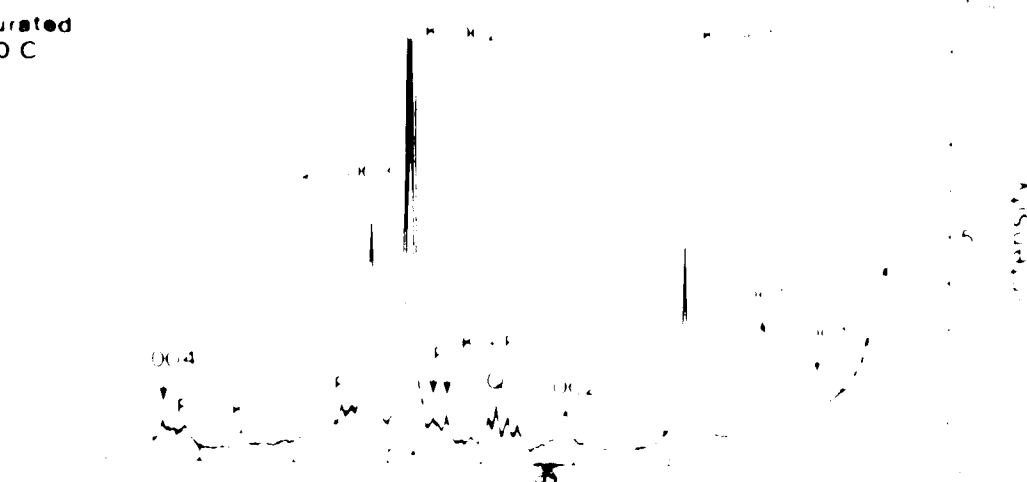


Type III cont

K saturated
54% R.H.



K saturated
300 C



K-saturated
550 C

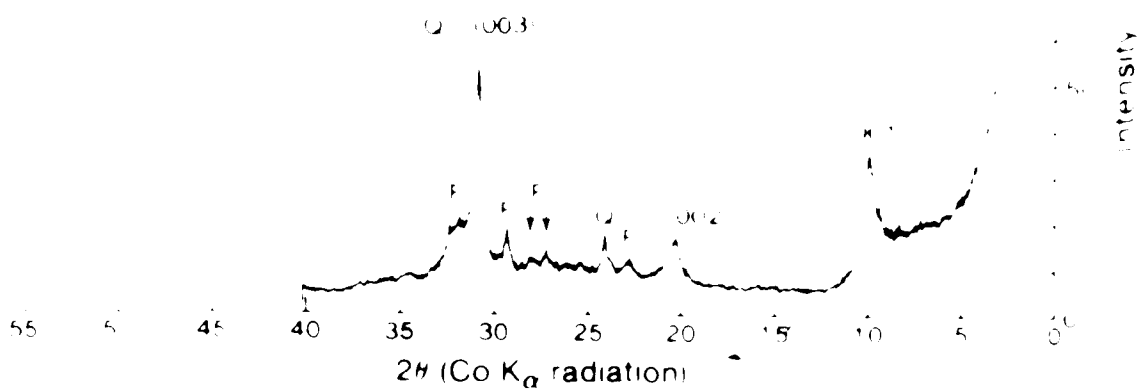


Figure 22A and B

X-ray diffractograms representing a shale interbed in the carbonate cemented sandstone of facies 6 type II clay assemblage. This sample contains 55 per cent illite. Note the peak at 12 Å labelled "S". Upon glycolation, the 12 Å reflection loses intensity and shifts to about 14 Å. The reflection probably represents a randomly interstratified illite-smectite.

Type III

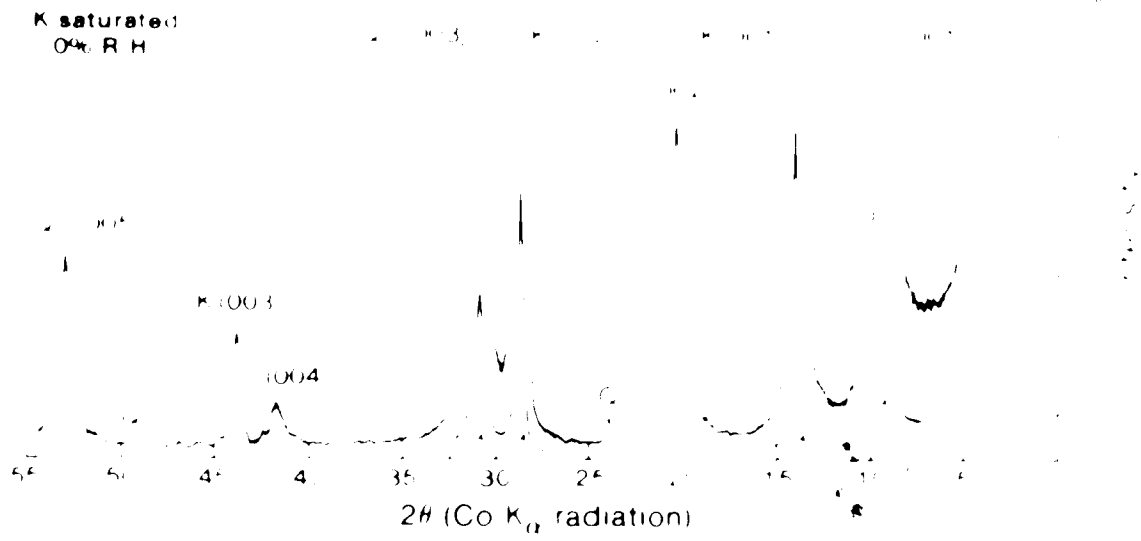
Ca-saturated
54% R.H.



Ca-saturated
glycolated



K saturated
0% R.H.



Type III cont.

K-saturated
54% R.H.



K-saturated
300°C



K-saturated
550°C

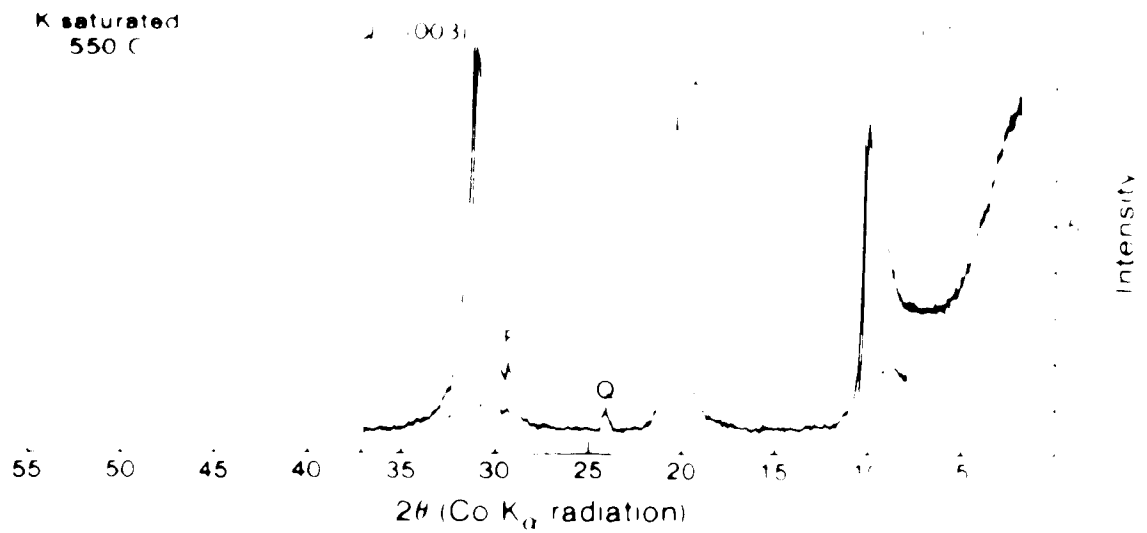
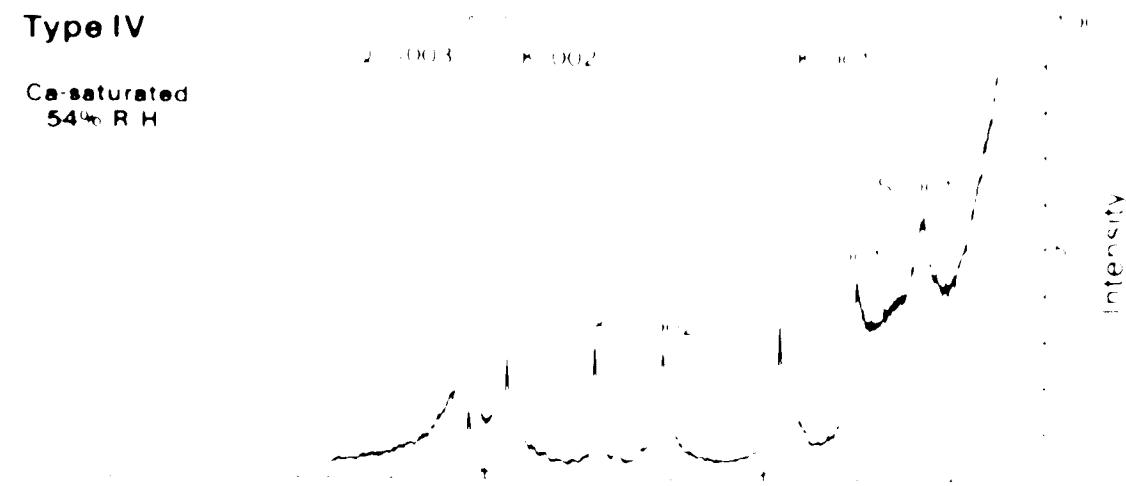


Figure 25 A and B

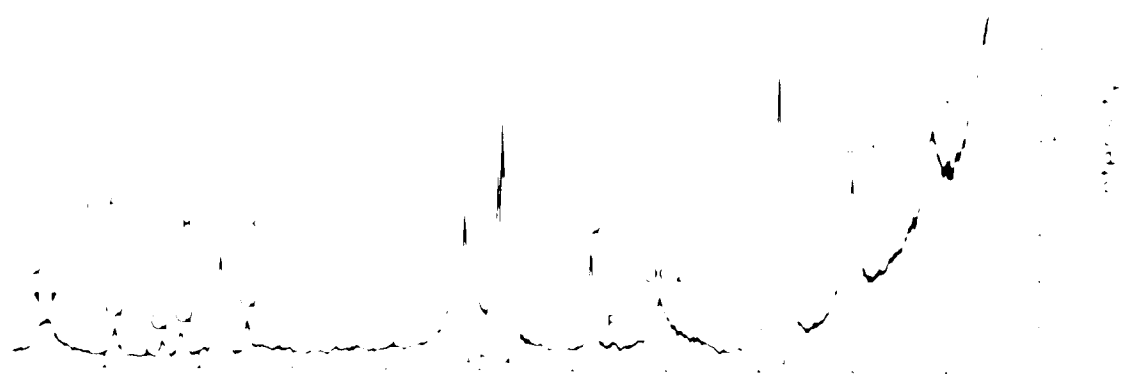
X-ray diffractograms representing the +2 micrometre fraction of an oil-saturated sandstone of facies 4. Type IV clay assemblage. Smectite S content is less than 5 per cent. The smectite M_1 peak is relatively sharp. Clay-saturated patterns. Dismalite M_1 intercalates in trace amounts.

Type IV

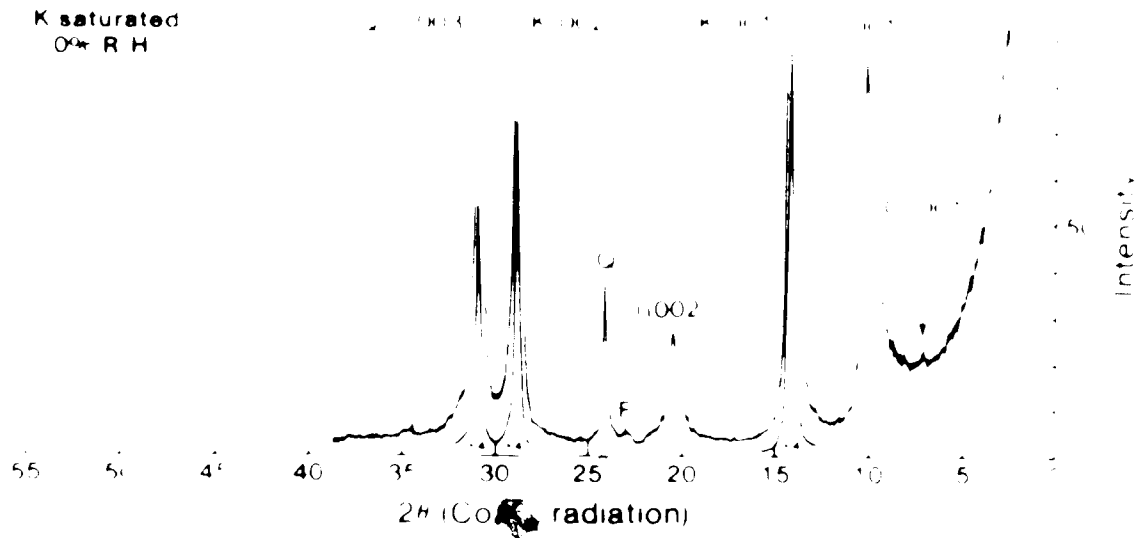
Ca-saturated
54% R.H.



Ca-saturated
glycolated

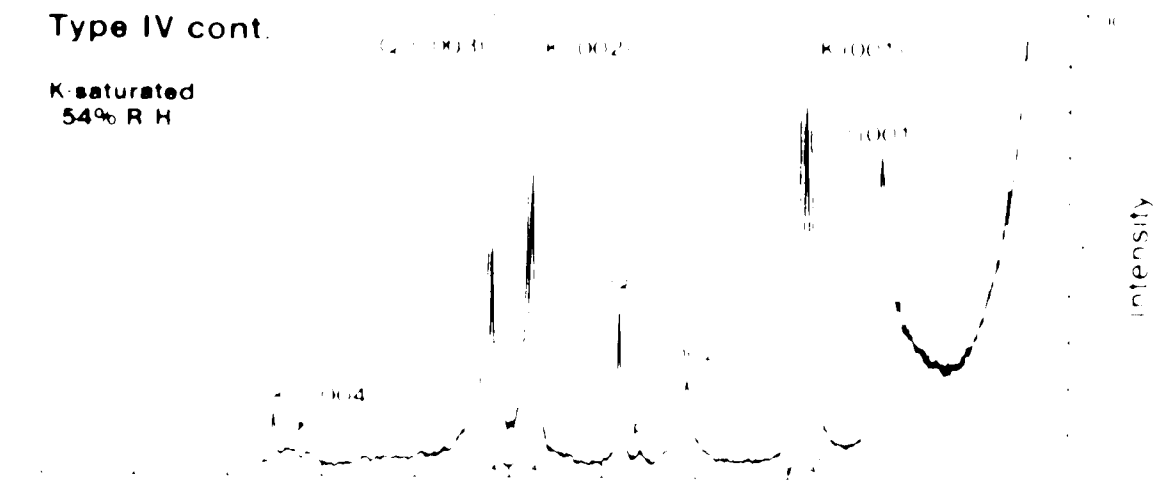


K saturated
0% R.H.

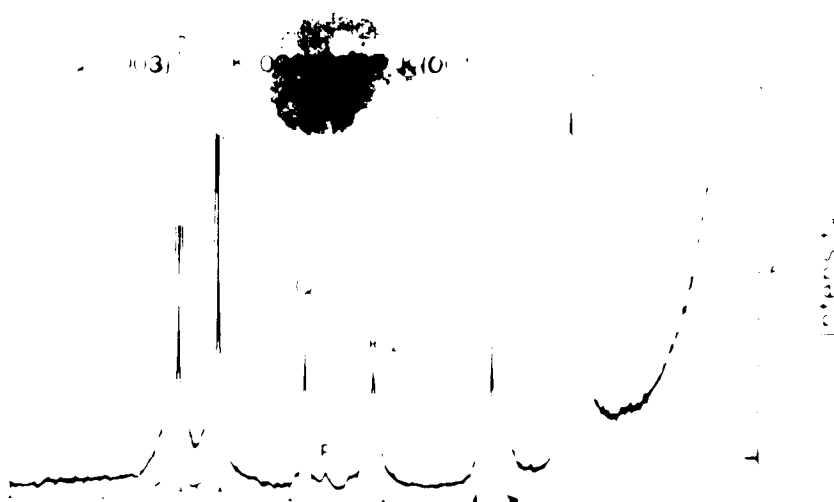


Type IV cont.

K-saturated
54% R.H.



K-saturated
300 C



K-saturated
550 C

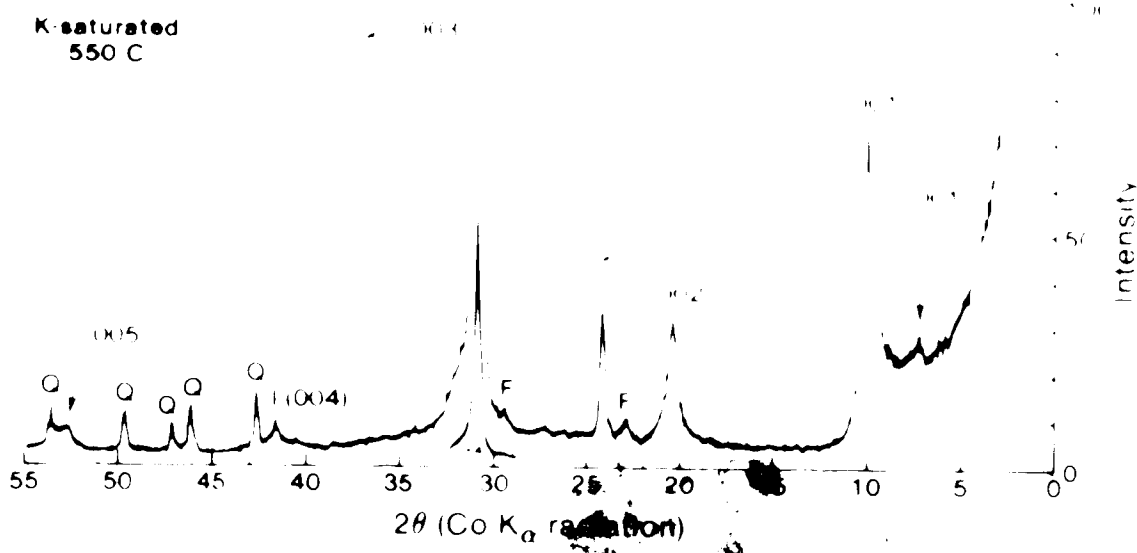


Figure 24A and B

X-ray diffractograms representing the < 2 micrometre fraction of an air-saturated sandstone of facies 4 type IV clay assemblage. Smectite content is less than 1 percent. Smectite (S) is represented by a broad 15 Å reflection which expands to 17 Å upon saturation with ethylene glycol. Discrete chlorite occurs in trace amounts. The chlorite (Ch) peak (10.2 Å) is enhanced upon heating to 550°C (Fig. 24B) and shows as a low intensity broad peak.



Type IV

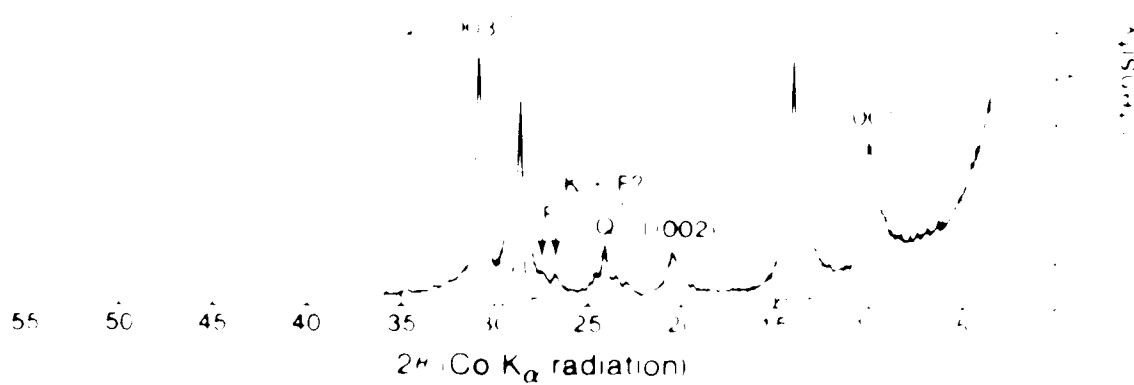
Ca-saturated
54% R.H.



Ca-saturated
glycolated



K-saturated
0% R.H.



Type IV cont.

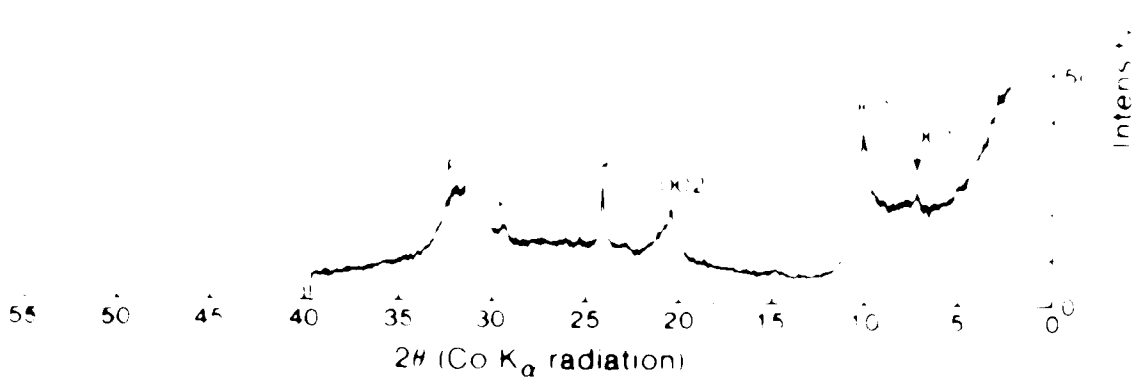
K-saturated
54% R.H.



K-saturated
300°C



K-saturated
550°C



• Paragenetic Sequence

Estimating the paragenetic sequence of the various minerals in a metamorphic rock is based on the following principles:

- **Minerals are stable in certain environments.** This means that a mineral will remain stable as long as it is exposed to the same environment. If the environment changes, the mineral may react with other minerals or with the surrounding rock to form new minerals.
- **Minerals form in a specific sequence.** This means that certain minerals will always form in a specific sequence, regardless of the environment. For example, garnet will always form after kyanite, and staurolite will always form after garnet.
- **Minerals are stable in certain environments.** This means that a mineral will remain stable as long as it is exposed to the same environment. If the environment changes, the mineral may react with other minerals or with the surrounding rock to form new minerals.
- **Minerals form in a specific sequence.** This means that certain minerals will always form in a specific sequence, regardless of the environment. For example, garnet will always form after kyanite, and staurolite will always form after garnet.

• Estimating Paragenesis

Estimating the paragenetic sequence of the various minerals in a metamorphic rock is based on the following principles:

- **Minerals are stable in certain environments.** This means that a mineral will remain stable as long as it is exposed to the same environment. If the environment changes, the mineral may react with other minerals or with the surrounding rock to form new minerals.
- **Minerals form in a specific sequence.** This means that certain minerals will always form in a specific sequence, regardless of the environment. For example, garnet will always form after kyanite, and staurolite will always form after garnet.
- **Minerals are stable in certain environments.** This means that a mineral will remain stable as long as it is exposed to the same environment. If the environment changes, the mineral may react with other minerals or with the surrounding rock to form new minerals.
- **Minerals form in a specific sequence.** This means that certain minerals will always form in a specific sequence, regardless of the environment. For example, garnet will always form after kyanite, and staurolite will always form after garnet.

the upper reaches of the river. At that time, a large segment of the lake was dry, and the water level was about 150 feet above the lake stage. A great amount of material was washed down from the mountainous areas, and the lake became filled with sand and mud. The water level gradually fell, and the lake became a shallow body of water. The lake became filled with silt and mud, and the water level gradually fell again. This process repeated itself several times, creating a series of lakes of varying sizes, some of which are still present today. The lake eventually became a shallow body of water, and the water level gradually fell again. This process repeated itself several times, creating a series of lakes of varying sizes, some of which are still present today. The lake eventually became a shallow body of water, and the water level gradually fell again. This process repeated itself several times, creating a series of lakes of varying sizes, some of which are still present today. The lake eventually became a shallow body of water, and the water level gradually fell again. This process repeated itself several times, creating a series of lakes of varying sizes, some of which are still present today. The lake eventually became a shallow body of water, and the water level gradually fell again. This process repeated itself several times, creating a series of lakes of varying sizes, some of which are still present today. The lake eventually became a shallow body of water, and the water level gradually fell again. This process repeated itself several times, creating a series of lakes of varying sizes, some of which are still present today. The lake eventually became a shallow body of water, and the water level gradually fell again. This process repeated itself several times, creating a series of lakes of varying sizes, some of which are still present today.

Environmental Management

The environmental management of Lake Superior has been a concern for many years. The lake is a major source of drinking water for the surrounding communities, and it is also a popular destination for tourists and recreationists. The lake is home to a variety of fish species, including salmon, trout, and lake whitefish. The lake is also a habitat for many other aquatic life forms, such as mussels, snails, and insects. The lake is a significant part of the local ecosystem, and its health is closely monitored by various government agencies and organizations. The lake is a major source of drinking water for the surrounding communities, and it is also a popular destination for tourists and recreationists. The lake is home to a variety of fish species, including salmon, trout, and lake whitefish. The lake is also a habitat for many other aquatic life forms, such as mussels, snails, and insects. The lake is a significant part of the local ecosystem, and its health is closely monitored by various government agencies and organizations. The lake is a major source of drinking water for the surrounding communities, and it is also a popular destination for tourists and recreationists. The lake is home to a variety of fish species, including salmon, trout, and lake whitefish. The lake is also a habitat for many other aquatic life forms, such as mussels, snails, and insects. The lake is a significant part of the local ecosystem, and its health is closely monitored by various government agencies and organizations. The lake is a major source of drinking water for the surrounding communities, and it is also a popular destination for tourists and recreationists. The lake is home to a variety of fish species, including salmon, trout, and lake whitefish. The lake is also a habitat for many other aquatic life forms, such as mussels, snails, and insects. The lake is a significant part of the local ecosystem, and its health is closely monitored by various government agencies and organizations. The lake is a major source of drinking water for the surrounding communities, and it is also a popular destination for tourists and recreationists. The lake is home to a variety of fish species, including salmon, trout, and lake whitefish. The lake is also a habitat for many other aquatic life forms, such as mussels, snails, and insects. The lake is a significant part of the local ecosystem, and its health is closely monitored by various government agencies and organizations. The lake is a major source of drinking water for the surrounding communities, and it is also a popular destination for tourists and recreationists. The lake is home to a variety of fish species, including salmon, trout, and lake whitefish. The lake is also a habitat for many other aquatic life forms, such as mussels, snails, and insects. The lake is a significant part of the local ecosystem, and its health is closely monitored by various government agencies and organizations.

Third Stage Diagnosis

The first stage of education is pre-school, which is optional. The second stage is primary school, which is mandatory. The third stage is secondary school, which is also mandatory. The fourth stage is tertiary education, which is optional.

the first stage of the research project. The second stage of the project will be the analysis of the data collected during the first stage. This will involve the use of statistical methods to identify patterns and trends in the data. The third stage of the project will be the interpretation of the results obtained from the analysis. This will involve the use of qualitative methods to interpret the results and draw conclusions. The final stage of the project will be the presentation of the findings and recommendations to the relevant stakeholders.

the first time in the history of the world, the people of the United States have been compelled to go to war to defend their country against a foreign nation.

Fourth Stage Stage

the following statement of additional information which may be helpful in the investigation:

The subject is a man of average height and weight, with brown hair and brown eyes. He has a mustache and wears glasses. He is wearing a light-colored shirt and a dark-colored jacket. He is carrying a briefcase.

The subject is a man of average height and weight, with brown hair and brown eyes. He has a mustache and wears glasses. He is wearing a light-colored shirt and a dark-colored jacket. He is carrying a briefcase.

VI. RESERVOIR QUALITY

The reservoir quality of a rock matrix depends on its ability to conduct
fluids after being deformed and fractured. In the early permeability experiments,
it was found that very little information could be derived from the initial
permeability values due to the large amount of fluid required to measure it.

A. Facies A

In the early permeability measurements, the samples were cut from the
matrix of the sandstone, and the rock was then saturated with water.
After the sample had been saturated, the pressure was reduced to 100 psi.
This pressure was considered to be the hydrostatic pressure at the bottom
of the reservoir. At this pressure, the water was found to have a permeability
of approximately 0.0005 Darcies. This value was found to be representative
of the permeability of the sandstone. The permeability of the sandstone
was determined by the use of the pressure drop method. The pressure
was increased in small increments, and the corresponding change in
permeability was measured. The results of these measurements are shown
in the following table. It can be seen that the permeability of the sandstone
is relatively constant, and the permeability of the sandstone is
approximately 0.0005 Darcies. The permeability of the sandstone
was found to be approximately 0.0005 Darcies. The permeability
of the sandstone was found to be approximately 0.0005 Darcies.

B. Permeability and Continuity

PERMEABILITY AND IRREDUCIBLE WATER SATURATION. The relationship between permeability and water saturation has been studied by many researchers. In general, permeability is proportional to water saturation. However, the relationship is not linear. At low water saturations, permeability increases rapidly with increasing water saturation. At higher water saturations, the rate of increase in permeability decreases. This is because at higher water saturations, the water molecules begin to interfere with each other and with the solid particles, reducing the effective pore space available for fluid flow. The relationship between permeability and water saturation can be described by a logarithmic equation:

$$K = K_0 \cdot S^{n-1}$$

where K is permeability, K_0 is a constant, S is water saturation, and n is a constant. The value of n is typically between 0.5 and 1.0. The value of K_0 depends on the rock type and grain size.

PERMEABILITY AND CONTINUITY. The continuity of a reservoir is determined by the size of the pores and the degree of cementation. A reservoir is considered continuous if it contains a single, interconnected system of pores that can be connected by a single path from any point in the reservoir to the surface or to another point in the reservoir. If the reservoir is discontinuous, it consists of separate, isolated systems of pores that are not interconnected. This can occur if the reservoir is fractured or if it contains large amounts of clay minerals that have replaced the original rock matrix.

C. Detrital Clay

DETERRITAL CLAY. Detrital clay is a type of clay that is derived from the weathering of older rocks. It is composed of fine-grained mineral particles that are too small to be classified as silt or sand. Detrital clay is often found in sedimentary rocks, such as shale and mudstone. It is also found in metamorphic rocks, such as schist and gneiss. Detrital clay is often associated with organic matter, such as plant remains and animal fossils. It is often found in association with other minerals, such as quartz and feldspar.

D. Irreducible Water Saturation

THE ARGILLACEOUS SANDSTONES. The argillaceous sandstones are characterized by their high water saturation due to the abundance of detrital kaolinite. Argillaceous sandstones have a high water saturation because they have a high surface area and thus has high irreducible water saturation (Grim 1959). The water is held in the tight sand because of the physical attraction of the water to the clay mineral.

sandstones log calculations may indicate that water saturations are too high for a productive interval. However, the reservoir may be capable of essentially water-free production because the water is predominantly irreducible.

E Fluid Sensitivity

The main concern related to fluid sensitivity in this reservoir pertains to the dispersion of fine kaolinite. Many of these kaolinite plates are very closely attached to grain surfaces and could easily be dispersed by moving fluids and become lodged in pore throats. Gray and Rex (1966) report that damage caused by migration of fines can drop a very permeable sandstone to less than 1 percent of its original permeability within a few hours of time.

Iron-containing minerals are sensitive to oxidation. These minerals dissolve precipitate water, expand, and cause reservoir damage. Although Fe²⁺ is relatively inert at temperatures below 200°C., there is a rapid oxidation rate above 200°C.

Effect of the Application of Wet Forward Combustion on the Reservoir

Wet forward combustion laboratory experiments under simulated field conditions show that the combustion of crude oil in air at ambient temperature is limited where the oil is oxidized at a very small amount of oxygen. The oxygen is adsorbed onto the oil droplets and is rapidly removed by diffusion and volatilization. This results in a rapid increase in the viscosity of the oil. This problem leads to the need for a catalyst to facilitate the conversion of the hydrocarbons to CO₂. The basic requirement for a catalyst is that it be stable, durable, and able to withstand temperatures up to 1,000°C. and pressures up to 100 atm. Mazzola and Murray (1979) report that the most promising catalysts are cobalt and nickel sulfide. They also report that the catalyst must be resistant to mineral acids. Murray and Murray (1979) also state that the combustion of oil in air at ambient temperature is limited by the diffusion of oxygen into the oil. They also suggest that the formation of smoke from the burning oil is the primary cause of heat loss and problems of energy efficiency.

Another reaction which may occur during the *in situ* recovery of bitumen by wet thermal methods is the dissolution and precipitation of SiO₂ (Boon 1979). Low quartz and amorphous silica may dissolve when temperature and pH are increased and precipitate as the fluid reaches cooler regions. Such fluid-rock interactions can lead to a change in reservoir properties such as reduced porosity and permeability and to an undesirable composition of produced fluids suspended clays, high dissolved silica and a high degree of hardness (Boon 1979). Chert percentage in the bitumen-saturated portion of the Glauconitic Sandstone in the SHOP project is about 20 per cent (Table 1). This chert may be particularly susceptible to dissolution under raised temperature and pH conditions.

VIII. CONCLUSIONS

Three factors control the distribution of hydrocarbons and the reservoir quality in the Glauconitic Sandstone within the Suffield area. They are (1) sedimentology, (2) structure, and (3) mineralogy and diagenesis.

A. Sedimentological Controls

Hydrocarbons are located along a northwest to southeast trending broad arch of thick, vertically continuous sandstone. The sandstone consists of facies representing in ascending order, the shoreface, foreshore, backshore, marsh and lagoonal or continental zones of a progradational beach or barrier island complex. The facies representing the foreshore zone (laminated sandstone cf. facies 4) was deposited under high energy conditions and has good reservoir properties: high porosity, low clay content, and good lateral and vertical continuity. Fluctuating energy conditions and bioturbation in the backshore zone created a rock with poor reservoir properties in facies 3 (argillaceous or bioturbated sandstone facies). This unit is characterized by low porosity and high clay content with only isolated porous zones. Tidal inlet and channel deposits occurring along the sandstone trend disrupt the continuity of the reservoir.

B. Structural Controls

Basement faults, possibly related to tectonic activity associated with the North Battleford Arch and active during late Mannville time, have caused downfaulting of blocks of sandstone such that nondepositional facies changes occur. Thus the major trapping mechanism is stratigraphic with some structural effects.

Movement on basement faults during deposition of the Glauconitic Sandstone is most likely responsible for the locally occurring unusually thick (45m) progradational beach deposits. Areas with the thickest sandstone accumulations were probably located over downfaulting basement blocks. The rate of subsidence equalled the rate of sediment input such that the shoreline remained in a relatively stable position and facies accumulated vertically.

C. Mineralogical and Diagenetic Controls

The Glauconitic Sandstone is a litharenite composed of quartz, chert, other sedimentary rock fragments, and trace amounts of feldspar. The dominant clay mineral is kaolinite which occurs in both detrital and authigenic forms. It is the abundance of detrital kaolinite present in the rock which determines the reservoir quality. The bioturbated or structureless facies 3 with abundant detrital clay forms a poor reservoir whereas the clean nonargillaceous facies 4 has good reservoir qualities. Porosity and permeability is only slightly reduced in the clean sandstones by diagenetic forms such as kaolinite, quartz overgrowths and deformed rock fragments.

The paragenetic sequence is: (1) first stage calcite cement and pyrite crystallization; (2) quartz cementation and kaolinite growth; (3) second stage calcite cementation, feldspar leaching, minor kaolinite illite development, and growth of calcite crystals; and (4) smectite chlorite crystallization and the emplacement of hydrocarbons.

The main concern related to fluid sensitivity is the dispersion of kaolinite, iron-containing minerals (pyrite and Fe-chlorite) which are sensitive to acidification occur only in trace amounts. When the temperature of the reservoir is raised during the wet combustion process, kaolinite, quartz and dolomite may react to form the swelling clay smectite. Further reduction in permeability, may result from dissolution and reprecipitation of SiO₂-quartz and particularly chert.

D Recommendations for Future Work

Areas for further study include regional sedimentology and diagenesis. Preliminary examination of core from the eastern sandstone belt centred in range 7 townships 19 and 20 suggest that conglomerates with shale interbeds within this belt represent offshore storm deposits. Further study is necessary to negate or substantiate this idea. The Glauconitic Sandstone in the Suffield area is only a small part of the extensive regional Glauconitic Sandstone for which the entire depositional picture is yet to be understood. Stable isotope analyses are needed to develop a further understanding of water-rock interaction during diagenesis. With similar objectives in mind, new cores should be drilled in the SHOP project site after the combustion front has past through the area. Samples from these new cores should be examined in thin section and by SEM to

evaluate any reservoir damage due to water-rock interaction during stimulation

PLATE 1: Core Photographs for Facies 6 to Facies 3d.

- 1 **Facies 6b** Light grey to light brown very fine to fine grained sandstone with well-defined laminations
 Left Wave-rippled sandstone with a thin shale interbed at the base of the photograph
 Centre Ripple troughs and subhorizontal planar laminations defined by carbonaceous debris
 Right Cross-laminated very fine grained sandstone near the base of the Glauconitic Sandstone
- 2 **Facies 6b** Calcite-cemented siltstone or very fine grained sandstone
 Left Calcite-cemented sandstone with low angle planar laminations. The circular homogenous patches in the lower right of the photograph are probably burrows
 Right Calcite-cemented sandstone with interbeds of carbonaceous shale. The shale has syneresis cracks and the bed is partially bioturbated
- 3 **Facies 6a** Bioturbated structureless or indistinctly laminated fine grained sandstone
 Left Generally structureless sandstone poorly defined laminations in lower portion of photograph
 Right Bioturbated zone in upper portion of photograph to structureless in the lower portion
- 4 **Facies 5** Medium grained sandstone interbedded and interlaminated with fine-grained sandstone
 Left Thicker medium grained sandstone bed with erosional base. The bed fines upward to fine grained sandstone
 Right Low angle planar laminated medium and fine grained sandstone
- 5 **Facies 4** Horizontal laminated to low angle cross laminated fine grained sandstone. Low angle cross laminations
- 6 **Facies 4** Low angle planar laminations. The black piece of core at the top of the photograph is an uncleaned oil-saturated portion
- 7 **Facies 3d** Fine grained sandstone with variable sedimentary structures and argillaceous zones. This facies is characterized by patches with good oil saturation interrupted by zones with poor oil saturation or no saturation
 Left Zone with irregular bedding and patchy oil saturation. The upper part of the slab has been cleaned but the lower portion demonstrates an oil saturated lens surrounded by a nonsaturated clay rich sandstone
 Left centre Slightly coarser sandstone interbeds and lenses. This slab has been cleaned
 Right centre Relatively high angle laminated nonargillaceous sandstone. Both pieces have been cleaned but they probably had good oil saturation originally
 Right Sandstone breccia. The laminated breccia blocks are angular and randomly oriented. The matrix is a slightly coarser clay rich sandstone

Scale: An core in the photographs is 3 inches (7.6 cm) wide

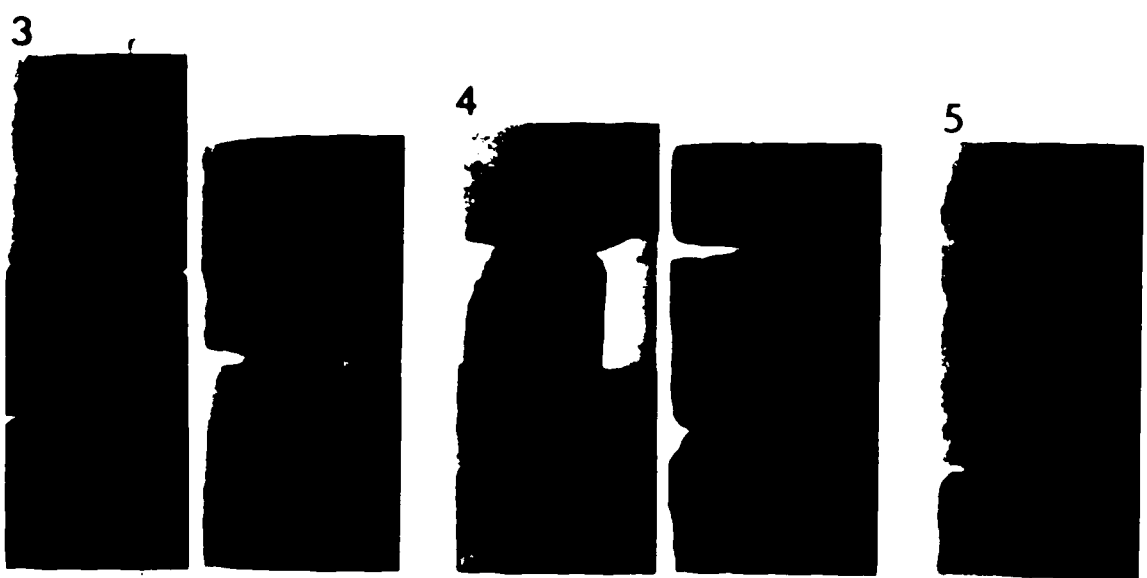
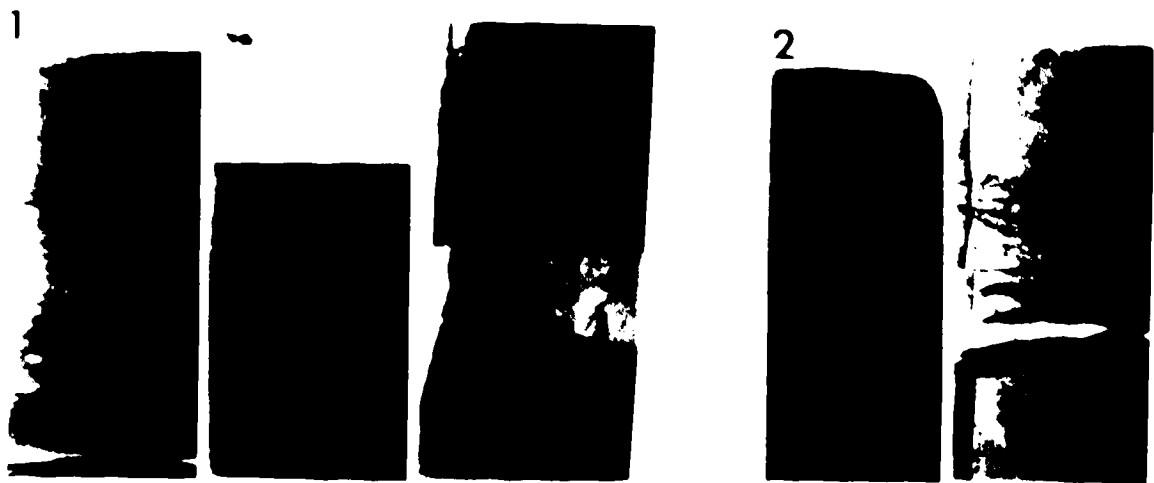


PLATE 2 Core Photographs for Facies 3c to Facies 1

- 1 **Facies 3c** Facies 3c is more argillaceous than facies 3d and lacks any regular bedding
 Left Indistinctly bedded sandstone with patchy oil saturation
 Centre Bioturbated sandstone
 Right Structureless argillaceous sandstone
- 2 **Facies 3bi** Bioturbated argillaceous sandstone
 Left Bioturbated to structureless sandstone
 Right Bioturbated sandstone with clay streaks
- 3 **Facies 3bii** Cross-laminated sandstone unit overlain by a breccia
 Left Structureless fine-grained sandstone containing coarse grained pyrite overlain by cross-laminated sandstone
 Right Breccia Disrupted zone with carbonaceous rootlets and irregularly shaped subrounded blocks. Breccia blocks are finer grained than the matrix
- 4 **Facies 3biii** Laminated to low angle cross laminated argillaceous sandstone
 Laminations are defined by coarse sand sized magnetite grains
- 5 **Facies 3a** Light brown rooted argillaceous sandstone
- 6 **Facies 2** Carbonaceous sandstone and shale
 Left Dark grey sandy shale The base of the unit is an irregular boundary marked by a colour change from medium or light grey (facies 3) to dark grey facies 2
 Right Poor quality coal overlain by bioturbated carbonaceous shale
- 7 **Facies 1** Very fine grained sandstone siltstone and shale
 Left Structureless to laminated medium grey shale with light grey silt interlaminations and small burrows
 Right Interlaminated siltstone and shale rippled to cross laminated with shelled burrows carbonaceous debris along some laminations

Scale All core in the photographs is 3 inches (6 cm) wide

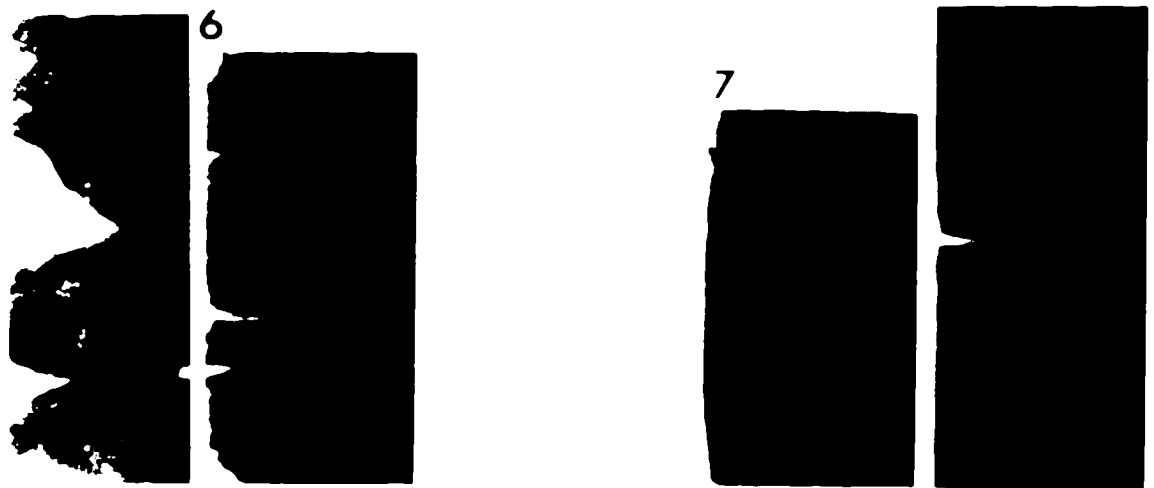
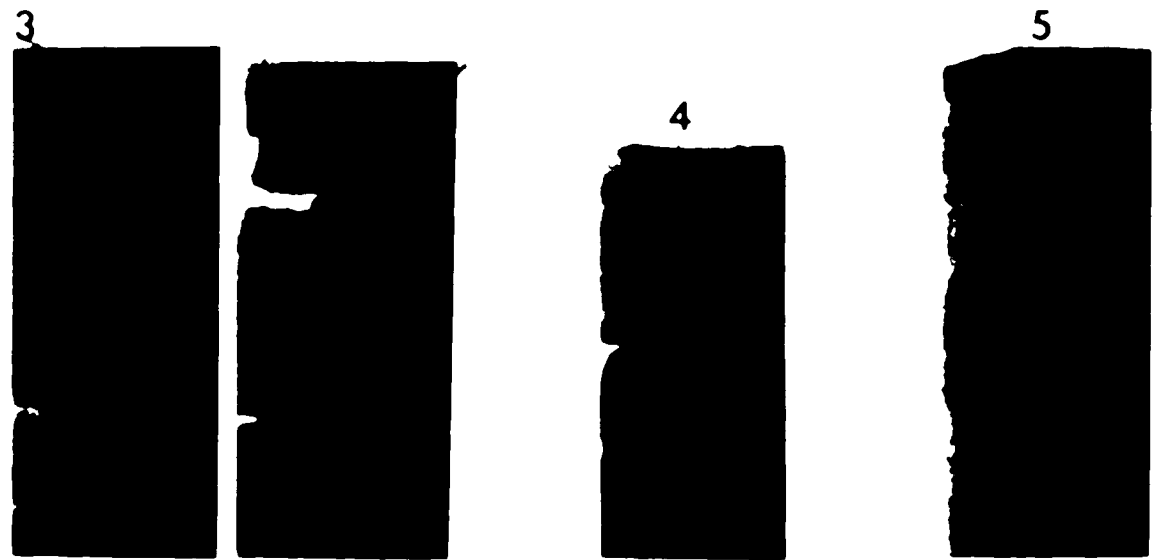


PLATE 3 Thin Section Textures for Facies 5 and Facies 3bIII

- 1 Facies 5 Thin section photomicrograph of a sample from facies 5 showing bimodal grain size with coarser chert grains (Ch) and fine quartz (Q). Chert grains have low sphericity and are more angular than the quartz. Plane polarized light.
- 2 Facies 3bIII Thin section photomicrograph of a sample from facies 3bIII showing the preferential horizontal fabric resulting from compaction flattening of soft rock fragments (RF) and orientation of elongate chert grains (Ch). Feldspars (F) (K feldspar and plagioclase) are more abundant than in other facies. Plane polarized light.

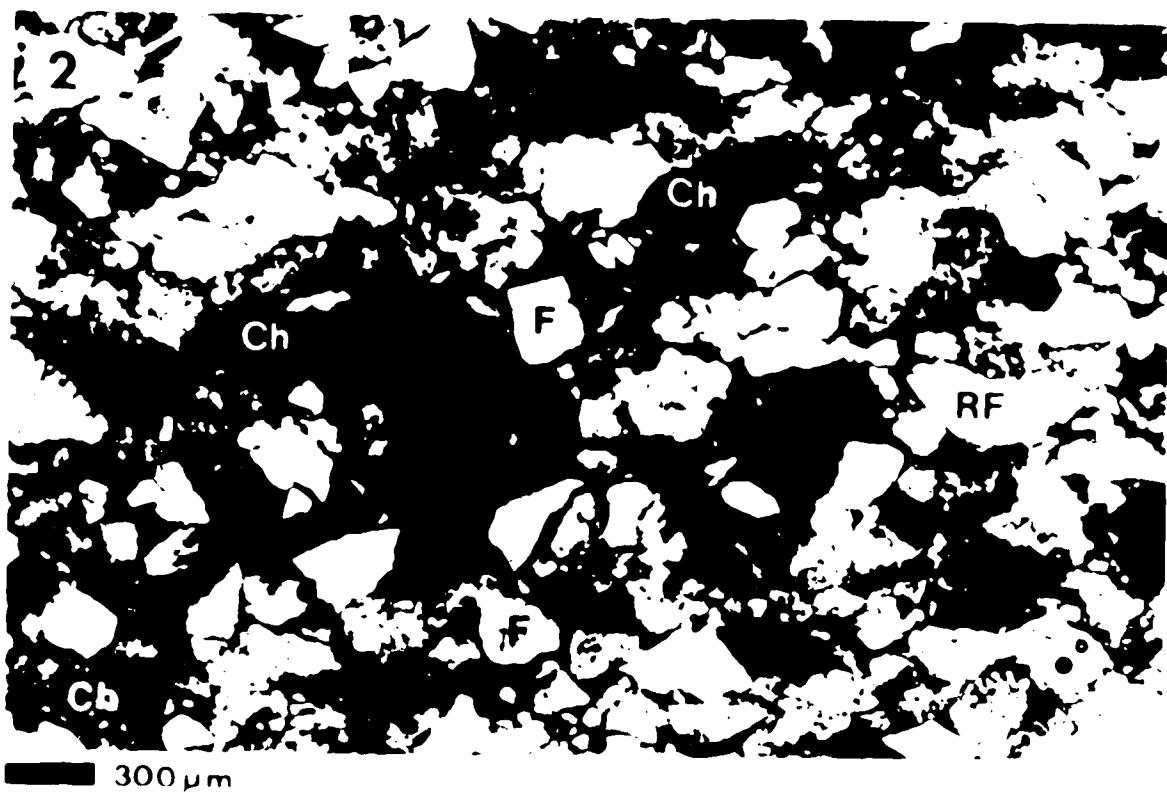
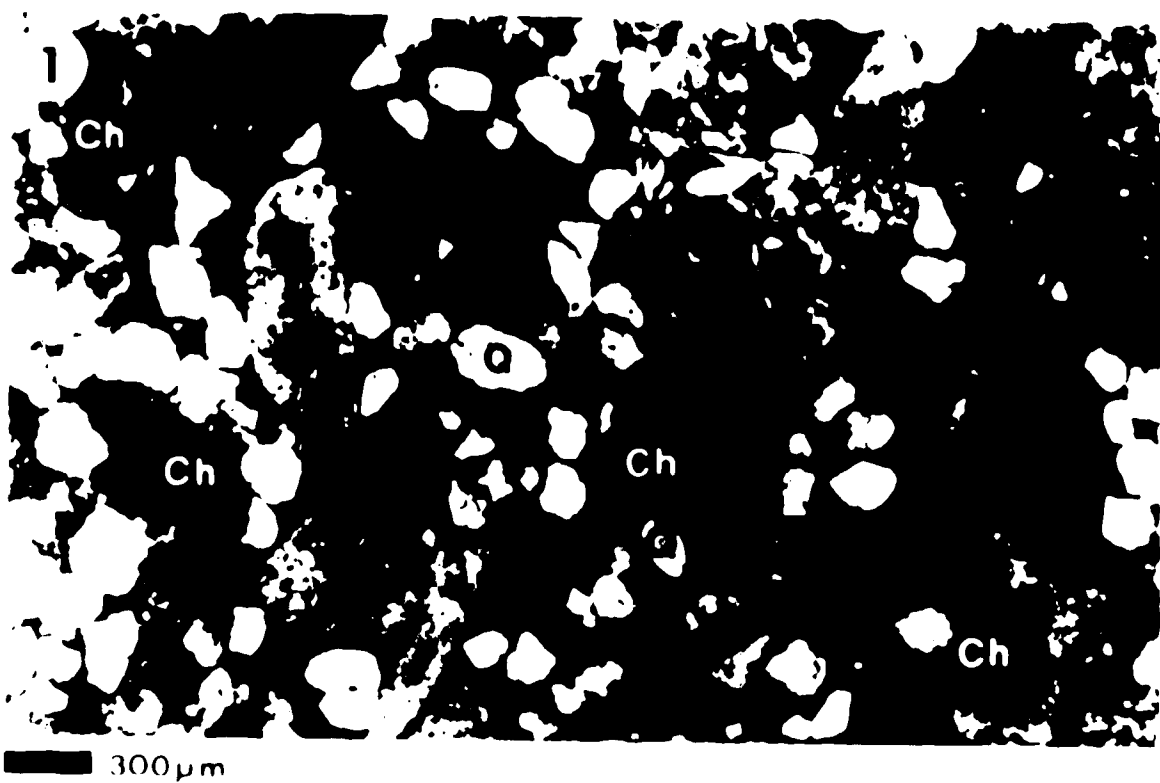


PLATE 4 Bulk Mineralogy

- 1 The detrital shape of some quartz grains is defined by a thin line of abundant inclusions trapped at the boundary between detrital and authigenic quartz (short arrow right side of thin section photomicrograph). Other quartz overgrowths produce an interlocking of quartz grains (long arrows left side of photomicrograph) such that original detrital shape is not obvious. Plane polarized light Scale bar is 100 micrometres
- 2 Thin section photomicrographs showing:
 - (a) microcrystalline chert Plane polarized light
 - (b) macrocrystalline chert Crossed nicols
 - (c) chalcedonitic chert Crossed nicolsScale bar is 100 micrometres
- 3 Thin section photomicrograph showing a deformed siltstone fragment (RF). Plane polarized light Scale bar is 100 micrometres
- 4 Thin section photomicrograph showing a deformed argillaceous rock fragment (RF). Note the lack of intergranular pore space associated with the rock fragment. Plane polarized light Scale bar is 100 micrometres

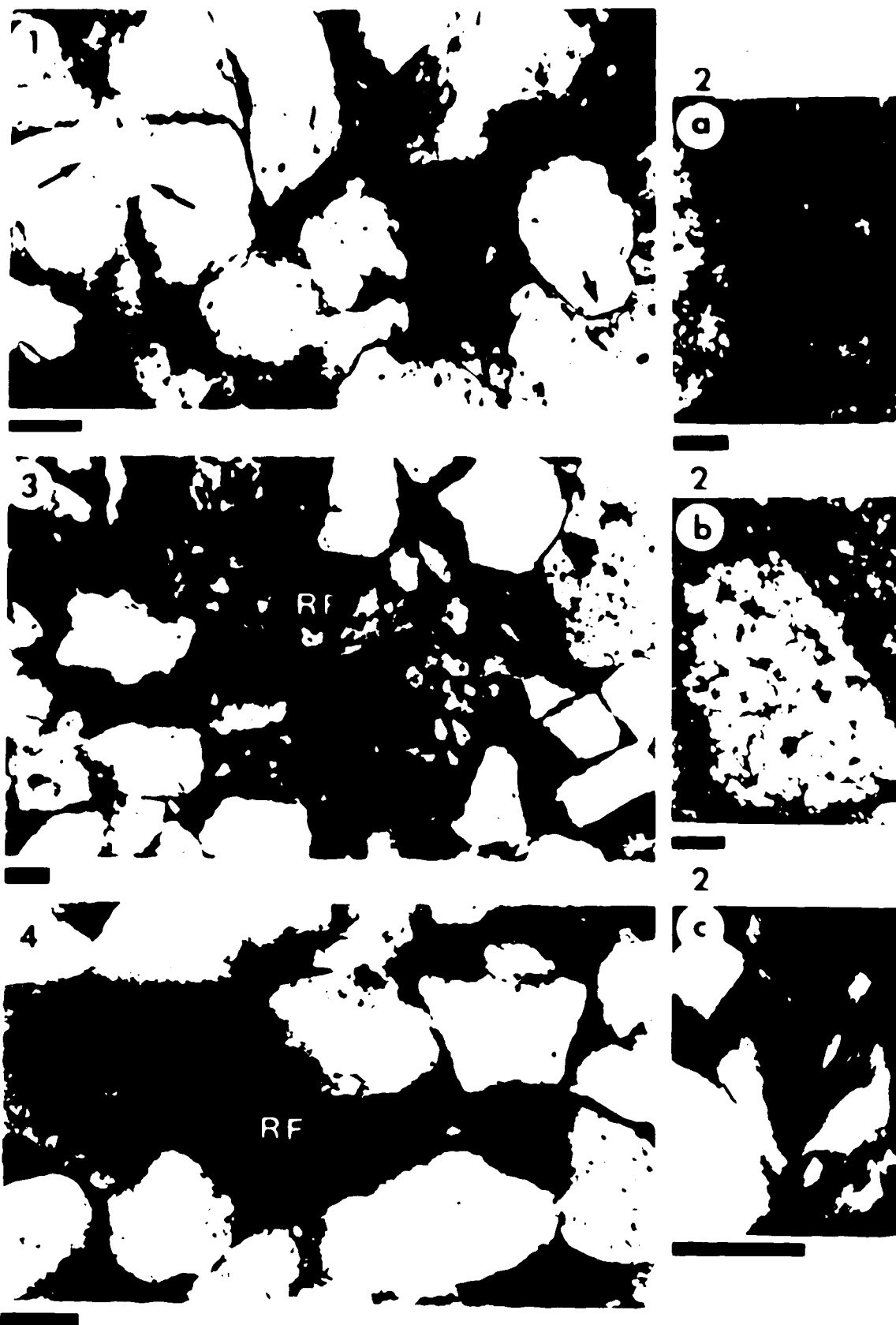


PLATE 5: Bulk Mineralogy and Texture of the Argillaceous Sandstone, Facies 3

- 1 Thin section photomicrograph showing the skeletal framework of a corroded feldspar (F). Note the secondary porosity (P) created by the corrosion of the grain Plane polarized light
- 2 Thin section photomicrograph showing carbonate grains (dolomite or siderite). The black arrow (upper left) points to a median grain sized zone of carbonate which has interlocking contacts with adjacent grains. The interlocking contacts may be either the result of remobilization of a carbonate grain or due to a combination of both quartz and carbonate overgrowths. The white arrows point to a carbonate zone which is a larger than median grain size. Contacts with adjacent grains are interlocking and this carbonate probably represents a very local early diagenetic cement Plane polarized light
- 3 SEM photomicrograph of pyrite (Py) associated with clay on a pore wall
- 4 SEM photomicrograph of an organic structure replaced by pyrite (Py) subfacies 3a
- 5 SEM photomicrograph of a very argillaceous sample from facies 3. Masses of very fine kaolinite coat the grains and fill the pores
- 6 Thin section photomicrograph showing a silt size quartz and clay matrix surrounding sand sized grains (Q) chert (Ch) Plane polarized light

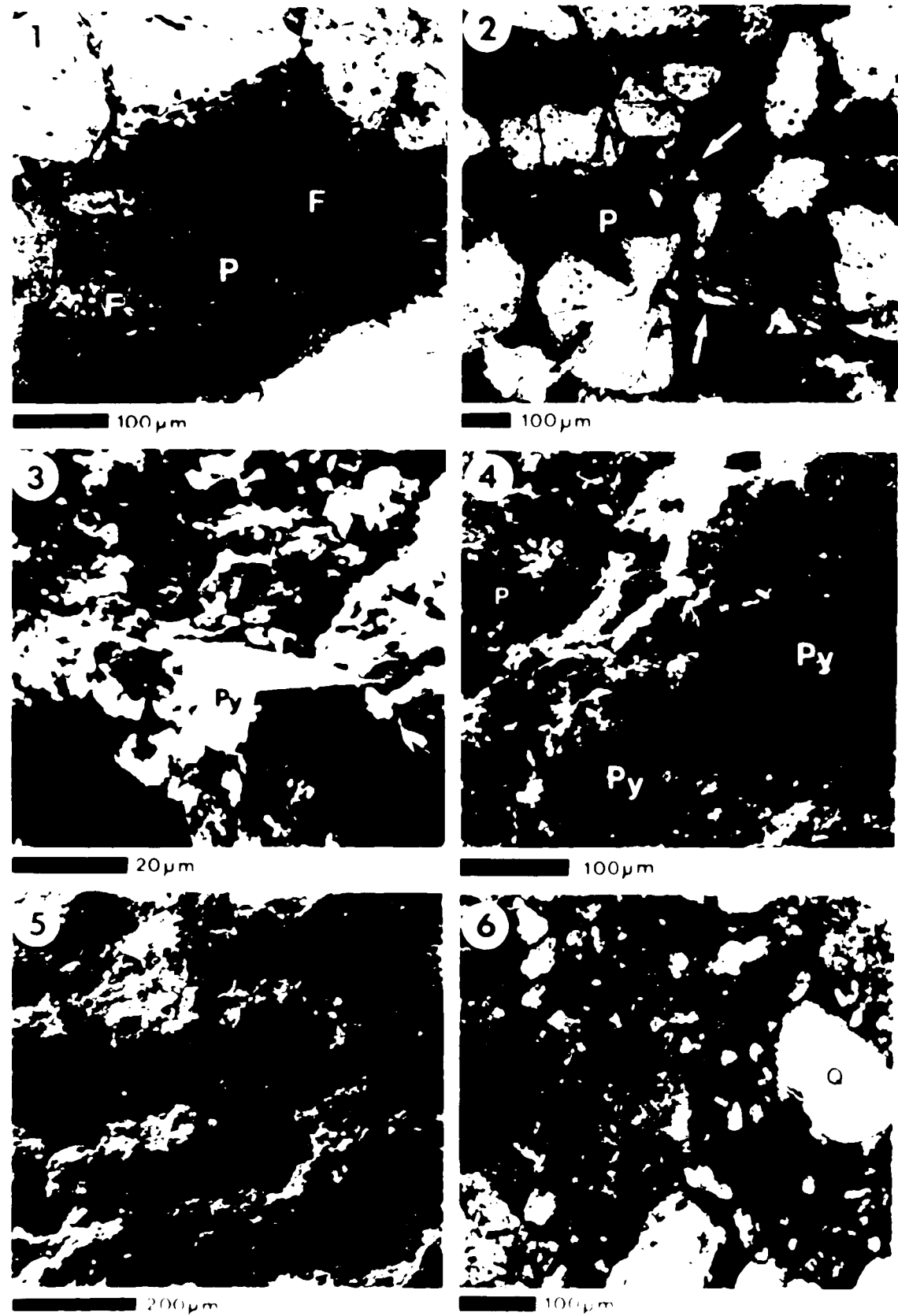


PLATE 6. Pore Space Reduction by Kaolinite and Quartz

- 1 SEM photomicrograph showing a sheet composed of very fine clay attached to a detrital grain and extending into the pore space
- 2 SEM photomicrograph showing the majority of pore space filled by fine detrital kaolinite (dK). Most of the remaining pore space is filled by authigenic kaolinite (ak) and quartz overgrowths (Q)
- 3 SEM photomicrograph of large authigenic vermicular kaolinite (vk) filling much of the pore space. Note the smaller vermicular kaolinite (white arrow) on the surface of the large kaolinite
- 4 SEM photomicrograph showing the occlusion of porosity by vermicular kaolinite (vk) and quartz overgrowths (Q). Note the smaller authigenic kaolinite (arrows) sitting on the larger forms
- 5 SEM photomicrograph showing a mass of kaolinite booklets (k) sitting on quartz overgrowths (Q) and reducing pore space. This kaolinite-quartz relationship indicates that kaolinite formed after completion of the quartz overgrowth
- 6 SEM photomicrograph showing a silt-sized cluster of authigenic quartz (q) and kaolinite (k) reducing the pore size. This kaolinite-quartz relationship suggests that quartz and kaolinite grew at approximately the same time

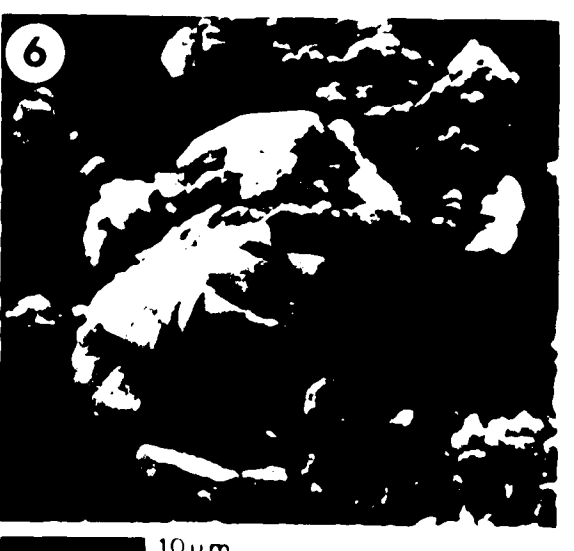
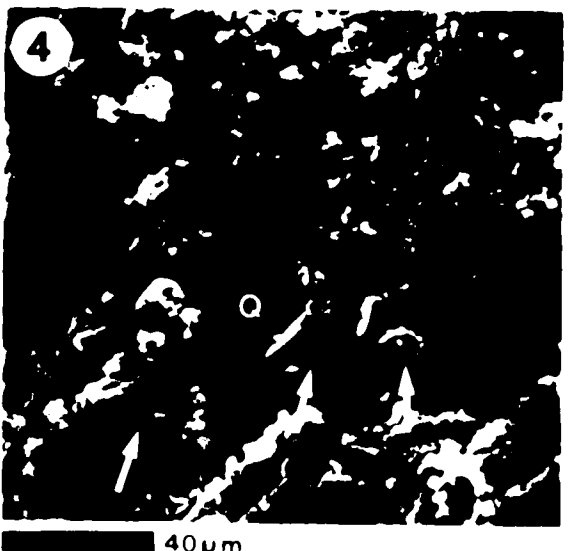
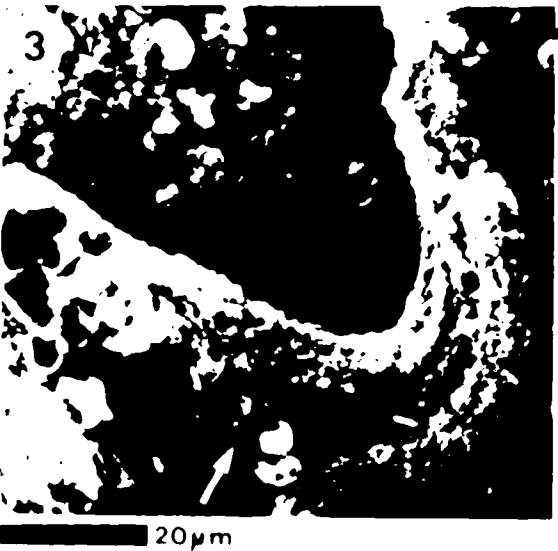
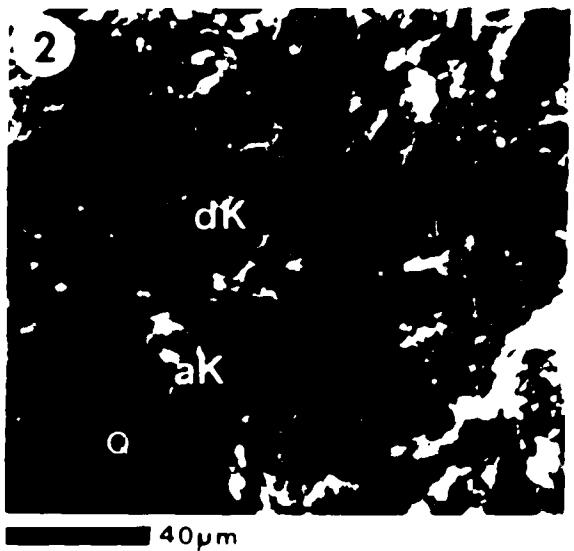
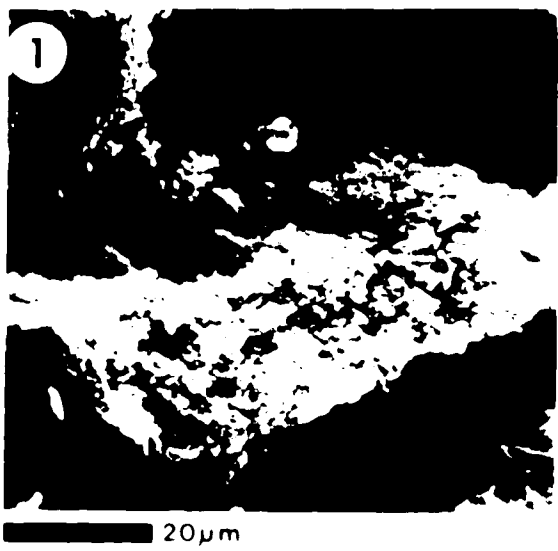


PLATE 7: Morphologies of Illite and Smectite

- 1 SEM photomicrograph of a clay ridge on a detrital grain. This clay ridge has an illitic component but may contain very fine detrital kaolinite or a mixed layer illite-smectite
- 2 SEM photomicrograph of a very fine grained, delicate clay coating (white arrow) on a kaolinite booklet and extending across a pore space. This authigenic clay coating is probably illite or interstratified illite-smectite
- 3 SEM photomicrograph showing a rare occurrence of smectite in a honeycomb-like growth habit (white arrow)
- 4 SEM photomicrograph of a sample with approximately 5 per cent smectite in the clay fraction. Note the abundance of clay ridges on the detrital grains

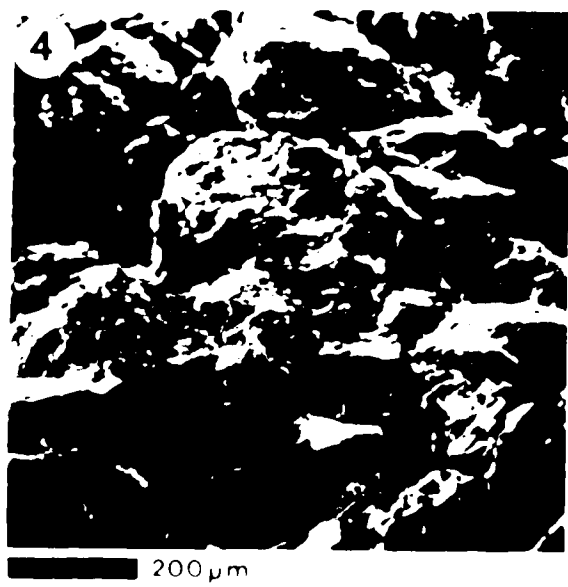
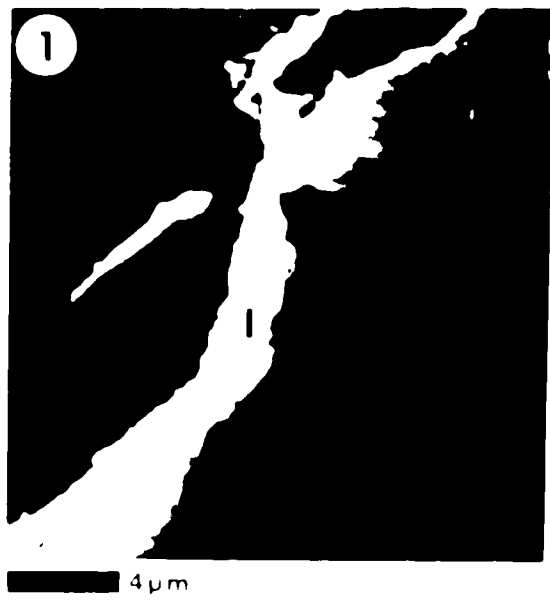


PLATE 8: Paragenetic Sequence

- 1 Thin section photomicrograph of a calcite-cemented sandstone. Dark material surrounding grains is calcite cement (C). Note the loose grain packing with few grain-to-grain contacts, and the lack of clay rims around grains. This sandstone was probably cemented very soon after sedimentation. Plane polarized light.
- 2 Thin section photomicrograph showing a close-up of the calcite cement (C). Note the coarse texture of the cement. The dark patches in the cement are zones which have stained a darker pink. These zones have fewer impurities than the lighter pink patches and may represent partial recrystallization of the early calcite cement. Crossed nicols.
- 3 SEM photomicrograph showing a close association of kaolinite (K) and quartz overgrowths (Q). The arrow points to a zone where the presence of the kaolinite inhibited completion of the quartz overgrowth. The quartz overgrowth probably began forming before the kaolinite grew but continued after kaolinite formation.
- 4 SEM photomicrograph showing a kaolinite booklet (K) embedded in calcite cement (C). The kaolinite was present at the time of carbonate cementation.
- 5 SEM photomicrograph showing kaolinite (K) in the pore space created by feldspar (F) dissolution. This association of kaolinite with the corroded feldspar grain suggests that kaolinite was formed as a result of the feldspar dissolution. An earlier stage kaolinite (black K) grew on the uncorroded feldspar surface.
- 6 SEM photomicrograph of calcite cubes in the pore space created by dissolution of feldspar. This association indicates that calcite crystals grew after feldspar dissolution.

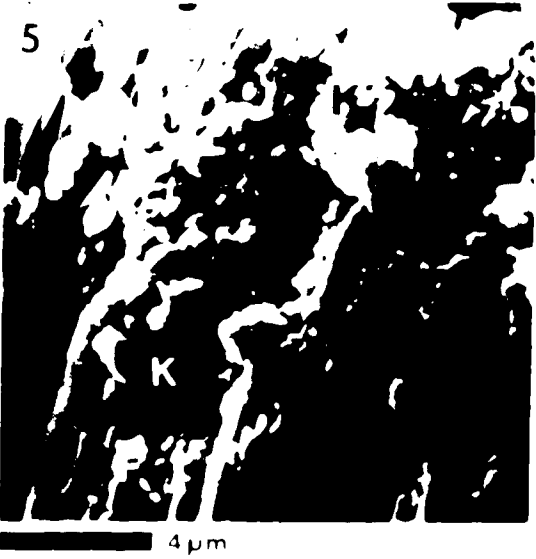
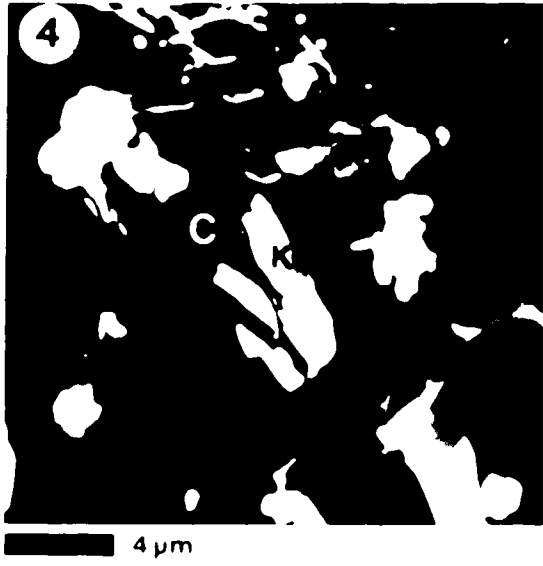
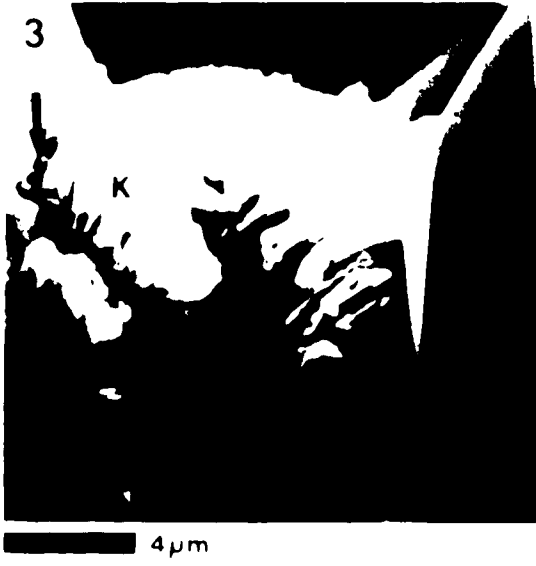
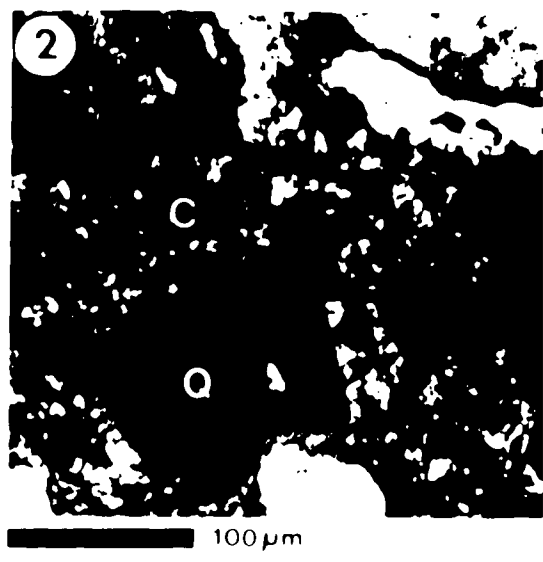
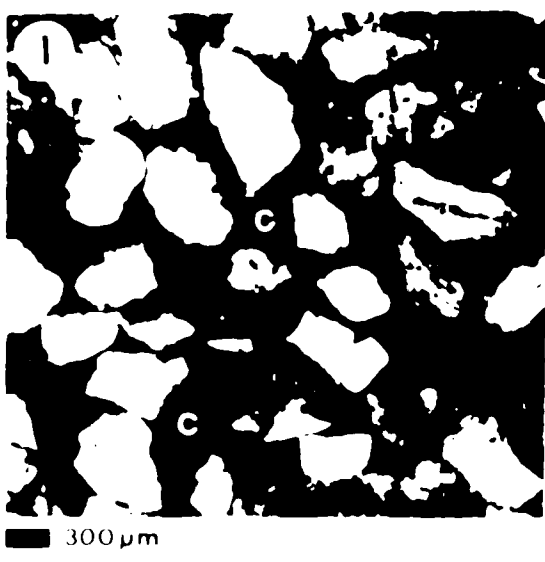
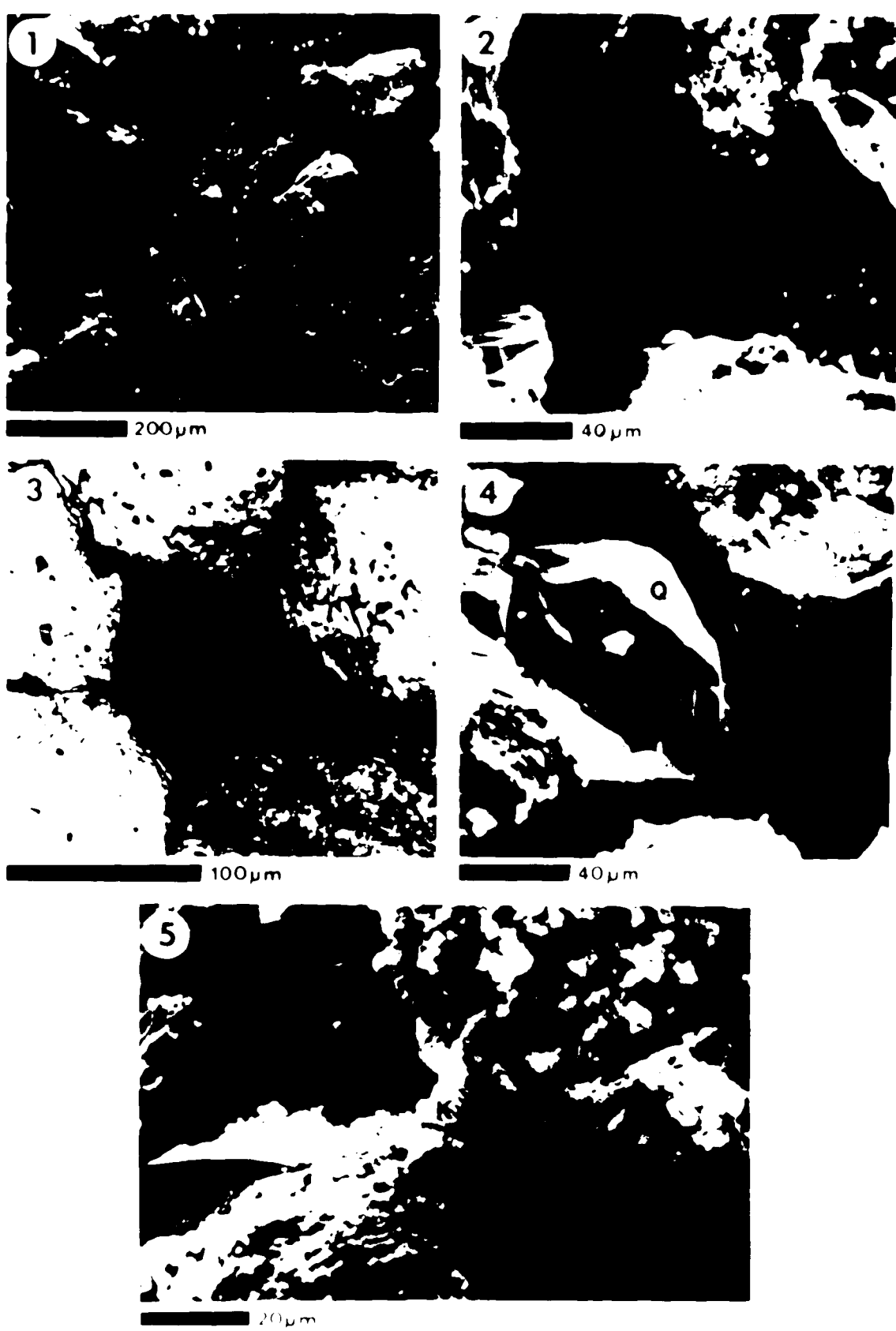


PLATE 9 Pore Morphology

- 1 SEM photomicrograph of a sample from the laminated facies 4. Note the good porosity slightly reduced by quartz overgrowths and scattered clusters of authigenic clays.
- 2 SEM photomicrograph showing a typical clean pore from a sample representing facies 4. The pore space has been reduced in size slightly by local clusters of authigenic kaolinite (AK) and quartz overgrowths (Q).
- 3 Thin section photomicrograph showing a pore space (P) lined by masses of authigenic kaolinite (AK). Plane polarized light.
- 4 SEM photomicrograph showing the occlusion of pore space by quartz overgrowths (Q).
- 5 SEM photomicrographs showing a cluster of kaolinite coating the grain and extending across the pore to form a pore bridge and permeability barrier.



IX. REFERENCES

- AAPG Nomenclature Committee. 1980. Summary of recommendations of AAPG Nomenclature Committee (Clays and Clay Minerals). Vol. 28, No. 1, p. 1-10.
- Alberta Energy Petroleum Geologists. 1960. *Lexicon of Geologic Names in the Western Canada Sedimentary Basin and Arctic Archipelago*. John C. McAna Limited, Calgary. 380p.
- Anderson, V.H. and Davies, J.H. 1979. Regional diagenetic trends in the lower metasediments of Muddy Sandstone Flounder River Basin. In: Peter A. Scholle and Paul H. Schluger (eds.), *Aspects of Diagenesis*. SEPM Special Publication No. 26, p. 319-341.
- Barnes, S.E. 1977. Chlorites and hydroxy-interlayered vermiculite and smectite. In: D.L. Clark and J.B. Weed (eds.), *Minerals in Soil Environments*, 2nd. ed., p. 1-16. American Society of Masicology, p. 357-389.
- Davies, J.H. and Davies, J.A. 1977. Low temperature synthesis of smectite, illite, quartz and kaolinite. Clay and Clay Minerals, v. 25, p. 114-119.
- Hemond, G., Moore, R.S. and Rodney, S. 1979. Alberta Energy Company test number 4. Department of Chemical Engineering, University of Alberta.
- Hennings, M.A., Le Blanc, R. and MacEachern, F. 1962. The eastern Gulf of Mexico - Southeast Texas Province of the East and Central Texas gulf coast. Geological Survey, p. 138-224.
- Holland, T. H. 1965. Mineralogy and sedimentation in the recent deep sea off the Atlantic Ocean and adjacent seas and oceans. Beaufortia Series, 1st. America, Bulletin, v. 16, p. 81-182.
- Blatt, Harve. 1979. Diagenetic processes in sandstones. In: Peter A. Scholle and Paul H. Schluger (eds.), *Aspects of Diagenesis*. SEPM Special Publication No. 26, p. 141-157.
- Rodney, A. 1977. Fluid-rock interactions during steam injection. In: J. A. Reynolds and A. Greenstock (eds.), *The Oil Sands of Canada*. Venezuela, 1977. The Canada Institute of Mining and Metallurgy, p. 135-158.
- Ward, J.W. 1980. Order-disorder in clay mineral structures. In: J.W. Brindley and J.B. Way (eds.), *Crystal Structures of Clay Minerals and their X-ray Identification*. Mineralogical Society, London. 495p.
- Brindley, Rodney S. 1976. Computer analysis of sand and petroleum distribution in the Mannville Group, Turner area, Southern Alberta. University of Alberta M.Sc. thesis. 104p.
- Carter, Charles M. 1978. A regressive barrier and barrier-protected deposit.

- Depositional environments and geographic setting of the late Tertiary
Cochransey Sand. *Journal of Sedimentary Petrology*, vol. 48, No. 3, p.
933-950.
- Conybeare, C. B. 1976. Geomorphology of Oil and Gas Fields in Sandstone Bodies.
Developments in Petroleum Science. 4. Elsevier Scientific Publishing
Company, New York, p. 231-233.
- Murray, R. and Moore, D.G. 1964. Holocene regressive off-shore sand, Costa (De Nayarit)
Mexico. In: M. van Straaten (ed.), *Deltas and Shallow Marine Deposits*.
Developments in Sedimentology. Elsevier, Amsterdam, p. 76-82.
- van Vliet, M., Meijerink, B.B., and Mulder, J. 1967. Laboratory study of rock softening
and means of prevention during steam injection waterflood. *Journal of Petroleum Technology*, v. 19, p. 113-117.
- Wade, James. 1977. The Co-Operative Geological Atlas of Alberta Information on the
Tuktoyaktuk Peninsula, NW 1/4, Section 10, Delta Formation, September 1976. *Canadian Petroleum Geology*, v. 5, p. 1-16.
- Wade, K. and L. G. Setzer. 1979. Petrology and diagenesis of karstic sandstones from
the Norwegian Jan Mayen Bay, North Sea. American Association of Petroleum
Geologists Bulletin, v. 63, No. 1, p. 18-32.
- Wade, K. 1979. *Karstic Diagenesis and bedding-est. sedimentation, development and
facies*. Elsevier, New York, p. 1-12.
- Fanning, T. and Hernandez, J. Z. 1977. Melendez, B. L., and Soto-Vieira, Eds., *Minerals
in Soil Environments*. Elsevier, New York, America, Madrid, Mexico, 1977, p.
198-204.
- Wade, K. 1980. *Petrology, Diagenesis, and Depositional Facies*. Texas, 1-12.
- Gas-Way, W. L. et al. 1979. Diagenetic controls on reservoir quality of delta-derived
sandstones: implications for petroleum exploration. In: Peter A. Björnerud and David
H. Schlager (eds.), *Aspects of Diagenesis: SEPM Special Publication*, v. 26, p.
251-267.
- Hastings, R. 1959. Lower Cretaceous of southern Alberta and adjacent area. In:
The American Association of Petroleum Geologists Bulletin, v. 43, p. 57-79,
89-162.
- May, H. and Rex, R.W. 1966. Formation damage in sandstones caused by clay
dispersion and migration. 14th National Conference on Clay and Clay
Minerals, p. 355-366.
- Grim, R.E. and Johns, W.D. 1954. Clay mineral investigation of sediments in the northern
Gulf of Mexico. Clays and Clay Minerals, National Academy Sciences, National
Research Council, Publication 32, p. 1-111.

- Hartness, J.C., Southard, J.B., Spearing, D.K. and Walker, R.G.: 1975, 'Depositional environments as interpreted from primary sedimentary structures and stratification sequences', SEPM Short Course No. 2, Dallas, 161p.
- Hayes, B.K.: 1982, 'Upper Jurassic and Lower Cretaceous stratigraphy of Southern Alberta and Northern Montana', University of Alberta Ph.D. thesis, 234p.
- Hayes, M. and Kana, J.W.: 1976, 'Tectogenous Clastic Depositional Environments: Some Modern Examples', American Association of Petroleum Geologists Field Course, University of South Carolina Technical Report No. 11, p. RD-315p.
- Henderson, G.J.: 1974, 'Petroleum geology of Sweetgrass Arch, Alberta', The American Association of Petroleum Geologists Bulletin, v. 58, N. 11, p. 1222-1244.
- Henderson, G.J., Hopkins, J. and Lawton, J.: 1982, 'Upper Mannville sandstone channels - the Bow area, Alberta', Geological Models for Seismic Interpretation Abstracts Booklet, Abstracts AAPG Annual Convention, June 21-30, 1982.
- Henderson, G.J. and van Vliet, J.A.: 1976, 'A marine barrier island-barrenheit in southeastern Alberta', 4th Conference Alberta Society of Petroleum Geologists, St. Albert, 1976, p. 34-41.
- Henderson, G.J. and Wierman, H.: 1968, 'Comparison of modern and ancient beach barriers along the rigid east American coast', American Association of Petroleum Geologists Bulletin, v. 52, p. 29-53.
- Henderson, M.: 1979, 'Sedimentological Analysis - Advanced Course 1979', in: 'Teaching field sheets, author of Manuscript, 1979', 1979.
- Holland, C.H.: 1971, 'Sedimentary facies patterns and geological significance of the Permian transgression of the Tethys', in: 'Evolution of the Tethys', ed. by A. Boucsein and J. Burchfiel, p. 11-18.
- Humbert, J. and Sloss, L.P.: 1963, 'Stratigraphy and sedimentation in the Mississippi River delta', Freeman and Company, San Francisco, 306p.
- Jordan, J.M. and Hodges, C.W.: 1969, 'Origin and development of the Texas shelf - Transgression of the Gulf of California', Geologische Rundschau, v. 59, p. 191-221.
- Kelvin, A.A. and Van Heege, A.W.: 1966, 'The hydrothermal synthesis of mineral-carbonate group minerals from kaolinite, quartz and various carbonates', The American Mineralogist, v. 51, p. 495-508.
- Kramer, J.M.: 1957, 'Useful Biarmic environments in central and southern Alberta, Canada', American Association of Petroleum Geologists Bulletin, v. 41, N. 11, p. 1348-1367.
- McCubbin, D.G.: 1982, 'Barrier island and strand plain facies', in: P.A. Scholle and D. Spearing (eds.), 'Sandstone Depositional Environments', American Association

Canadian Petroleum Geologists' Circular, Vol. 41, p. 100

- Morin, Enrique (1976) Diagenesis in Tertiary sandstones from Eketemar, North Dome, California. *Diagenetic mineralogy, Journal of Sedimentary Petrology*, v. 48, No. 1, p. 320-336.
- Perry, C. and Elliott, E. (1979) The formation and behaviour of montmorillonite during the use of wet pyrolysis combustion in the Alberta oil sand deposits. *Bulletin of Canadian Petroleum Geologists*, v. 27, No. 3, p. 314-326.
- Thompson, Edward G. (1979) Gravity diagenesis and productive capacity of sandstone reservoirs. In Peter A. Cookson and Faulkner, (eds.), *Aspects of Diagenesis*. SERM Special Publication No. 26, p. 159-174.
- Thompson, E. G. (1981) Facies Models: Materials and Systems. In Cookson, P. A. (ed.), *Facies Models*, p. 1-14.
- Thompson, E. G. (1984) The development of facies models. In Cookson, P. A. (ed.), *Modern Approaches to Facies Models*, p. 1-14.
- Thompson, E. G., Fletcher, J. C., and McLean, J. R. (1984) Montmorillonite and the geological history of Western Canada. The Alberta section. In *Canadian Petroleum Geologists' Circular*, v. 32, p. 15-18.
- Thompson, E. G. (1979) A color illustrated guide to authigenic elements and minerals of Sandstone and Associated Rock. American Association of Petroleum Geologists Special Publication 26.
- Thompson, A. (1964) Authigenic kaolinite in sandstone. *Journal of Sedimentary Petrology*, v. 34, p. 101-108.
- Thompson, A. (1969) Calcarenous clastic-barrier facies. In Shepard, N. S., Pfleiderer, and Cookson, (eds.), *Recent Sediments Northwest Gulf of Mexico*. American Association of Petroleum Geologists' Circular, v. 47, p. 1-22.
- Thompson, A. (1973) Beaches and shales in estuarine environments. In Cookson, P. A. (ed.), *Sheridan, A. (ed.), *Beaches and Shales in Estuarine Environments**, p. 11-18.
- Thompson, Graham R. and Hawley, John H. (1978) The mineralogy of clay minerals and clay minerals. *Clay Minerals*, v. 16, p. 249-317.
- Taylor, J. M. (1958) The development of the Sweetgrass Aquifer, Alberta. Alberta Proceedings of the Geological Association of Canada, v. 17, p. 119-124.
- Tive, Robert C. (1981) Isomorphie evolution and stratigraphic framework of the early capers inlets, South Carolina. University of South Carolina M.S. Thesis, 140p.
- Waldron, C. M. (1965) Effect of steam on permeabilities of water-sensitive formations. *Journal of Petroleum Technology*, v. 17, p. 1219-1222.

Wilson MD and Pittman ED (1977) Authigenic clays in sandstones recognition and influence on reservoir properties and paleoenvironmental analysis Journal of Sedimentary Petrology Vol 47 No 1 p 3-31

Workman LE (1958) Glauconitic Sandstone in Southern Alberta Journal of Alberta Society of Petroleum Geologists Vol 6 p 237-245

X APPENDICES

Appendix A: Core Logs for Wells from the SHOP Project (see attached pocket)

Appendix B Analytical Methods for Detailed XRD Analyses

Samples were gently crushed by hand and treated with a 3 per cent bleach solution (sodium hypochlorite) at 50°C for three days to remove any organic phases. This less hypochlorite solution was then removed by repeated washings (high speed centrifugation). The mineral material was then dispersed in distilled water using an ultrasonic probe and allowed to settle in columns for the appropriate period of time to extract the particles with an equivalent spherical diameter of < 2 micrometres. The settling procedure was repeated three times for each sample and the < 2 micrometre material collected after each step combined. The < 2 micrometre material was treated with the 3 per cent sodium hypochlorite solution again at 50°C for two days in order to destroy residual organic materials and then repeatedly washed. The sample was split in fractions and separate portions saturated with K^+ and Ca^{++} . Once saturated, the < 2 micrometre material was thoroughly washed, freeze-dried and then precipitated by sucrose into a pringlean dish. The < 2 micrometre Ca and K disks were analyzed in the X-ray diffractometer using the following conditions:

Intensity of alpha radiation obtained by means of a graphite monochromator
1 DEGREE DIVERGENCE +
1 DEGREE TWIN theta minute at 60 mm

Time constant 1 s

Scanning rate 10°/min

The following X-ray patterns were obtained for the < 2 micrometre samples:

a) 35° at 54% relative humidity, 1.05°/degree theta, theta

b) 35° at 54% relative humidity, 1.05°/degree theta

c) 35° at 54% relative humidity, 1.05°/degree theta

d) 35° at 54% relative humidity, 1.05°/degree theta

e) 35° at 54% relative humidity, 1.05°/degree theta

Relative humidity gradients were constructed by varying the 20°/min scanning rate.

Settling time was calculated by means of Stokes law for a spherical particle of about a falling spherical body combined with the differential specific gravity and the gravitational instant (Jackson 1979).

The d-spacings and intensities of smectite and vermiculite are decreased by potassium saturation and increased by calcium saturation (Jackson 1979). These XRD analyses of both Ca and K points are valuable for the identification of the mineral

the analysis of the sample on the diffractometer. The glycolated Ca-disc was prepared by placing the Ca-saturated disc in an enclosed ethylene glycol environment. The disc was heated in this environment at 65°C for 14 hours and then left for one day to allow the ethylene glycol to fully penetrate into the clay structures.

Relative percentages of kaolinite, illite and smectite were estimated using the weighted peak-area method described in Biscaye (1965). The peaks and weighting factors used were the area of the 17A glycolated peak for smectite four times (4X) the 10A peak area (glycolated trace) for illite and twice (2X) the 7A peak area for kaolinite. Since kaolinite and chlorite have a common 7A peak, the 3.5A peaks for these minerals are used to determine the relative proportion of kaolinite and chlorite. The kaolinite peak at 3.58A and the chlorite at 3.54A form a couplet which can sometimes be resolved (Biscaye 1975). In the clay samples from the Glauconitic Sandstone there is generally no indication of a couplet at 3.5A. Thus the 7A peak is calculated as 100 per cent kaolinite.

NAME AEC et al 01 SHUFFIELD

LOCATION 4-10-20-8 W4

KB 755.16 m **DATE LOGGED** March 1981

LOGGED BY B.J. Tilley



SYMBOL LEGEND

GRAIN SIZE

- Mean
 - Median
 - * Largest grain

LITHOLOGY

- | | |
|--|-------------------------|
| | Conglomerate |
| | Sandstone c.v.c.m.v.f.t |
| | Siltstone |
| | Shale |
| | Breccia |
| | Coal |
| | Calcareous |

BEDDING CONTACTS

- Flat
— Erosional

SEDIMENTARY STRUCTURES

- Homogenous, structureless
 - Parallel laminated/angle
 - Cross bedded/angle
 - Trough cross bedded
 - Ripple cross laminae
 - Ripple troughs
 - Oscillation ripples
 - Discontinuous laminae
 - Flaser bedding

ORGANIC MATTER

- Carbonaceous fragments
 - Carbonaceous laminae
 - Rootlets
 - Discontinuous laminae
 - Carbonaceous grains

INDURATION

- | | | |
|---|-----------------|--|
| 1 | Unconsolidated | grains falling apart
in dry conditions |
| 2 | Friable | grains can be detached
using a fingernail |
| 3 | Moderately hard | grains can be detached
with a knife |
| 4 | Hard | sample breaks around
most grains |

P - Pyrite, G - Glauconite, C - Carbonate Cement

NOTE: All depths have been adjusted so that lithologic log depths correspond to geophysical log depths.

910						
3-146	top of glauconitic ss	UH	X	P		
3-147		UC	X			
3-148		H	X			
915						
3-143		BM	U	>13		
320						
325						
3-151		H		P		
930						
935						

1 / 909.00 - 918.75 / 9.00

2 / 921.00 - 927.00 / 9.55 / 9.00

3 / 927.00 - 936.00 / 9.00 / 9.00

908.9-910.4 SHALE, medium grey, inter laminated with light grey SILT and carbonaceous material, parallel laminated to low angle xbedded, local small scale ripples, pyrite is disseminated along laminations and also occurs as larger nodules

910.4-910.7 SHALE, brownish-grey

910.7-911.1 SHALE black to dark grey, carbonaceous and COAL with some sand grains

911.1-912.0 SAND, fine grained, argillaceous, medium grey, structureless with some lighter grey mottles

912.0-913.8 SAND, less argillaceous, no rootlets, light grey-white with larger bent grain appearing as dark specks, structureless and bioturbated with local hint of bedding, patchy oil saturation

913.8-922.6 SAND, high angled, irregularly laminated beds interbedded with faintly mottled bioturbated zones, irregular laminations disrupted by burrows, patchy oil saturation, non oil saturated clay rich lenses occur within oil saturated bed

918.9 non oil-saturated sand lenses surrounded by oil-saturated sand

921.4 non oil-saturated sand lens surrounded by oil-saturated sand

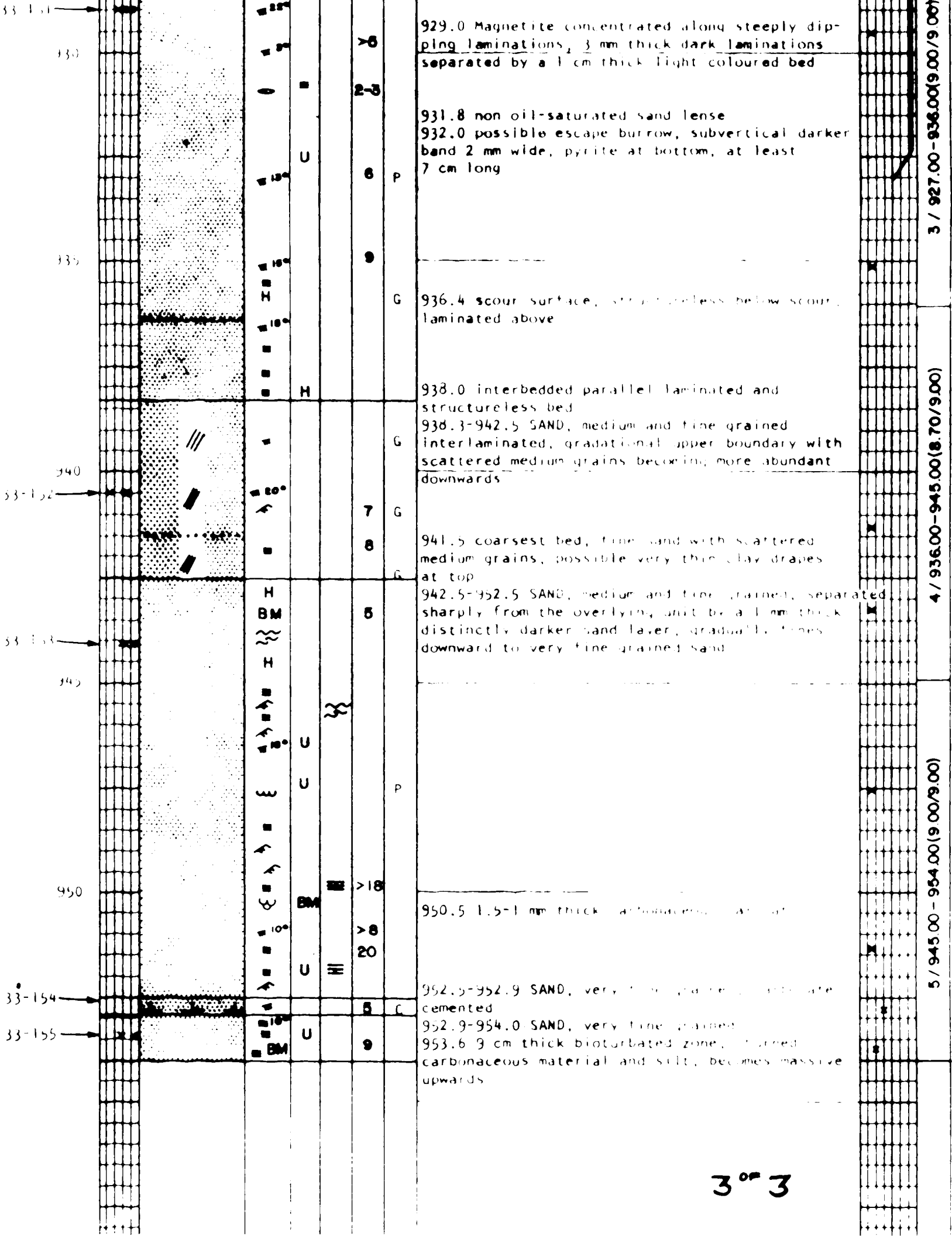
922.6-938.3 SAND, parallel to low angle xlaminated, clean continuously oil-saturated with very rare non oil-saturated lenses above the oil-water contact, laminations are alternations of dark and light coloured sand layers of similar fine grain size

2 of

929.0 Magnetite concentrated along steeply dipping laminations, 3 mm thick dark laminations separated by a 1 cm thick light coloured bed

931.8 non oil-saturated sand lens

932.0 possible escape burrow, subvertical darker band 2 mm wide, pyrite at bottom, at least 7 cm long



3°3

NAME ABC et al 02 SUFFIELD

LOCATION 4-10-20-8 W4

KB 754.87 m

DATE LOGGED

March 1981

LOGGED BY B. J. Tilley



GRAIN SIZE

- Mean
- Median
- ✖ Largest grain

SYMBOL LEGEND

SEDIMENTARY STRUCTURES

- H Homogeneous structureless
- Parallel laminated angle
- ✖ Cross bedded angle
- ↙ Trough cross bedded
- ↖ Ripple cross laminae
- ↘ Ripple troughs
- ↔ Oscillation ripples
- ~~ Discontinuous laminae
- ↔ Flash bedding

- Contorted laminae
- Vertical burrows
- Horizontal burrows

BM Burrow mottled

S S Scour and fill

L Lenses

NV Structures not visible due to oxidation

R Rip up clasts

P Penecontemporaneous faults

LITHOLOGY

- Conglomerate
- Sandstone (cv) m vft
- Siltstone
- Shale

B Breccia

Coal

Calcareous

BEDDING CONTACTS

Flat

Erosional

ORGANIC MATTER

- Carbonaceous fragments
- ☰ Carbonaceous laminae
- ✖ Rootlets
- ↔ Discontinuous laminae
- Carbonaceous grains

INDURATION

- 1 Unconsolidated grains falling apart in dry conditions
- 2 Fissile grains can be detached using a fingernail
- 3 Moderately hard grains can be detached with a knife
- 4 Hard sample breaks around moist grains

NOTE All depths have been adjusted so that lithologic log depths correspond to geophysical log depths.

DEPTH - TOPS SAMPLES

1000-660 660-580
220-300 300-280
530-320 320-220

LITHOLOGY

SEDIMENTARY STRUCTURES

ORGANIC MATTER

BEDDING THICKNESS

CEMENT/ACC MINERALS

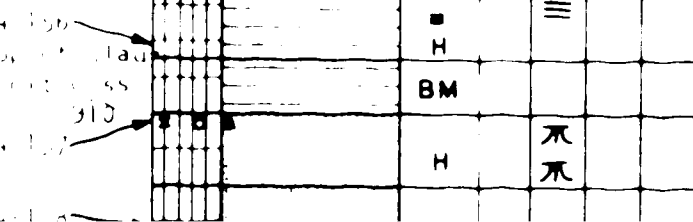
DESCRIPTION

INDURATION

SATURATION

CORE/CORE DEPTH RECOVERY

70/8 25)



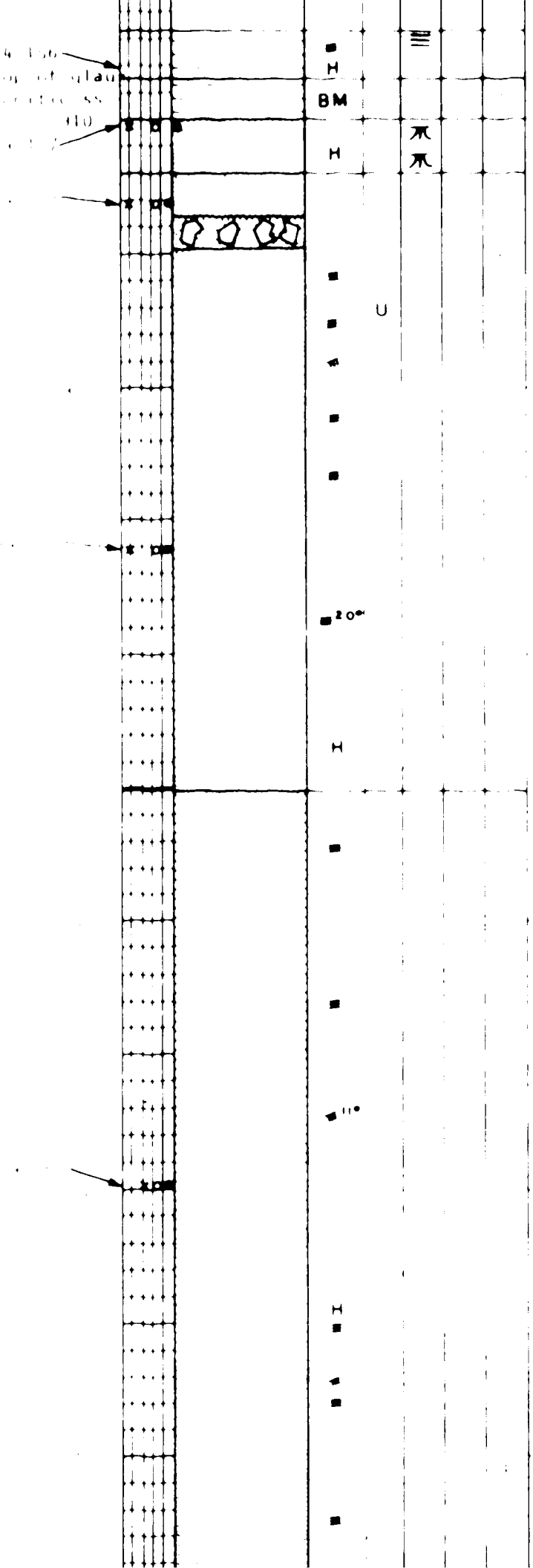
1 / 909 00 - 9725 (70/825)

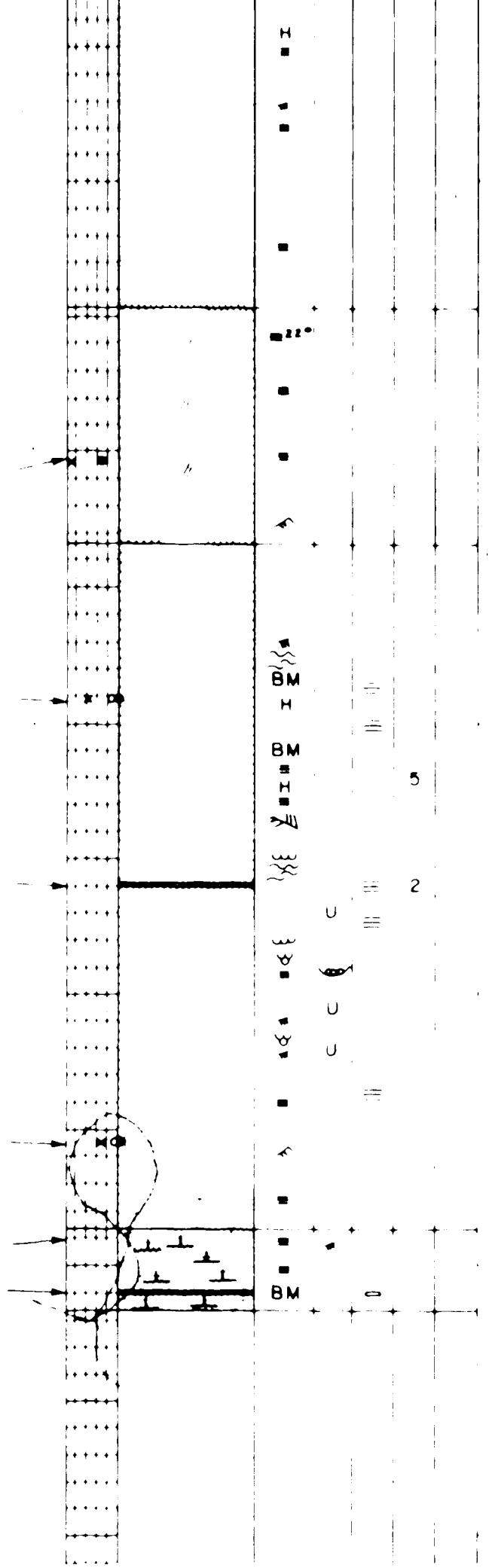
2 / 91725-92625(725/900)

3 / 92625-93525(785/900)

400

2 of





303

6 / 95325-95525 05/2001 5 / 94425-95325(900/900)

4 / 93525-94425(900/900)

3 /

NAME ALICE C. DEE SUFFIELD

LOCATION 1070 NW4

KB 1000

DATE LOGGED

May 16, 1981

LOGGED BY S. ELLIOTT

RESEARCH COUNCIL
GEOLOGICAL SURVEY

SYMBOL LEGEND

GRAIN SIZE

- Mean
- Median
- Largest grain

LITHOLOGY

- Conglomerate
- Sandstone
- Shale
- Breccia
- Coal
- Calcarenous

BEDDING CONTACTS

- Flat
- Cross-bed

SEDIMENTARY STRUCTURES

- Horizontal bedding
- Parallel linear angle
- Cross bedded surface
- Truncation surface
- Ripple cross-cutting
- Ripple troughs
- Horizontal surface
- Current line surface
- Fossils

SEDIMENTARY STRUCTURES

- Confolated laminae
- Vertical burrows
- Horizontal burrows
- Burrow modified
- Rooted surface
- Lenses
- Structures indicating organic activity
- Biopellets
- Preferred orientation of sedimentary structures

ORGANIC MATTER

- Detrital organic fragments
- Charcoaceous laminae
- Rootlets
- Detrital organic laminae
- Charcoaceous grains

INDURATION

- Very soft
 - Soft
 - Moderate
 - Hard
- Induration is measured in centimeters. The scale is logarithmic.
- Very soft = less than 1 cm.
 Soft = 1 to 10 cm.
 Moderate = 10 to 100 cm.
 Hard = greater than 100 cm.

DEPTH TOPS SAMPLES

LITHOLOGY

GRAIN SIZE

SEDIMENTARY
STRUCTURES

ORGANIC MATTER

BEDDING THICKNESS

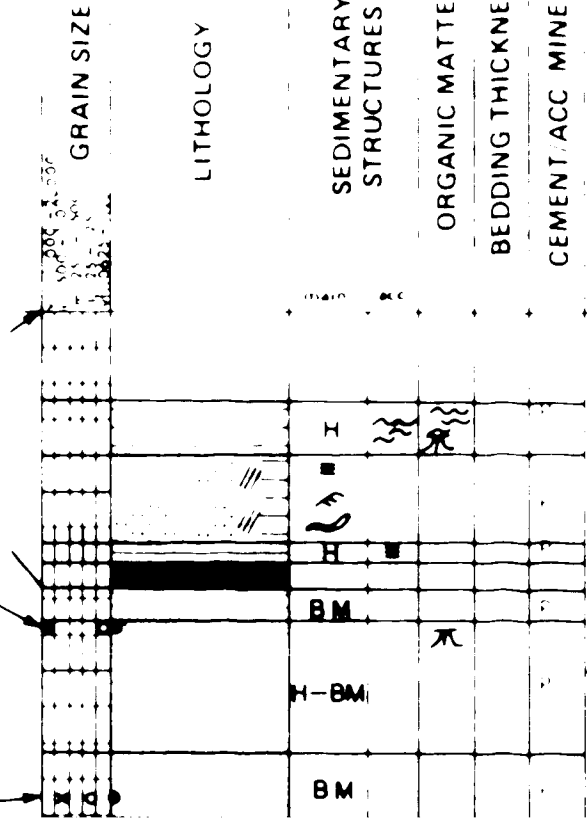
CEMENT/ACC MINERALS

DESCRIPTION

INDURATION

SATURATION

CORE/CORE DEPTH RECOVERY



0-9200(980/900)

1 / 91100-92000-93800-93500-900

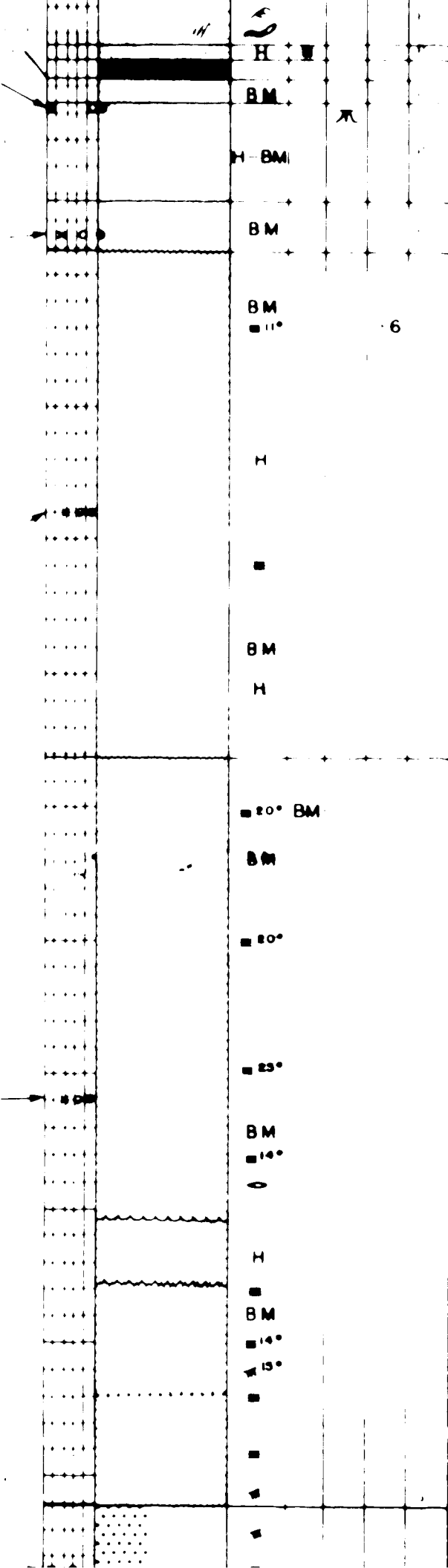
2 / 92000-92900-935/900

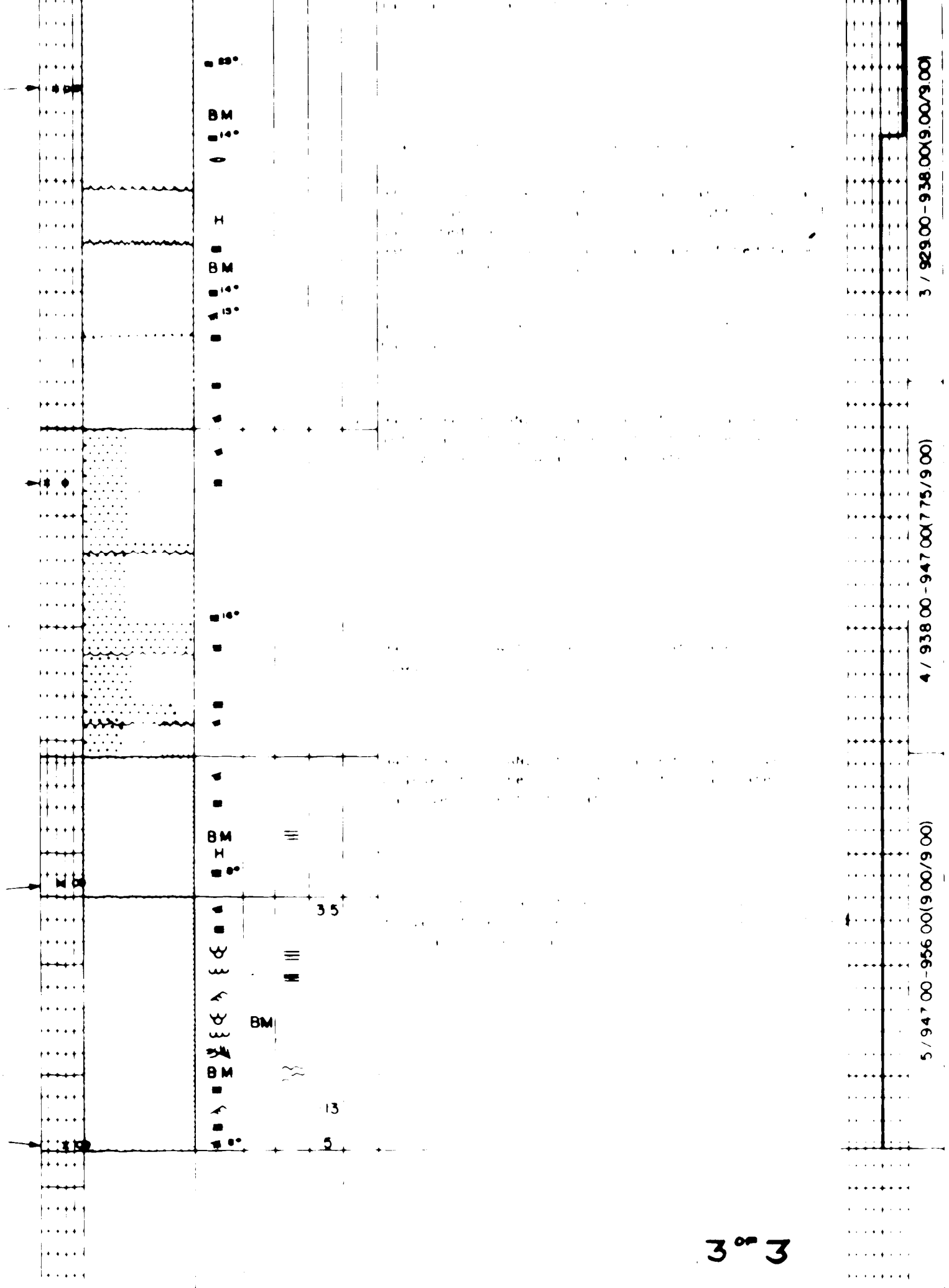
3 / 92600-93800-900/900

4 / 9300

2 of

6





3 / 929 00 - 938 00 (900/900)

4 / 938 00 - 947 00 (775/900)

5 / 947 00 - 956 00 (900/900)

Metric Log Form

1 OF

NAME

LOCATION

B

DATE LOGGED

LOGGED BY

RESEARCH COUNCIL
GEOLOGICAL SURVEY

SYMBOL LEGEND

GRAIN SIZE

- Mean
- Median
- ✖ Largest grain

LITHOLOGY

- Conglomerate
- Sandstone
- Siltstone
- Shale
- Breccia
- Coal
- Calcareous

BEDDING CONTACTS

- Flat
- Erosional

SEDIMENTARY STRUCTURES

- ↑↓ Parallel or oblique linear
- ↖↗ Parallel or oblique angle
- ↔ Cross-bedding angle
- ↙↗ Trough cross-bedding
- ↖↗ Ripple-cross-bedding
- ↙↗ Ripple troughs
- ↔ Oscillation ripples
- ↖↗ Discoidal ripples
- ↔ Faser bedding

ORGANIC MATTER

- Coal
- III Detrital organic matter
- Mucilins
- Sphaerotilus
- Diatomaceous

INDURATION

- Hard
- Soft
- Very soft
- Detached
- Broken
- Detached with a break
- Detached with a break and a fissure

Note: All depths have been adjusted so that thickness is from the corresponding top to the bottom of the deposit.

DEPTH TOPS SAMPLES

GRAIN SIZE

LITHOLOGY

SEDIMENTARY
STRUCTURES

ORGANIC MATTER

BEDDING THICKNESS

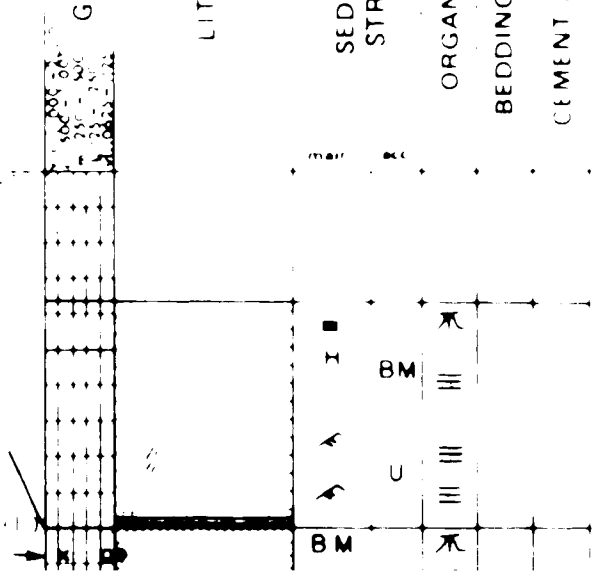
CEMENT ACC MINERALS

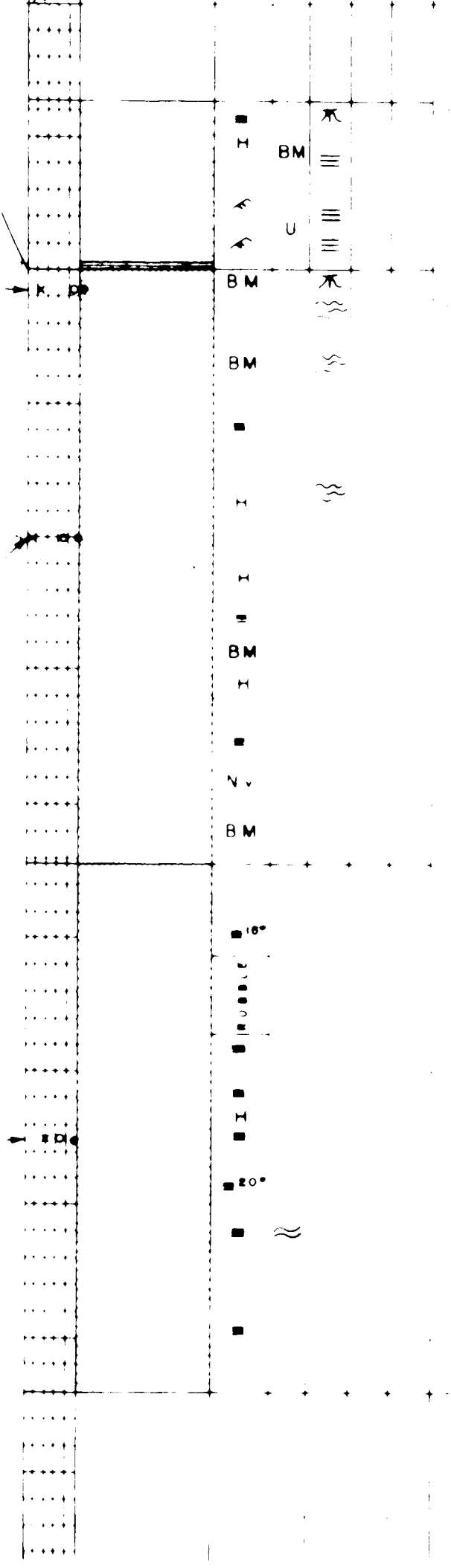
DESCRIPTION

INDURATION

SATURATION

CORE CORE DEPTH RECOVERY





1 / 907 00 - 916 00 (8 00 / 9 00)

2 / 916 00 - 924 00 (8 00 / 8 00)

3 / 924 00 - 931 00 (6 75 / 7 00)

2 of 2

Metric Log Form

1 of

NAME ALC ET AL F2 SUFFIELD

LOCATION 4-10-20-8W4

755.25 m

DATE LOGGED March 1951

LOGGED BY

SYMBOL LEGEND

SEDIMENTARY STRUCTURES

- Mean
 - Median
 - × Largest gram

- ## LITHOLOGY

- ### Geographical

- VI. Sandviken

- Suisse

- + Snaile

- 1 —

- Breccia

- Cool

- L Calcareous.

BEDDING CONTACTS

δ δ'

DEPTH TOPS SAMPLES

GRAIN SIZE

LITHOLOGY

SEDIMENTARY
STRUCTURES

ORGANIC MATTER

BEDDING THICKNESS

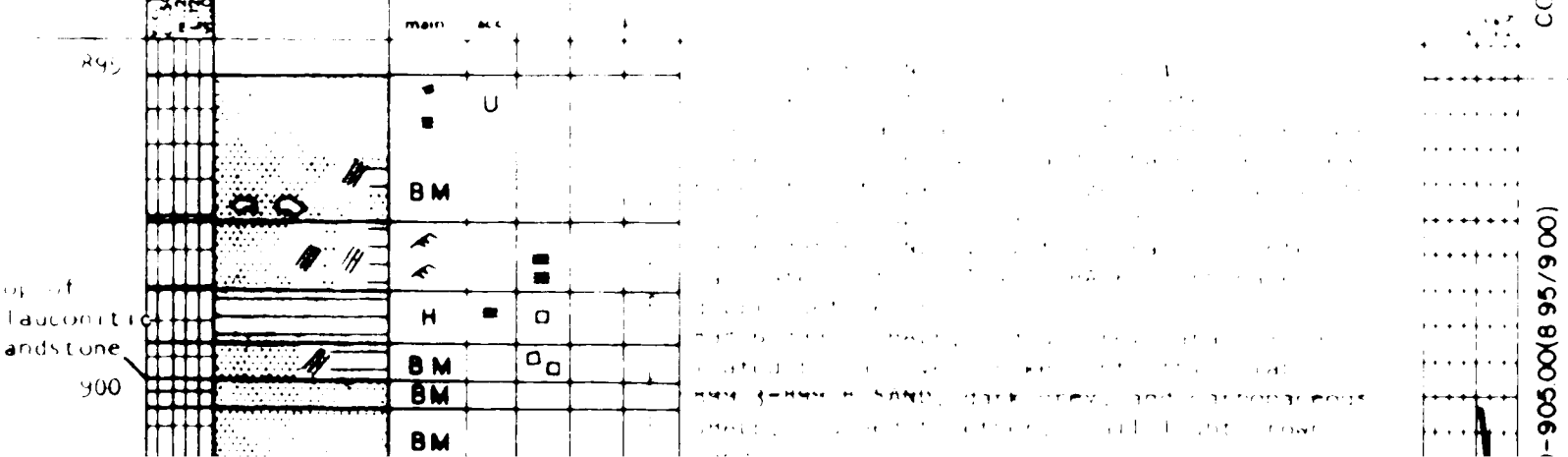
CEMENT ACC MINERALS

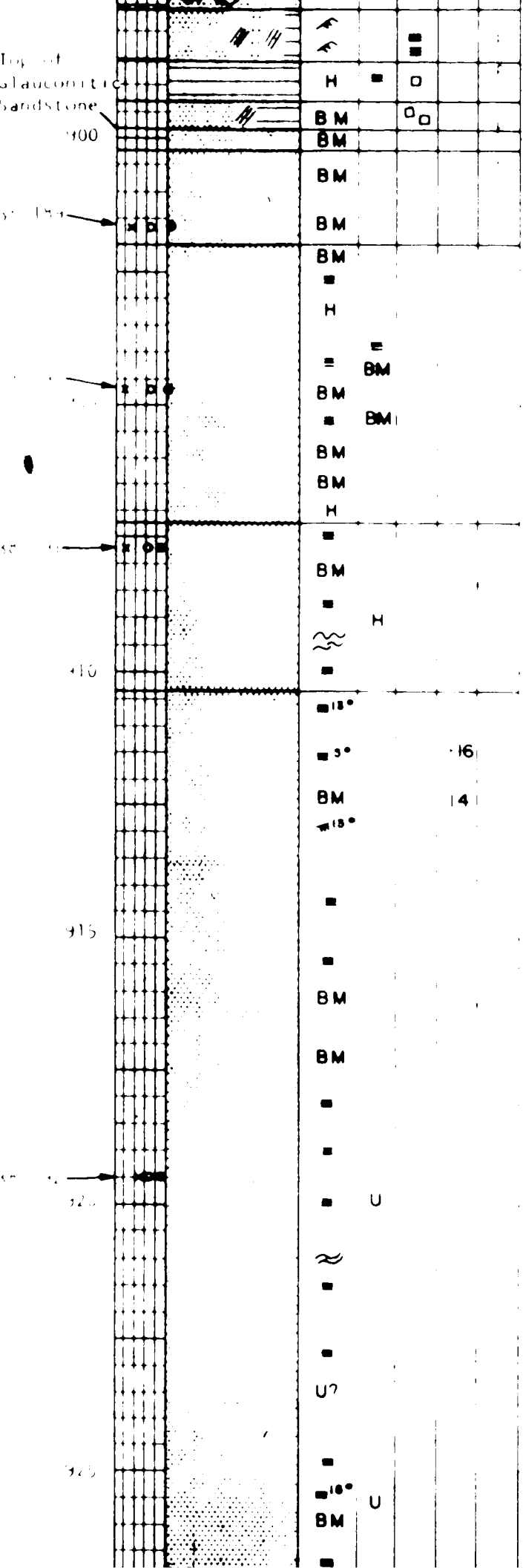
DESCRIPTION

INSTITUTION

SATURATION

CORE CORRECTIONAL RECOVERY



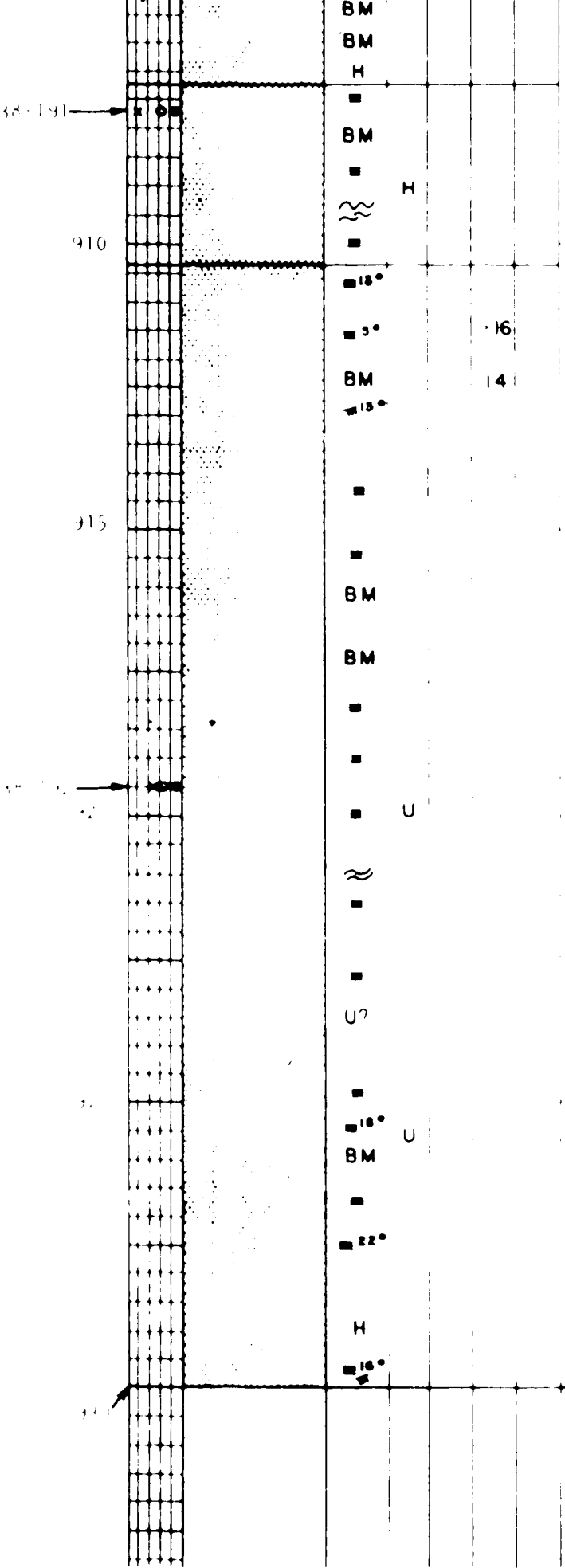


2 of

3 / 914 00-923 00(870/9.00)

2 / 905.00-94 00(8.60/9.00)

8



3°3

4 / 92300-93100(780/800)

3 / 914 00-923 00(870/9.00)

2 / 905.00-914 00(8.60/9.00)

108

NAME _____

LOCATION _____

KB _____

DATE LOGGED 10/10/81

LOGGED BY _____

RESEARCH COUNCIL
GEOLOGICAL SURVEY

SYMBOL LEGEND

GRAIN SIZE

- Mean
- Median
- ✖ Largest grain

SEDIMENTARY STRUCTURES

LITHOLOGY

Conglomerate
Sandstone
Siltstone
Shale
Breccia
Coal
Calcareous

- H Homogeneous structureless
- || Parallel laminated angle
- ↖ ↗ Cross bedded angle
- ↙ ↘ Trough cross bedded
- ↗ Ripple cross laminae
- ↖ Ripple troughs
- ↔ Isoclinal ripples
- ~~~~ Oscillatory laminae
- ↖ ↗ Flaser bedding

- Contorted laminae
- Vertical burrows
- Horizontal burrows
- BM Burrow mottled
- ↙ ↘ Scour and fill
- ↔ Lenses
- NV Structures not visible due to oil saturation
- ↑ Rip-up clasts
- ↖ ↗ Penetrating anomalous faults

ORGANIC MATTER

- Carbonaceous fragments
- ☰ Carbonaceous laminae
- ✖ Rocklets
- ↔ Discontinuous laminae
- ◆ Carbonaceous grains

INDURATION

- 1 Unconsolidated grains falling apart in dry conditions
- 2 Frangible grains can be detached using a fingernail
- 3 Moderately hard grains can be detached with a knife
- 4 Hard sample breaks around most grains

NOTE: All depths have been adjusted so that lithological depths correspond to geophysical depths.

DEPTH - TOPS SAMPLES

1000 800 600 400 200
1000 800 600 400 200
1000 800 600 400 200
1000 800 600 400 200

GRAN SIZE

LITHOLOGY

SEDIMENTARY
STRUCTURES

ORGANIC MATTER

BEDDING THICKNESS

CEMENT ACC MINERALS

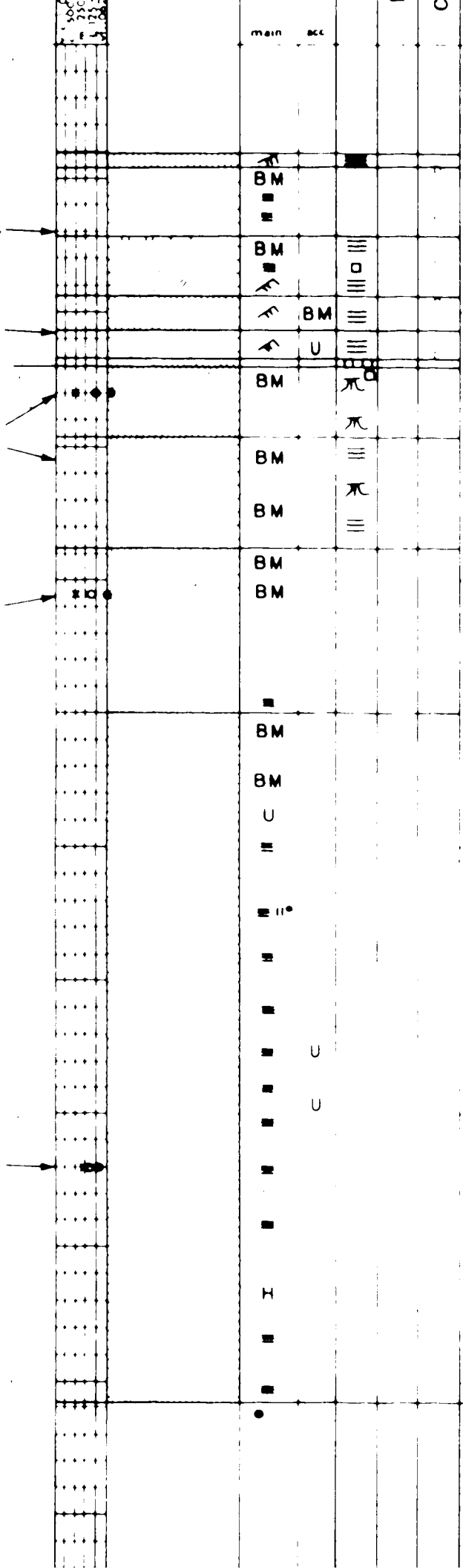
DESCRIPTION

INDURATION

SATURATION

CORE/CORE DEPTH (RECOVERY)

300 ft Top of
Top of
1000 (800/900)



CASE 40700-91600(880/900)
SUBCASE 1: THE SYSTEM IS CONNECTED
TO THE MAIN COMPUTER BY A BUS.
THE COMPUTER IS CONNECTED TO THE
SYSTEM BY A BUS. THE COMPUTER IS
CONNECTED TO THE SYSTEM BY A BUS.
THE COMPUTER IS CONNECTED TO THE
SYSTEM BY A BUS. THE COMPUTER IS
CONNECTED TO THE SYSTEM BY A BUS.

THE COMPUTER IS CONNECTED TO THE
SYSTEM BY A BUS. THE COMPUTER IS
CONNECTED TO THE SYSTEM BY A BUS.
THE COMPUTER IS CONNECTED TO THE
SYSTEM BY A BUS. THE COMPUTER IS
CONNECTED TO THE SYSTEM BY A BUS.
THE COMPUTER IS CONNECTED TO THE
SYSTEM BY A BUS. THE COMPUTER IS
CONNECTED TO THE SYSTEM BY A BUS.

THE COMPUTER IS CONNECTED TO THE
SYSTEM BY A BUS. THE COMPUTER IS
CONNECTED TO THE SYSTEM BY A BUS.
THE COMPUTER IS CONNECTED TO THE
SYSTEM BY A BUS. THE COMPUTER IS
CONNECTED TO THE SYSTEM BY A BUS.
THE COMPUTER IS CONNECTED TO THE
SYSTEM BY A BUS. THE COMPUTER IS
CONNECTED TO THE SYSTEM BY A BUS.

THE COMPUTER IS CONNECTED TO THE
SYSTEM BY A BUS. THE COMPUTER IS
CONNECTED TO THE SYSTEM BY A BUS.

1 0P

NAME AEC et al E4 SUFFIELD

LOCATION 4 10-20-8 W4

XB 152.00 m

DATE LOGGED May 11, 1971

LOGGED BY B.J. Tilley

RESEARCH COUNCIL
GEOLOGICAL SURVEY

GRAIN SIZE

- Mean
- Median
- ✖ Largest grain

LITHOLOGY

- Conglomerate
- Sandstone - coarse
- Siltstone
- Shale

- Breccia
- Coal

CALCAREOUS

BEDDING CONTACTS

- Flat
- Erosional

SYMBOL LEGEND

		SEDIMENTARY STR.
●	Mean	H Homogeneous, structureless
○	Median	■ Parallel laminated, angle
✖	Largest grain	▲ Cross bedded, angle
		◎ Thoroughly cross bedded
		↗ Ripple cross laminar
		↙ Ripple troughs
		↔ Oscillation ripples
		≈ Discontinuous laminae
		↔ Flaser bedding
		ORGANIC MATTER
		□ Carbonaceous fragments
		III Carbonaceous laminae
		■ Rootlets
		NN Discontinuous laminae
		○ Carbonaceous grains
		INDURATION
		● Dissociated grains falling apart in dry conditions
		○ Detached grains can be detached using a fingernail
		■ Moderately hard grains can be detached with a knife
		● Hard sample breaks around most grains

NOTE: All depths have been adjusted so that thicknesses correspond to geophysical log depths.

DEPTH TOPS SAMPLES

500-550' 550-600'
500-550' 550-600'
500-550' 550-600'
500-550' 550-600'
500-550' 550-600'

LITHOLOGY

SEDIMENTARY
STRUCTURES

ORGANIC MATTER

BEDDING THICKNESS

CEMENT/ACC MINERALS

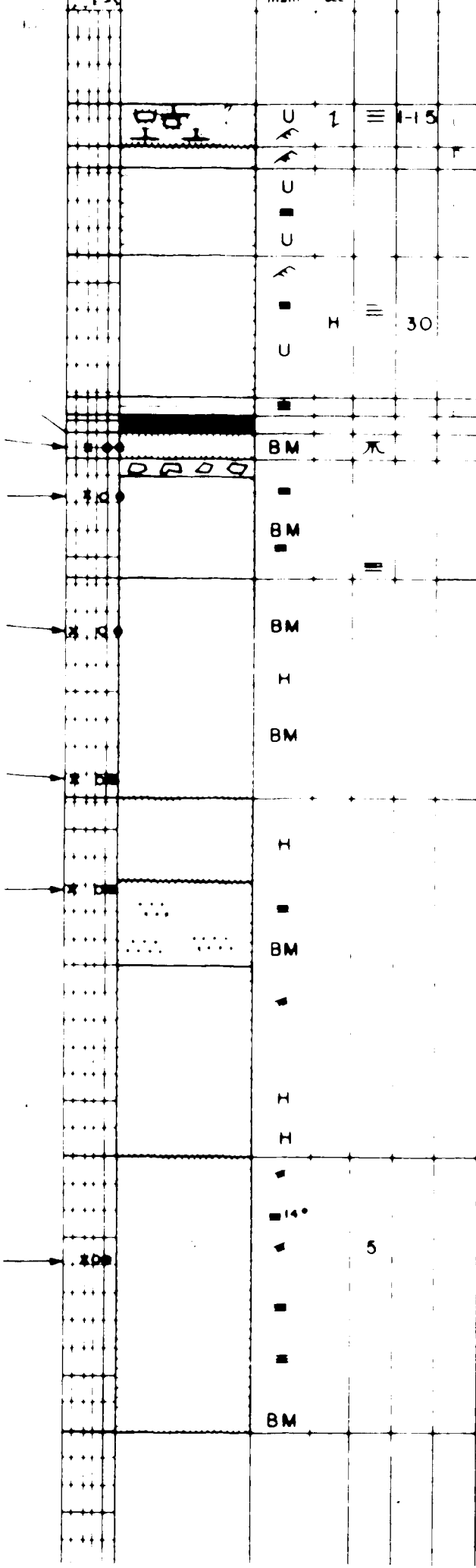
DESCRIPTION

INDURATION	DETACHED
SATURATION	DRY
CORE/DEPTH RECOVERY	100%

1 / 907 00 - 96 00 (8 85/900)

2 / 916 00 - 925 00 (8 80/900)

3 / 925 00 - 934 50 (6 50/6 50)



Metric Log Form

1 OF

NAME

LOCATION

KB

DATE LOGGED

RESEARCH COUNCIL
GEOLOGICAL SURVEY

LOGGED BY

SYMBOL LEGEND

GRAIN SIZE

- Med
- Med. s
- ✖ Largest grain

LITHOLOGY

- Igneous
- Sedimentary
- ✖ Metamorphic
- Conglomerate
- Sandstone
- ✖ Shale
- Breccia
- Lignite
- ✖ Coal

BEDDING CONTACTS

- Flat
- Irregular

SEDIMENTARY STRUCTURES

- Horizontal bedding
- Parallel laminated
- ✖ Cross-bedded
- ✖ Tabular cross-bedding
- Ripple-cross laminae
- ✖ Ripple troughs
- Isoclinal dips
- ✖ Subhorizontal dips
- ✖ Tabular

- Vertical tabular
- Horizontal tabular
- Horizontal wavy
- Horizontal
- Lenses
- Structures indicating saturation
- Mud cracks
- Horizontal sedimentary facies

ORGANIC MATTER

- Carbonaceous fragments
- Carbonaceous detritus
- ✖ Nodules
- Carbonaceous detritus with carbonized grains

INDURATION

- Hard
- Soft
- Faint
- Grains falling apart in dry conditions
- Grains can be detached using a fingernail
- Moderate
- Detached
- Very soft
- Grains break around existing grains

DEPTH TOP SAMPLES

GRAIN SIZE

LITHOLOGY

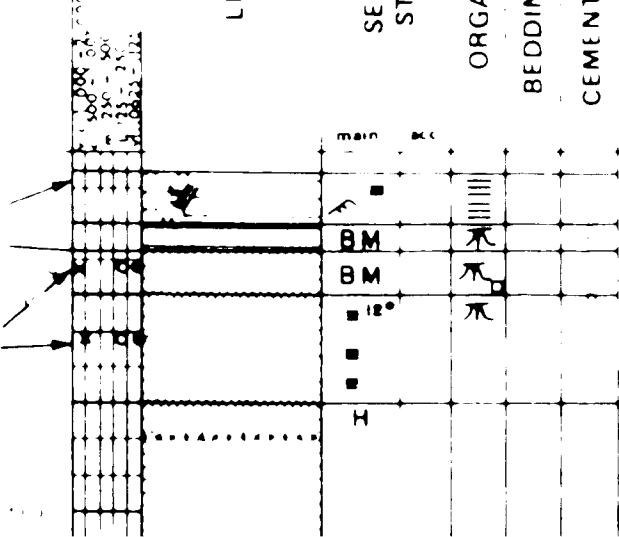
SEDIMENTARY
STRUCTURES

ORGANIC MATTER

BEDDING THICKNESS

CEMENT ACC MINERALS

DESCRIPTION



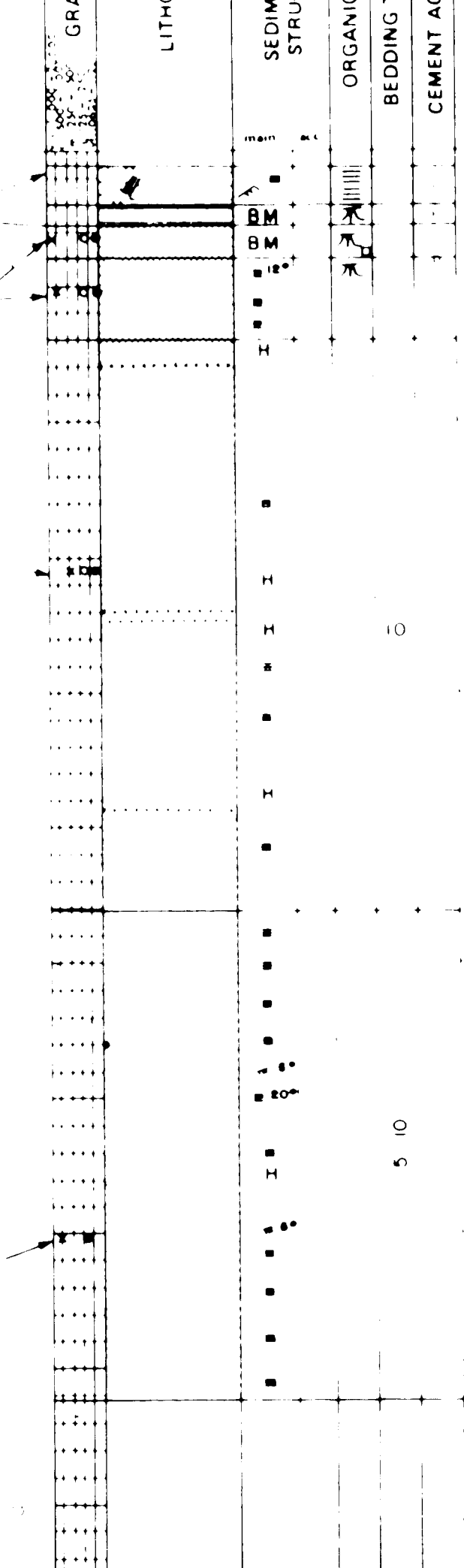
INDURATION

SATURATION

CORE/DEPTH/RECOVERY

-91700(900/900)

DEPTH - TCC

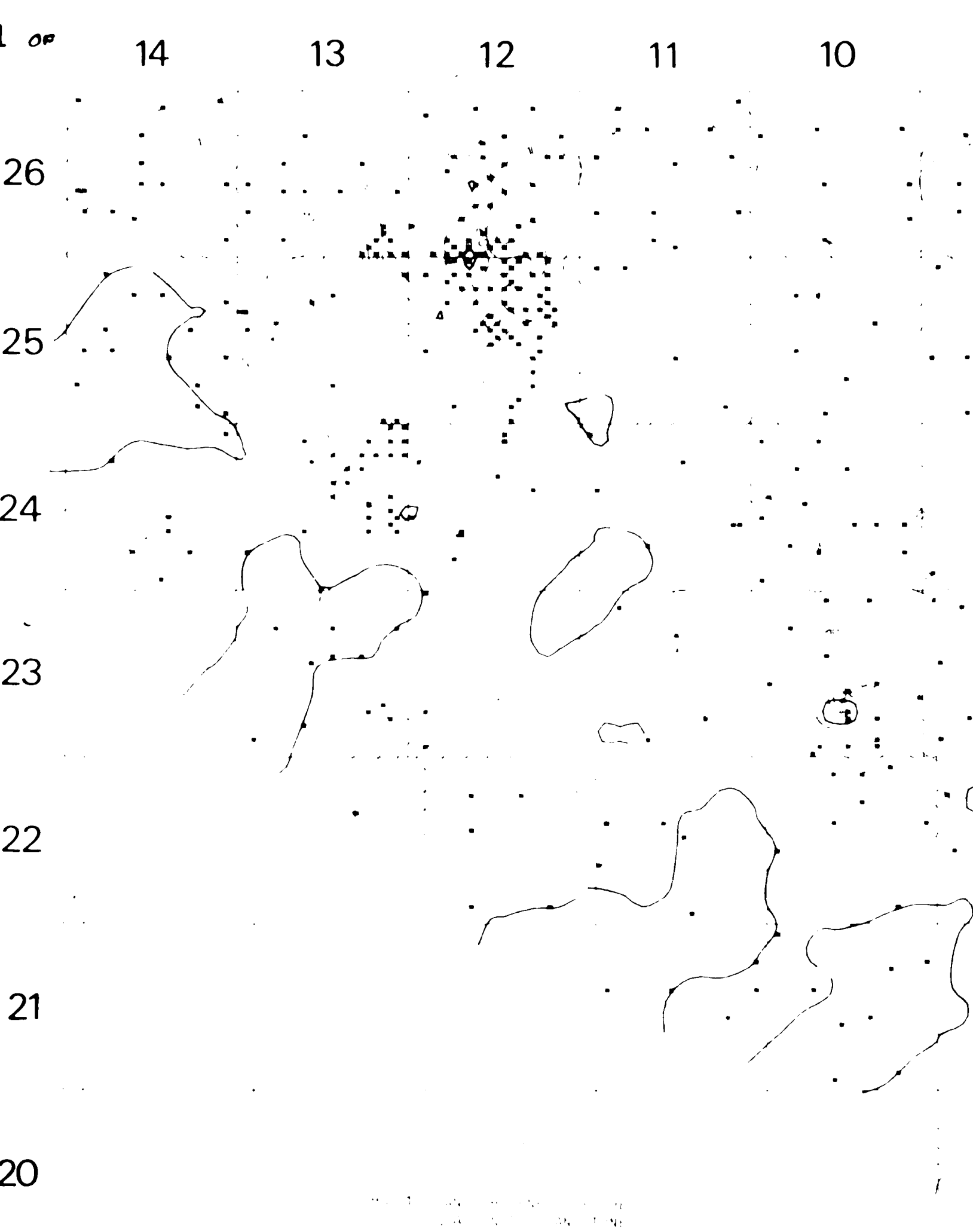


CORE CORE 1
1 / 908 00 - 917 00 (9 00/9 00)

2 / 917 00 - 925 00 (7 50/8 00)

3 / 925 00 - 930 00 (5 50/5 00)

INDU
SATU



9

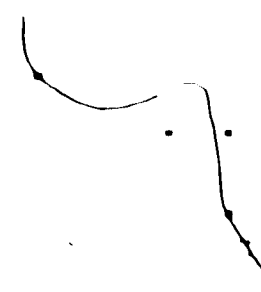
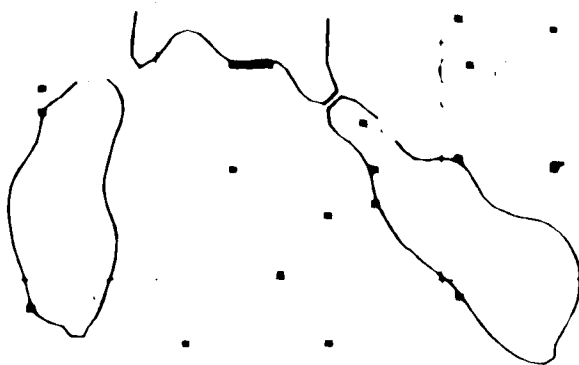
8

7

6

5 W4

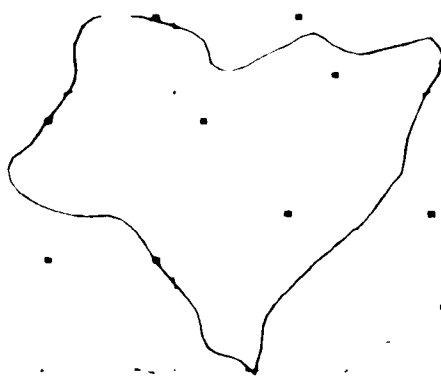
2 OF



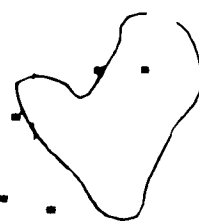
26

25

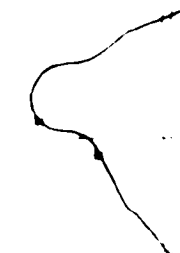
24



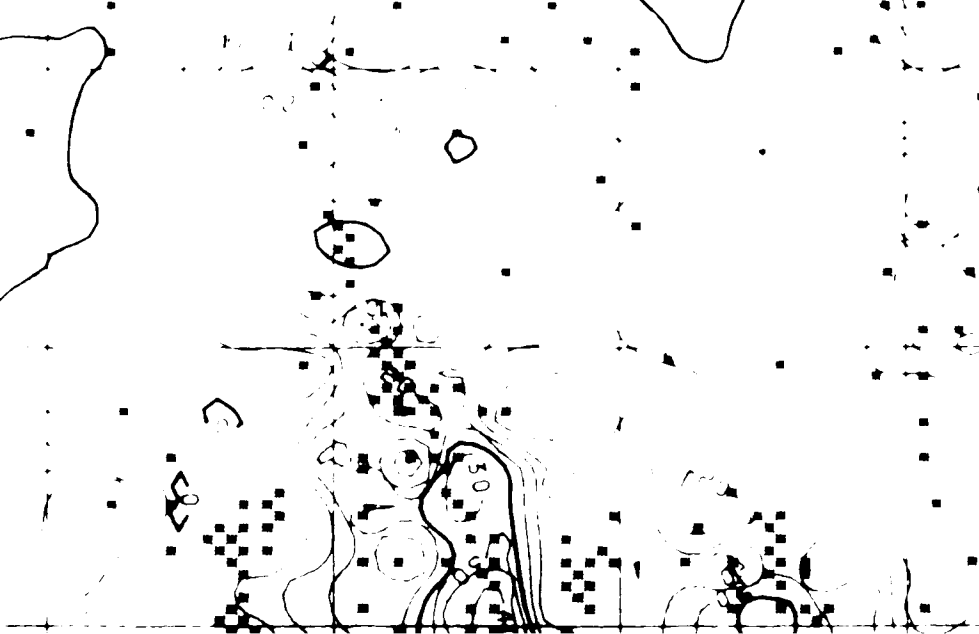
23



22



21



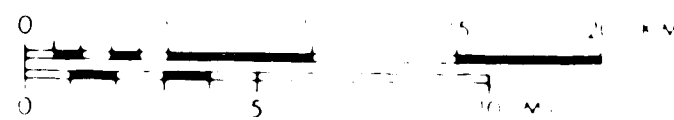
20

22

21

20

19



18

17

16

15

3 of

22

21

20

19

18

17

16

15

404